O-GlcNAc – a posttranslational modification implicated in Alzheimer disease?

DISSERTATION

zur

Erlangung des Doktorgrades (Dr. rer. nat.)

der

Mathematisch-Naturwissenschaftlichen Fakultät

der

Rheinischen Friedrich-Wilhelms-Universität Bonn

vorgelegt von

Sarah Förster

aus

Tel Aviv

Bonn, 2014

Angefertigt mit Genehmigung der Mathematisch-Naturwissenschaftlichen Fakultät der Rheinischen Friedrich-Wilhelms-Universität Bonn.

1. Gutachter: Prof. Dr. Brigitte Schmitz (em.)

2. Gutachter: Prof. Dr. Norbert Koch

Tag der Promotion:15.01.2015

Erscheinungsjahr: 2015

Aus dieser Dissertation hervorgegangene Publikationen:

Artikel in Fachzeitschriften

Förster S, Welleford AS, Triplett JC, Sultana R, Schmitz B, Butterfield DA (2014). Increased O-GlcNAc levels correlate with decreased O-GlcNAcase levels in Alzheimer disease brain. *Biochim Biophys Acta* 1842(9): 1333-1339.

Kongressbeiträge

Vortrag:

O-GlcNAc – a posttranslational modification implicated in Alzheimer disease? International Meeting of the GBM study group "Molecular Neurobiology", 11.-13. September 2014, Bochum.

Poster:

Förster S, Gehrig BJ, Balzen S, Diestel S, Schmitz B. Analytical tools for the identification of O-GlcNAc modified proteins: from Western blots to mass spectrometric sequencing. 63. Mosbacher Kolloquium der Gesellschaft für Biochemie und Molekularbiologie, 29.-31. März 2012, Mosbach/Baden.

Förster S, Strempel N, Gehrig BJ, Schmitz B. Development of an *in vitro* OGT assay using recombinant OGT. 22th Joint Glycobiology Meeting of the "Studiengruppe Glykobiologie der Gesellschaft für Biochemie und Molekularbiologie", the „Niederlandse Vereinigung voor Glycobiologie", the „Groupe Lillois de Glycobiologie" and the „Belgian Working Group for Glycosciences", 28.-29. November 2011, Lille, Frankreich.

Abstract

O-linked N-acetylglucosamine (O-GlcNAc) is a highly dynamic posttranslational modification which has been found on a myriad of nucleocytoplasmic proteins. O-GlcNAc addition and removal are catalyzed by two conserved enzymes, O-GlcNAc transferase (OGT) and O-GlcNAc hydrolase (OGA).

Alzheimer disease (AD) is one of the most common forms of dementia. The histopathological hallmarks of AD brain include neurofibrillary tangles of hyperphosphorylated tau and senile plaques consisting mainly of aggregated amyloid β-peptides which are generated from a larger transmembrane protein, the amyloid precursor protein (APP).

O-GlcNAc has been extensively studied in the context of AD. However, contradicting results have demonstrated either increased or decreased O-GlcNAcylation in AD brain. To date the underlying cause(s) as well as potential consequences of altered O-GlcNAcylation in AD are unknown. Both the microtubule-associated protein tau and APP are O-GlcNAc-modified. While some studies show that increased O-GlcNAcylation reduces tau hyperphosphorylation, the function of the O-GlcNAc modification of APP is not yet understood.

In this work, the potential involvement of O-GlcNAc in different aspects of AD pathology was investigated. For this purpose, a recently established *in vitro* OGT assay was used to demonstrate the O-GlcNAcylation of cyclin-dependent kinase 5 (cdk5), a kinase that phosphorylates both APP and tau and has been implicated in AD pathogenesis. The functional role of O-GlcNAcylation of cdk5 remains to be elucidated. Since OGT assays are useful tools for the analysis of OGT activity or for the identification of novel OGT targets, the established *in vitro* OGT assay was further refined using the nuclear pore protein Nup62 as a model substrate. To investigate the (potential) role of APP´s O-GlcNAcylation, effects of O-GlcNAc modulation on the proteolytic processing of APP were analyzed in cell culture studies. Increased O-GlcNAc expression by OGA inhibition did, however, not alter levels of the APP cleavage products sAPPα and sAPPβ. Furthermore, O-GlcNAc and, for the first time, O-GlcNAc cycling enzymes were investigated in brain samples of subjects with AD and amnestic mild cognitive impairment (MCI), a prodromal stage of AD. In AD brains, increased O-GlcNAcylation correlated with reduced OGA expression and activity while OGT expression was unaltered when compared with age-matched controls. In MCI brains, no changes in O-GlcNAc, OGA or OGT expression were observed.

Taken together this work suggests that O-GlcNAc may not play a direct role in APP processing and that altered O-GlcNAcylation may be a late event in the progression of AD. In combination with recent reports demonstrating positive effects of OGA inhibition in animal models of AD, it is obvious that further studies are needed to elucidate the role of O-GlcNAc in AD.

Table of Content

List of abbreviations

2D	Two-dimensional
AD	Alzheimer disease
ADAM	A disintegrin and metalloprotease
AICD	APP intracellular domain
AP	Alkaline Phosphatase
APLP1/2	Amyloid precursor protein-like protein 1/2
ApoE	Apolipoprotein E
APP	Amyloid precursor protein
APP_{695}	APP isoform with 695 amino acids
Aβ	Amyloid β
$Aβ_{40/42}$	Amyloid β-peptide ending at amino acid 40/42
BACE	β-site APP cleaving enzyme
BEMAD	β-elimination and Michael addition of dithiothreitol
BSA	Bovine serum albumin
C	Control
C. elegans	*Caenorhabditis elegans*
Cdk5	Cyclin-dependent kinase 5
CK	Casein kinase
ConA	Concanavalin A
C-terminus	Carboxy-terminus
CTFα/β	Carboxy-terminal fragment after α/β-cleavage
Cy	CyDye
DMEM-LG	Dulbecco´s Modified Eagle Medium low glucose
DI water	Deionized water
E. coli	*Escherichia coli*
e.g.	for example (from Latin: *exempli gratia*)
ECD	Electron capture dissociation
ECL	Enhanced chemiluminescence
ELISA	Enzyme-linked immunosorbent assay
ER	Endoplasmic reticulum
et al.	and others (from Latin: *et alii*)
ETD	Electron transfer dissociation
FL-OGA	Full-length OGA
GAPDH	Glyceraldehyde-3-phosphate dehydrogenase
GlcNAc	N-acetylglucosamine
GlcNAz	N-azidoacetylglucosamine
GLUT	Glucose transporter
GST	Glutathione S-transferease
HBP	Hexosamine biosynthetic pathway

HCD	High-energy collision dissociation
i.e.	that is (from Latin: *id est*)
IEF	Isoelectric focusing
IP	Immunoprecipitation
IPG	Immobilized pH gradient
IPL	Inferior parietal lobule
IPTG	Isopropyl-β-D-thiogalactopyranosid
MALDI-TOF	Matrix-assisted desorption/ionization time-of-flight
MCI	Mild cognitive impairment
MGEA5	Meningioma-expressed antigen 5
MMSE	Mini-Mental State Examination
mOGT	Mitochondrial OGT
MS	Mass spectrometry
NButGT	1,2-dideoxy-2´-propyl-α-D-glucopyranoso-[2,1-D]-Δ2´-thiazoline
ncOGT	Nucleocytoplasmic OGT
Ni	Nickel
NTA	Nitrolotriacetid acid
N-terminus	Amino-terminus
Nup62	Nucleoporin 62
NV-OGA	Nuclear-variant of OGA
OD	Optical density
OGA	O-GlcNAc hydrolase or O-GlcNAcase
O-GlcNAc	O-linked N-acetylglucosamine
OGT	O-GlcNAc transferase
PAGE	Polyacrylamide gel electrophoresis
PBS	Phosphate-buffered saline
pI	Isoelectric point
PMA	4β-Phorbol 12-myristate 13-acetate
PMI	Post-mortem interval
pNP-GlcNAc	p-nitrophenyl N-acetyl-β-D-glucosaminide
POD	Peroxidase
PS1/2	Presenilin 1/2
PUGNAc	O-(2-acetamido-2-deoxy-D-glucopyranosylidene)amino-N-phenylcarbamate
rpm	Rounds per minute
sAPPα/β	Secreted ectodomain of APP after α/β-cleavage
SD	standard deviation
SDS	Sodium dodecyl sulfate
SEM	Standard error of the mean
sOGT	Short OGT
SY5Y-APP	SH-SY5Y cells stably transfected with the cDNA of human wild-type APP_{695}

TFA	Trifluoroacetic acid
TPR	Tetratricopeptide repeat
UDP	Uridine 5´-diphosphate
v/v	Volume per volume
w/v	Weight per volume
x g	fold gravitational force

List of figures

List of tables

List of units

°C	Degrees Celsius
µg	Microgram
µM	Micromolar
µm	Micrometer
A	Ampere
Da	Dalton
g	Gram
h	Hour
kDa	Kilodalton
L	Liter
M	Molar
mA	Milliampere
mg	Milligram
min	Minute
ml	Milliliter
mM	Millimolar
nM	Nanomolar
nm	Nanometer
s	Second
V	Volt

1 Introduction

1.1 O-GlcNAc

O-linked N-acetylglucosamine (O-GlcNAc) is a posttranslational modification consisting of a single N-acetylglucosamine (GlcNAc) attached to serine or threonine residues of proteins (Torres and Hart, 1984). In contrast to classical N- and O-glycosylation of membrane and secretory proteins, O-GlcNAc is not further elongated into more complex structures and it is localized to the nucleocytoplasmic compartment and to mitochondria (Holt and Hart, 1986; Hu *et al.*, 2009). Furthermore, and in analogy to protein phosphorylation, O-GlcNAcylation is reversible, highly dynamic, and changes in response to various stimuli (Kearse and Hart, 1991; Zachara *et al.*, 2004). O-GlcNAc cycling is facilitated by two highly conserved ubiquitously expressed enzymes, O-GlcNAc transferase (OGT) and O-GlcNAc hydrolase (O-GlcNAcase or OGA) (Lubas *et al.*, 1997; Gao *et al.*, 2001; see Figure 1A). Utilizing uridine 5´-diphosphate-N-acetylglucosamine (UDP-GlcNAc) as its donor substrate, OGT catalyzes the addition of the GlcNAc moiety onto proteins while OGA catalyzes its removal (Haltiwanger *et al.*, 1990; Dong and Hart, 1994). The high-energy sugar nucleotide UDP-GlcNAc is generated in the hexosamine biosynthetic pathway (HBP), a metabolic sideway through which 2-3 % of intracellular glucose are metabolized (Marshall *et al.*, 1991; illustrated in Figure 1B). As O-GlcNAc synthesis is dependent on glucose flux through the HBP, O-GlcNAcylation is often referred to as a nutrient sensor (Wells *et al.*, 2003).

To date, a myriad of proteins from almost all functional classes involved in various signaling pathways have been described to be O-GlcNAcylated. These proteins play important roles in transcription/translation, stress response and cell death, energy metabolism, cytoskeletal regulation, and protein stability/proteasomal degradation (reviewed in Hart *et al.*, 2007; Butkinaree *et al.*, 2010). However, the exact function(s) of O-GlcNAc on most proteins remain to be investigated. Interestingly, all identified O-GlcNAc proteins are also phosphoproteins indicating possible functional interplay between the two posttranslational modifications (see 1.1.2).

Despite being such an abundant modification O-GlcNAc was not described until the early 1980s because the detection and analysis of protein O-GlcNAcylation has been and still is quite challenging. The O-GlcNAc modification is substoichiometric, with as little as 0.1 GlcNAc residue per protein molecule in some cases (Kreppel and Hart, 1999). During cell lysis, lysosomal hexosaminidases are released which rapidly cleave O-GlcNAc off proteins if no precautionary measures are taken. O-GlcNAc is small and uncharged, thus its addition has no effect on the apparent molecular weight of a protein in gel electrophoresis. In

addition, analysis by mass spectrometry (MS) is difficult as the O-GlcNAc moiety is labile and it is often lost during standard ionization and fragmentation techniques. Site-directed mutagenesis, a method which is often used for functional analysis, can also affect phosphorylation and in consequence, it cannot be distinguished between effects mediated by the loss of phosphorylation or of O-GlcNAcylation of the investigated protein. Fortunately, the development of specific O-GlcNAc antibodies and the use of enzymatic and/or chemical tagging and enrichment methods in combination with new MS fragmentation techniques have greatly improved O-GlcNAc detection (Hart *et al.*, 2007; Hu *et al.*, 2010).

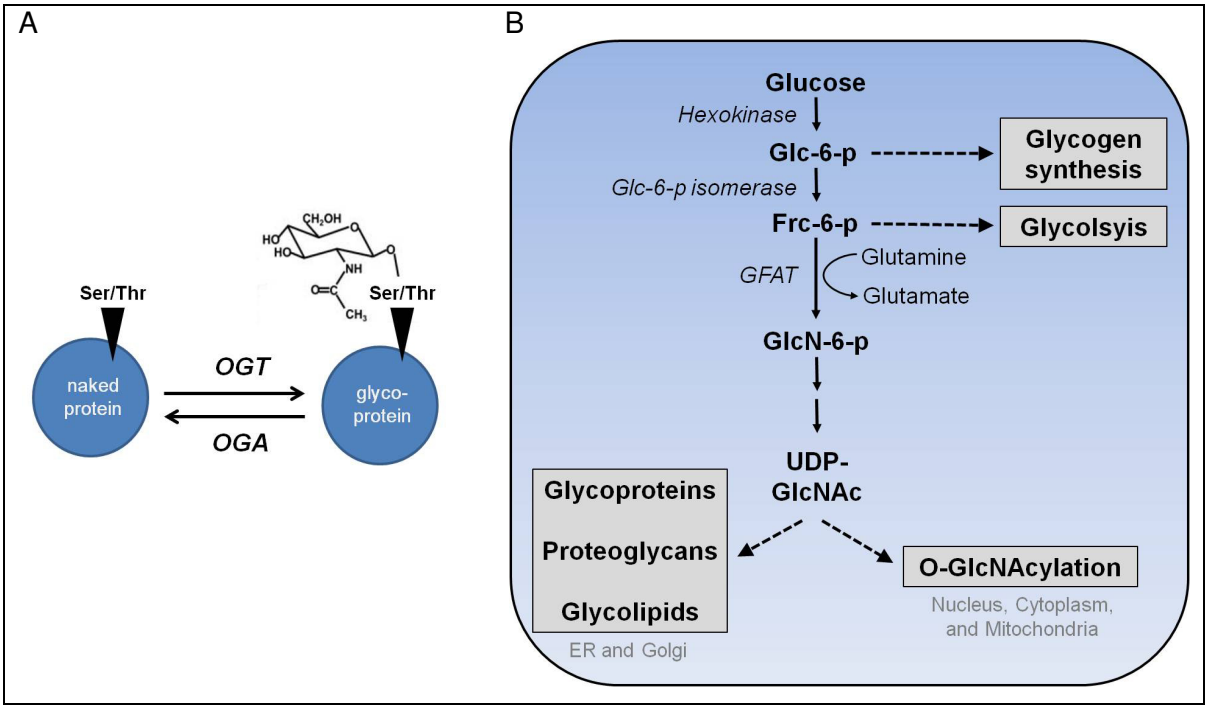

Figure 1: O-GlcNAc cycling and the hexosamine biosynthetic pathway

(A) Dynamic O-GlcNAc cycling is mediated by only two highly conserved enzymes. O-GlcNAc transferase (OGT) adds O-GlcNAc to serine or threonine residues of proteins while O-GlcNAc hydrolase (OGA) removes it (modified from Hart *et al.*, 2007 and Hu *et al.*, 2010). **(B)** UDP-GlcNAc is the final product of the hexosamine biosynthetic pathway, a metabolic side way through which about 2-3 % of intracellular glucose are metabolized. The rate-limiting enzyme glutamine:fructose-6-phosphate amido-transferase (GFAT) utilizes glutamine to convert fructose-6-phosphate (Frc-6-p) into glucosamine-6-phosphate (GlcN-6-p) which is then further metabolized to form UDP-GlcNAc. UDP-GlcNAc serves as the donor substrate for protein O-GlcNAcylation by the OGT and for the generation of various glycoconjugates. Glc-6-p: glucose-6-phosphate; ER: endoplasmic reticulum (modified from Buse, 2006; Issad and Kuo, 2008; Butkinaree *et al.*, 2010).

1.1.1 O-GlcNAc cycling enzymes: OGT and OGA

As described above, **OGT** catalyzes the addition of O-GlcNAc onto the hydroxyl groups of serine or threonine residues of target proteins (Haltiwanger *et al.*, 1990). The *ogt* gene is highly conserved from *Caenorhabditis elegans* (*C. elegans)* to humans and is ubiquitously expressed in all mammalian tissues analyzed with highest level in the pancreas (Lubas *et al.*, 1997; Kreppel *et al.*, 1997). Interestingly, OGT activity does not necessarily correlate with OGT protein level as it is highest in brain and thymus (Kreppel *et al.*, 1997). OGT is essential for life, as intact *ogt* gene is required for embryonic stem cell viability and mouse ontology (Shafi *et al.*, 2000). Furthermore, tissue-targeted deletion of the *ogt* gene causes adverse effects in several cell types. For example, neuron-specific *ogt* mutagenesis leads to tau hyperphosphorylation and neuronal dysfunction (O´Donnell *et al.*, 2004).

In humans, the *ogt* gene resides on the X chromosome and encodes three OGT isoforms of various lengths, subcellular localization, and distinct tissue-specific expression (Lubas *et al.*, 1997; Shafi *et al.*, 2000; Hanover *et al.*, 2003; Lazarus *et al.*, 2006). The nucleocytoplasmic and short OGT isoforms (ncOGT and sOGT) have apparent molecular weights of 116 and 75 kDa, respectively, and are localized to the nucleus and cytosol while mitochondrial OGT (mOGT), migrating at 103 kDa, resides in the mitochondria. OGT isoforms differ in the number of tetratricopeptide repeats (TPR) in their amino-terminus (N-terminus): ncOGT contains 11.5, mOGT contains 9, and sOGT contains only 2 TPRs (Hanover *et al.*, 2003).

TPRs are degenerate motifs composed of 34 amino acids which are often assembled in tandem arrays and mediate protein-protein interactions (Lamb *et al.*, 1995). In accordance, deletion studies have demonstrated the importance of TPRs for OGT´s substrate recognition and the three isoforms, with their varying numbers of TPRs, exhibit distinct substrate specificities (Lubas and Hanover, 2000; Hanover, *et al.*, 2003; Lazarus *et al.*, 2006; Clarke *et al.*, 2008). Furthermore, TPRs have been suggested to play a role in OGT multimerization and activity (Kreppel and Hart, 1999; Lubas and Hanover, 2000; Jínek *et al.*, 2004).

The carboxy-terminus (C-terminus) of OGT contains the catalytic domain and is identical in all three isoforms (Lubas and Hanover, 2000). The C-terminal region also includes a binding site for phosphatidylinositol-3,4,5-trisphosphate, the so called PPO domain, which is essential for the recruitment of OGT to the plasma membrane in response to insulin stimulation (Yang *et al.*, 2008). Uniquely, ncOGT contains a nuclear localization signal while mOGT contains a mitochondrial localization signal (Hanover *et al.*, 2003; Love *et al.*, 2003). An overview of OGT isoforms is depicted in Figure 2.

Although no consensus motif for O-GlcNAcylation has yet been identified, some distinct amino acid sequences are common to many OGT substrates. O-GlcNAcylation often takes

place at P-V-S/T-S/T motifs as well as at motifs consisting of two hydroxyl-containing amino acids adjacent to an alanine (Vosseller *et al.*, 2006).

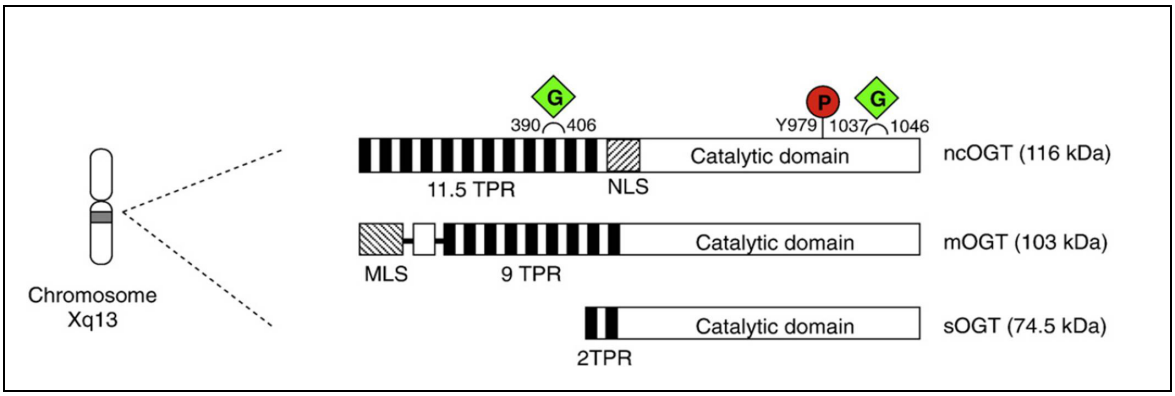

Figure 2: O-GlcNAc transferase (Butkinaree *et al.*, 2010)

The *ogt* gene resides on chromosome Xq13 and due to alternative splicing gives rise to three different OGT isoforms with identical C-terminal catalytic domains but varying N-termini: ncOGT contains 11.5 tetratricopeptide repeats (TPRs) and a central nuclear localization signal (NSL); mOGT contains 9 TPRs and an N-terminal mitochondrial localization signal (MLS); sOGT contains 2 TPRs. Posttranslational modifications of ncOGT include tyrosine phosphorylation and O-GlcNAcylation. G: O-GlcNAc; P: O-phosphate; nc: nucleocytoplasmatic; m: mitochondrial; s: short.

Regulation of OGT is highly complex and O-GlcNAcylation is responsive to various cellular signals and stimuli. While OGT is potently inhibited by free UDP and low concentrations of salts, GlcNAc and ATP have no effect on OGT activity *in vitro* (Haltiwanger *et al.*, 1990; 1992; Marshall *et al.*, 2003). The affinity of OGT towards different substrates as well as its activity is highly dependent on UDP-GlcNAc concentrations (Kreppel and Hart, 1999). OGT activity towards various substrates may further be influenced by interactions with different proteins. It has been demonstrated, for example, that OGT-interacting protein 106 targets OGT to RNA polymerase II (Iyer *et al.*, 2003); during glucose deprivation OGT can also be targeted to neurofilament H by p38 kinase (Cheung and Hart, 2008). OGT activity may also be regulated by posttranslational modifications as the enzyme is O-GlcNAcylated and tyrosine phosphorylated (Kreppel *et al.*, 1997; see Figure 2).

The removal of GlcNAc from proteins is catalyzed by **OGA** formally known as hexosaminidase C (Poenaru and Dreyfus, 1974; Dong and Hart, 1994; Gao *et al.*, 2001). Unlike lysosomal β-hexosaminidases, OGA activity is highest at neutral pH, shows cytoplasmic and nuclear localization, and is specific for β-linked GlcNAc (Dong and Hart, 1994). OGA is encoded by a highly conserved gene, originally identified as meningioma-expressed antigen 5 (*MGEA5*), and it is expressed ubiquitously with highest levels in the brain, followed by placenta and pancreas (Heckel *et al.*, 1998; Comtesse *et al.*, 2001; Gao *et al.*, 2001). Similar to *ogt* deletion studies, OGA knockout in mice causes embryonic or

neonatal lethality indicating that OGA is essential for development (Yang *et al.*, 2012). Interestingly, knockout of OGA or OGT homologues in *C. elegans* is not lethal and deletion of either gene results in similar phenotypes, i.e., altered macronutrient storage and dauer formation (Hanover *et al.*, 2005; Forsythe *et al.*, 2006).

In humans, the gene encoding OGA resides on chromosome 10, at a locus that has been implicated in AD and is associated with type 2 diabetes mellitus in Mexican Americans (Heckel *et al.*, 1998; Duggirala *et al.*, 1999; Bertram *et al.*, 2000; Lehman *et al.*, 2005). Alternative splicing of the *MGEA5* gene yields two OGA isoforms, full-length (FL) or long OGA and nuclear-variant (NV) or short OGA, with apparent molecular weights of 130 and 75 kDa, respectively (Comtesse *et al.*, 2001). Consistent with the localization of OGT and O-GlcNAcylated proteins, OGA is found in the cytosol, nucleus, and in mitochondria (Dong and Hart, 1994; Comtesse *et al.*, 2001; Hu *et al.*, 2009). OGA isoforms demonstrate distinct subcellular localization. FL-OGA resides predominantly in the cytoplasm whereas NV-OGA is located mainly to the nucleus but was recently also found on the surface of lipid droplets (Comtesse *et al.*, 2001; Keembiyehetty *et al.*, 2011). Both isoforms contain the N-terminal O-GlcNAcase domain, but NV-OGA lacks the C-terminal third of FL-OGA including a region that has been proposed to contain histone acetyl transferase activity *in vitro*; a finding which has later been contested (Comtesse *et al.*, 2001; Toleman *et al.*, 2004; Butkinaree *et al.*, 2008). Furthermore, OGA contains two caspase-3 consensus sequences predicted to generate C-terminal fragments of 83 and 63 kDa, respectively, and caspase-3 has been demonstrated to cleave FL-OGA *in vitro* (Wells *et al.*, 2002a). While both OGA variants show O-GlcNAcase activity *in vitro*, the catalytic efficiency of NV-OGA is approximately 400-fold lower than that of the full-length enzyme (Macauley and Vocadlo, 2009). An overview of OGA isoforms is depicted in Figure 3.

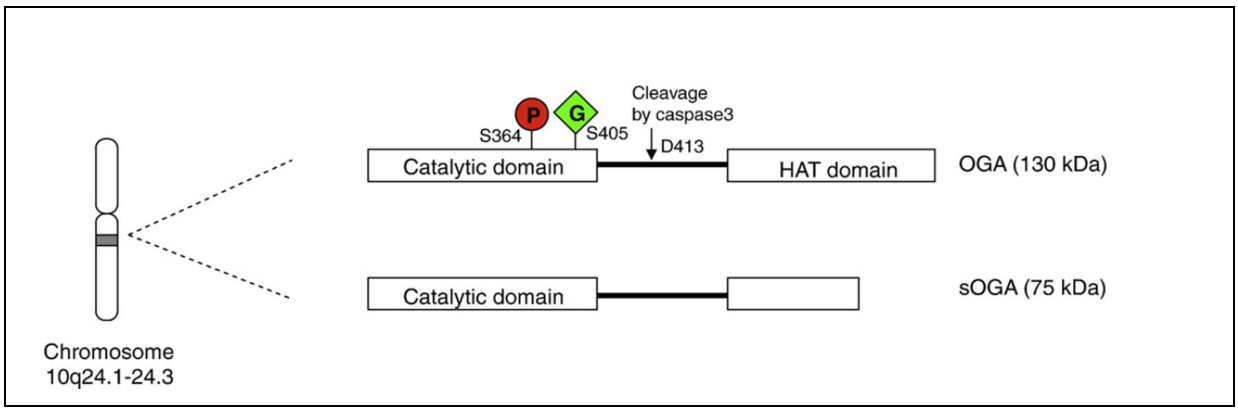

Figure 3: O-GlcNAc hydrolase (Butkinaree *et al.*, 2010)

The O-GlcNAc hydrolase (OGA) gene resides on chromosome X10q24 and gives rise to two OGA isoforms with identical N-terminal catalytic domains but different C-termini. Full-length OGA contains a caspase-3 cleavage site and a putative histone acetyl transferase (HAT) domain. Furthermore, it is posttranslationally modified by phosphorylation and O-GlcNAcylation. G: O-GlcNAc; P: O-phosphate; s: short.

Not much is known about the regulation of OGA activity or its targeting to substrates. Like OGT, OGA may also be regulated by posttranslational modifications, as the enzyme is phosphorylated and O-GlcNAcylated (Beausoleil *et al.*, 2004; Lazarus *et al.*, 2006; Khidekel *et al.*, 2007; see Figure 3). OGA interacts with OGT and it has been proposed that OGA may be sequestered to its substrates via its tight binding to OGT (Whisenhunt *et al.*, 2006). Furthermore, based on their different subcellular localizations and catalytic efficiencies, it has been suggested that OGA isoforms may have distinct cellular targets (Keembiyehetty *et al.*, 2011). The crystal structure of human OGA has not yet been solved, but the analysis of a bacterial OGA homologue indicates that OGA contains a highly conserved substrate-binding groove near its active site (Rao *et al.*, 2006). To date, it is not yet clear whether OGA´s substrate recognition is mediated via the GlcNAc moiety alone or by interactions with both the sugar moiety and the peptide backbone of the substrate (Rao *et al.*, 2006; Schimpl *et al.*, 2012; Shen *et al.*, 2012; Martin *et al.*, 2014).

1.1.2 Dynamic interplay between O-GlcNAcylation and phosphorylation

Since O-GlcNAcylation and phosphorylation both occur on serine and/or threonine residues, Hart *et al.* proposed the so-called "**yin-yang**" model of mutually exclusive O-GlcNAc and O-phosphate modification of proteins (Kelly *et al.*, 1993; Hart *et al.*, 1995). This hypothesis was strengthened by studies showing that increasing/decreasing global protein phosphorylation concomitantly reduced/elevated global O-GlcNAc expression (Griffith and Schmitz, 1999). A reciprocal relationship of both posttranslational modifications has also been demonstrated for individual proteins, for example, O-GlcNAcylation of p53 prevents phosphorylation of the protein (Yang *et al.*, 2006). However, it soon became apparent that the interplay between the two modifications was more complex than originally thought. For example, Wang *et al.* demonstrated that selective inhibition of glycogen synthase kinase-3 by lithium resulted in increased O-GlcNAcylation on some proteins but decreased O-GlcNAcylation on others (Wang *et al.*, 2007). A follow-up study demonstrated that global O-GlcNAc modulation also influenced protein phosphorylation bi-directionally (Wang *et al.*, 2008). Similarly, Tallent *et al.* showed that *in vivo* upregulation of O-GlcNAc expression resulted in elevated O-GlcNAcylation of synapsin I and, at the same time, site-specifically increased phosphorylation of synapsin I (Tallent *et al.*, 2009). By now, it seems that all possible combinations of both O-GlcNAc modification and phosphorylation can be found on proteins (Comer and Hart, 2000; Hart *et al.*, 2007) including but not limited to the following:

i. competitive occupancy of the same site, e.g. at Ser16 of estrogen receptor β (Cheng and Hart, 2001);
ii. competitive and alternative occupancy on adjacent sites, e.g. at Ser146 and Thr155 of p53 (Yang *et al.*, 2006);
iii. complex interplay of phosphorylation and O-GlcNAcylation of the same, adjacent and/or distant sites, e.g. on RNA polymerase II (Comer and Hart, 2001).

The extensive crosstalk of O-GlcNAcylation and phosphorylation is further demonstrated by the fact that O-GlcNAc cycling enzymes are phosphorylated and different kinases including glycogen synthase kinase-3β and casein kinase 2 (CK2) are O-GlcNAcylated (Kreppel *et al.*, 1997; Lubas and Hanover, 2000; Beausoleil *et al.*, 2004; Dias *et al.*, 2012). Furthermore, OGT associates with protein phosphatase 1 subunits and OGT, OGA, mitotic kinase Aurora B and protein phosphatase 1 have been demonstrated to form functional complexes during cytokinesis (Wells *et al.*, 2004; Slawson *et al.*, 2008). The recent findings that O-GlcNAcylation modulates tyrosine phosphorylation of insulin receptor substrate 1 and the discovery of phosphorylated O-GlcNAc add yet another level of complexity to the intricate interplay between the two modifications (Whelan *et al.*, 2010; Graham *et al.*, 2011).

1.1.3 Functions of O-GlcNAc

As demonstrated by knockout studies, O-GlcNAc and functional O-GlcNAc cycling are essential for life (Shafi *et al.*, 2000; Yang *et al.*, 2012). Protein O-GlcNAcylation plays important roles in transcription/translation, energy metabolism, cytoskeletal regulation, protein stability/proteasomal degradation, and cell death (reviewed in Hart *et al.*, 2007; Butkinaree *et al.*, 2010), and O-GlcNAc has been proposed to act as a nutrient and stress sensor (Wells *et al.*, 2003; Chatham and Marchase, 2010). In accordance with the significance of this modification, perturbations in O-GlcNAcylation are associated with different diseases such as cancer and type II diabetes (reviewed in Bond and Hanover, 2013). Based on the multitude of O-GlcNAc functions, only two exemplary aspects are briefly described below.

O-GlcNAc and protein stability

Many of the identified O-GlcNAcylated peptide sequences are reminiscent of “PEST” sequences (peptide regions rich in proline, glutamate, serine, and threonine) which are often subjected to phosphorylation and are known to target proteins for degradation by the ubiquitin-proteasomal system (Rechsteiner and Rogers, 1996; Vosseller *et al.*, 2006). In agreement, phosphorylation of the estrogen receptor β at Ser16 marks it for degradation, while O-GlcNAcylation of estrogen receptor β at Ser16 is thought to stabilize the protein

(Cheng and Hart, 2001). The same protective mechanism of O-GlcNAc has been demonstrated for the tumor suppressor p53 where O-GlcNAcylation at Ser149 prevents phosphorylation at Thr155 thus precluding ubiquitin-dependent proteolysis of the protein (Yang *et al.*, 2006).

Furthermore, key regulators of the ubiquitin-proteasomal system are O-GlcNAcylated and proteasomal function is directly modulated by O-GlcNAc as O-GlcNAcylation of the 26S proteasome inhibits its function (Cole and Hart, 2001; Zhang *et al.*, 2003; Guinez *et al.*, 2008). In agreement, downregulation of OGA has been demonstrated to compromise the proteasome (Keembiyehetty *et al.*, 2011).

O-GlcNAc and cellular stress

Cellular O-GlcNAc levels increase as a response to various forms of stress (Zachara *et al.*, 2004; Guinez *et al.*, 2008). For example in COS-7 cells, acute heat treatment induces O-GlcNAcylation via increased OGT activity. Importantly, this response is dynamic and reversible as O-GlcNAc levels returned to normal 48 hours post heat shock. Moreover, *in vitro* modulation of O-GlcNAc levels by OGT knockdown, OGT overexpression or OGA inhibition alters cellular thermotolerance. While the downregulation of O-GlcNAc renders cells more susceptible to heat stress, upregulation of O-GlcNAc results in increased cellular thermotolerance. Stress tolerance seems to be mediated by the induction the expression of heat shock proteins HSP40 and HSP70 (Zachara *et al.*, 2004).

This study and others indicate that short-term increases of O-GlcNAc levels in response to acute stress are protective and may be part of a pro-survival mechanism (Zachara *et al.*, 2004; Ho *et al.*, 2010). In contrast, chronically increased O-GlcNAcylation is associated with adverse effects in diseases like diabetes (Hu *et al.*, 2005; Chatham and Marchase, 2010).

1.2 Alzheimer disease

Dementia is characterized by the progressive deterioration of cognitive function. In 2010, 35.6 million people worldwide were living with dementia and this number is projected to nearly double every 20 years resulting in 115.4 million dementia cases in the year 2050. **Alzheimer disease** (AD) is one of the most common forms of dementia (Prince *et al.*, 2013).

1.2.1 Pathological hallmarks of AD

In 1907, the German psychiatrist Alois Alzheimer described the case of a 51-year-old patient with rapidly deteriorating memory. Post-mortem analysis of the patient´s brain revealed excessive atrophy as well as “changes of the neurofibrils” and “miliary foci (…) of a peculiar substance” (Alzheimer, 1907, translated by Jarvik and Greenson, 1987). These original observations are now known as the histopathological hallmarks of AD: intracellular **neurofibrillary tangles** of hyperphosphorylated tau protein and extracellular **senile plaques** consisting mainly of aggregated amyloid β (Aβ) peptides (Masters *et al.*, 1985; Grundke-Iqbal *et al.*, 1986a, b; Selkoe, 2001). Furthermore, substantial loss of synapses and increased neuroinflammation are observed in AD brain (Castellani *et al.*, 2010). Clinically, AD is characterized by progressive memory impairment, disordered cognitive function, altered behavior, and a progressive decline in language and motor function (Selkoe, 2001).

Tau pathology, as observed in AD but also in a number of other neurodegenerative disorders, is characterized by the accumulation of abnormally hyperphosphorylated **tau**. Physiologically, the microtubule-associated protein tau contains 2-3 moles phosphate per mole protein and promotes the assembly and stability of microtubules (Weingarten *et al.*, 1975; Köpke *et al.*, 1993). However, hyperphosphorylation of tau reduces its ability to bind tubulin, consequently leading to its dissociation from microtubules and the aggregation of tau protein into tangles of paired helical filaments (Grundke-Iqbal *et al.*, 1986a; Cruz and Tsai, 2004; Iqbal *et al.*, 2005).

Amyloid or senile plaques are microscopic lesions composed of extracellular deposits of Aβ peptides (Masters *et al.*, 1985). **Aβ peptides** of various lengths (39-43 amino acids) are derived from the so-called amyloid precursor protein (APP) (Kang *et al.*, 1987; Cappai and White, 1999). Senile plaques can be divided into two subtypes, diffuse and neuritic plaques, with the latter containing a core of highly insoluble Aβ aggregates that is surrounded by and associated with dystrophic neurites, microglia, and reactive astrocytes (Selkoe, 2001). The predominant Aβ species found in neuritic plaques are the forms ending at amino acid 42 ($A\beta_{42}$); however, also Aβ species ending at amino acid 40 ($A\beta_{40}$) are present in neuritic plaques. In contrast, diffuse or “preamyloid” plaques contain only $A\beta_{42}$ and are not surrounded by degenerating neurites (Iwatsubo *et al.*, 1994; Selkoe, 2001). It has been

suggested that these plaques may represent the immature form of neuritic plaques and in fact, diffuse plaques are often found in the brains of aged subjects free of AD (Selkoe, 2001).

1.2.2 AD subtypes, genes, and risk factors

The majority of AD cases (95 %) are late-onset or sporadic, with idiopathic etiology and symptom onset occurring after the age of 65 (Bertram and Tanzi, 2005; Tang, 2009). The number one risk factor for sporadic AD is age; however, there may also be a significant, yet unidentified, genetic component in late-onset AD since first-degree relatives of AD patients have an increased risk for the disease (Wu *et al.*, 1998). Furthermore, a polymorphism in the gene encoding apolipoprotein E (ApoE) which results in the presence of the ε4 allele is associated with an increased risk for sporadic AD (Strittmatter *et al.*, 1993; Schmechel *et al.*, 1993). The exact molecular mechanisms by which ApoE, a serum cholesterol transport protein, influences AD pathology are unknown but it has been suggested that the ε4 isoform of ApoE may decrease clearance and/or enhance the aggregation of Aβ (Bertram and Tanzi, 2005; Selkoe, 2011). Additional loci have been suggested to be genetically associated with late-onset AD but remain to be confirmed (Eisenstein, 2011).

In contrast, early-onset or familial AD is caused by autosomal dominant mutations in the genes encoding APP, presenilin 1 (PS1) or presenilin 2 (PS2). Although these mutations are found on three different chromosomes, they all lead to common biological consequences, i.e., altered processing of APP resulting in increased production and deposition of Aβ peptides (Selkoe, 2001). This phenotype can also be observed in Trisomy 21, where the triplication of chromosome 21 containing the *APP* gene results in a life-long increase of APP expression and Aβ generation; consequently, amyloid pathology is also found in the brains of subjects with Down syndrome (Masters *et al.*, 1985; Rumble *et al.*, 1989).

Table 1: Confirmed genetic risk factors for AD

Gene	Protein	Chromosome	Phenotype
APOE	ApoE	19	Unknown; possible impact on Aβ aggregation and/or lipid metabolism
APP	APP	21	Increased production of all Aβ species or specifically of $A\beta_{42}$ peptides
PSEN1	PS1	14	Increased $A\beta_{42}/A\beta_{40}$ ratio
PSEN2	PS2	1	Increased $A\beta_{42}/A\beta_{40}$ ratio

ApoE: apolipoprotein E; APP: amyloid precursor protein; PS1: presenilin 1; PS2: presenilin 2 (modified from Selkoe, 2001; Bertram and Tanzi, 2005).

Regardless of the genetic differences between AD subtypes, histopathology in the brains of subjects with familial and sporadic AD is virtually the same; the subtypes mainly differ in the

age of onset (Bertram and Tanzi, 2005). An overview of confirmed genetic risk factors of AD is provided in Table 1. Interestingly, despite the presence of neurofibrillary tangles in AD brain, no tau mutations are associated with the disease.

1.2.3 The amyloid precursor protein

The mammalian protein APP, its two homologues APP-like protein 1 and 2 (APLP1 and APLP2), together with APPL (*Drosophila melanogaster*) and APL-1 (*C. elegans*), comprise the members of the highly conserved APP family (Rosen *et al.*, 1989; Wasco *et al.*, 1992; 1993; Daigle and Li, 1993). Triple knockout of APP, APLP1 and APLP2 in mice leads to a severe phenotype with cranial abnormalities leading to early neonatal death (Herms *et al.*, 2004). In contrast, single knockout of APP, APLP1 or APLP2 results in viable mice showing only minor abnormalities (Zheng *et al.*, 1995; Heber *et al.*, 2000). These studies indicate an essential role of the APP family members in brain development but also point towards a certain degree of redundancy within the APP gene family (Zheng *et al.*, 1995; Heber *et al.*, 2000; Herms *et al.*, 2004).

APP is a type I transmembrane protein with a large N-terminal extracellular domain, a single membrane-spanning domain and a short cytoplasmic C-terminal region (Dyrks *et al.*, 1988; see Figure 4A). Importantly, only APP but not its family members contains the Aβ sequence (Wasco *et al.*, 1993). Alternative splicing of the *APP* gene gives rise to various APP isoforms with APP_{770}, APP_{751}, and APP_{695} comprised of 770, 751, and 695 amino acids, respectively, representing the major isoforms in mammals (Kang *et al.*, 1987; Kang and Müller-Hill, 1990). APP is ubiquitously expressed, the different isoforms, however, show differential tissue distribution. For example, APP_{695} is highly enriched in the brain and constitutes the major APP isoform in neurons (Kang and Müller-Hill, 1990; Ohyagi *et al.*, 1990). The exact function(s) of APP remain to be elucidated but it has been suggested to play a role in cell adhesion, neuronal migration, neurite outgrowth, synaptogenesis, modulation of synaptic plasticity, and in neuronal survival (reviewed in Jacobsen and Iverfeldt, 2009).

1.2.3.1 Trafficking of APP

Nascent APP is constitutively transported via the secretory pathway from the endoplasmic reticulum (ER) to the plasma membrane. During this transit, APP is posttranslationally modified, i.e., it undergoes phosphorylation, tyrosine sulfation as well as N- and O-glycosylation in the ER and Golgi (Weidemann *et al.*, 1989; Suzuki *et al.*, 1992; Haass *et al.*, 2012). Immature APP is only N-glycosylated while mature APP is both N- and O-glycosylated; these glycoforms, in addition to the various isoforms of APP, result in the apparent heterogeneity of the protein in gel electrophoresis (Weidemann *et al.,* 1989).

Complete glycosylation of APP is important for further processing as only mature APP is sorted via the trans-Golgi network and delivered to the plasma membrane (Weidemann *et al.,* 1989). Steady-state levels of full-length APP at the plasma membrane are low since cell surface APP undergoes ectodomain shedding or is quickly endocytosed (Nordstedt *et al.*, 1993; Thinakaran and Koo, 2008; Vetrivel and Thinakaran, 2010). From endosomes, APP can be recycled to the plasma membrane or targeted to lysosomes for degradation (Haass *et al.*, 1992a; Koo *et al.,* 1996; Thinakaran and Koo, 2008).

1.2.3.2 Processing of APP

As illustrated in Figure 4A, APP processing can be divided into the amyloidogenic and the non-amyloidogenic pathway (reviewed in Tang, 2009; Chow *et al.*, 2010; Haass *et al.*, 2012).

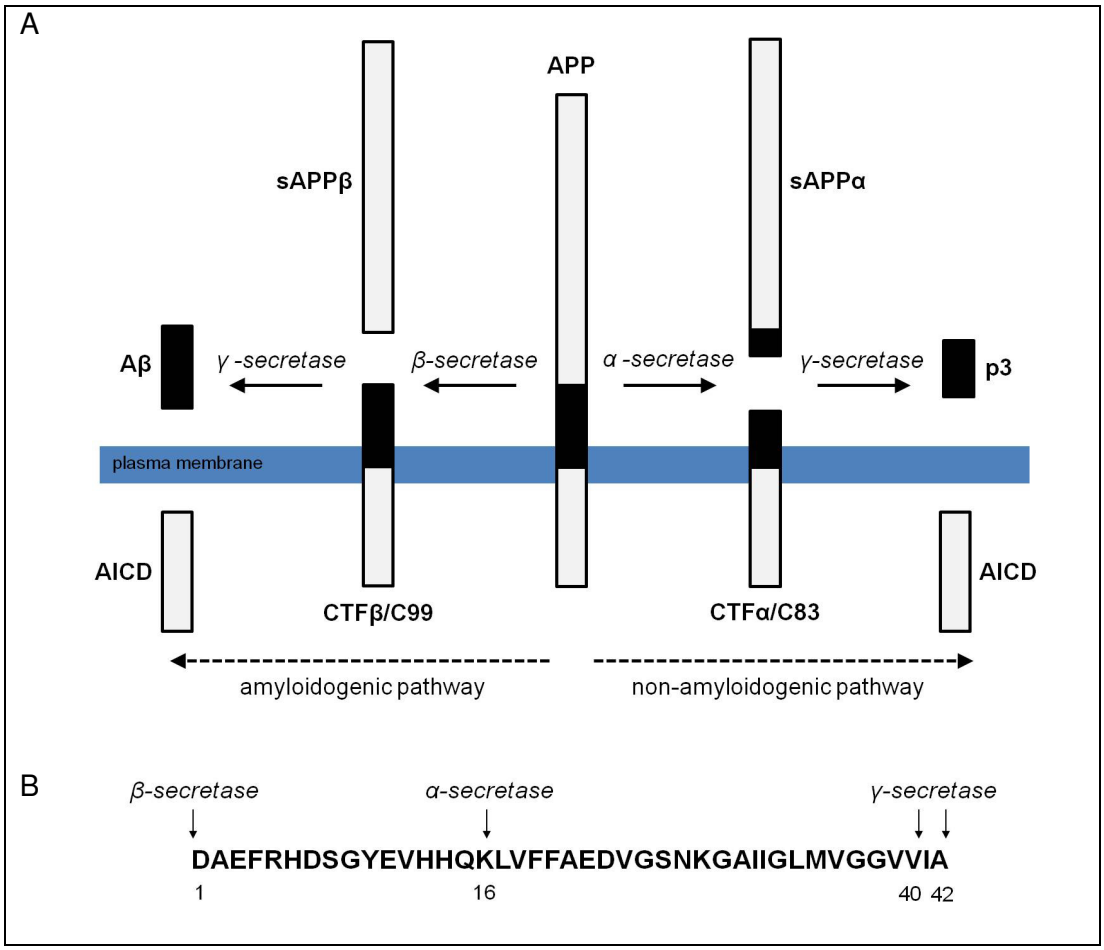

Figure 4: Proteolytic processing of APP

(A) The transmembrane protein APP can be processed via two separate pathways. In the amyloidogenic pathway (left side), APP is first cleaved by β-secretase releasing a large soluble ectodomain (sAPPβ). The membrane-bound C-terminal fragment of 99 amino acids (CTFβ or C99) is further processed by γ-secretase to generate Aβ and the APP intracellular domain (AICD). In contrast, in the non-amyloidogenic pathway (right side), APP is sequentially cleaved by α- and γ-secretases releasing sAPPα, the non-amyloidogenic p3 fragment, and AICD (modified from Tang, 2009). **(B)** Amino acid sequence of $A\beta_{42}$ including the major secretase cleavage sites as indicated by the arrows (modified from Chow *et al.*, 2010). APP: amyloid precursor protein; sAPP: secreted APP fragment; CTF: C-terminal fragment (picture is not drawn to scale).

The amyloidogenic pathway

In the amyloidogenic pathway, Aβ is generated through the sequential cleavage of APP by β- and γ-secretases (Figure 4A). Processing of APP by β-secretase releases a soluble N-terminal ectodomain, sAPPβ, while the remaining membrane-bound C-terminal fragment of 99 amino acids, termed CTFβ or C99, is then further cleaved by γ-secretase to generate Aβ (4 kDa) as well as the APP intracellular domain (AICD).

β-secretase activity is mediated by an aspartic protease termed β-site APP-cleaving enzyme (BACE) (Vassar *et al.*, 1999). Two BACE homologues, BACE1 and BACE2, with distinct expression patterns exist. BACE1 is expressed predominantly in the brain with highest abundance in neurons while BACE2 shows very little expression in the brain and therefore appears to be irrelevant for AD pathology (Vassar *et al.*, 1999; Bennett *et al.*, 2000; Chow *et al.*, 2010). As demonstrated by knockout studies, BACE1 activity is essential for the generation and deposition of Aβ (Luo *et al.*, 2001). In addition to the main β-cleavage site at position 1 of the Aβ sequence (see Figure 4B), β-cleavage can also occur at the so-called β´ site resulting in the generation of Aβ peptides beginning at residue 11 (glutamate) (Vassar *et al.*, 1999).

Like APP, BACE1 is a ubiquitously expressed type I transmembrane protein, it is core-glycosylated in the ER, further processed in the Golgi and finally targeted to endosomal compartments (Vassar *et al.*, 1999). BACE1 has also been demonstrated to cycle between endosomes and the cell surface and therefore small amounts of the enzyme can be found at the plasma membrane (Huse *et al.*, 2000; Riddell *et al.*, 2001). Consistent with the acidic pH optimum of the enzyme, cleavage by BACE1 preferentially occurs after internalization of APP in endocytic and/or recycling compartments (Koo and Squazzo, 1994; Vassar *et al.*, 1999). Furthermore, amyloidogenic processing of APP seems to be dependent on the integrity of cholesterol-rich lipid rafts (Ehehalt *et al.*, 2003).

Membrane-bound CTFs are further processed by **γ-secretase**, a protease complex comprised of PS1 or PS2, nicastrin, anterior pharynx defective 1, and presenilin enhancer-2 (Wolfe *et al.*, 1999; Yu *et al.*, 2000; Francis *et al.*, 2002; Haas *et al.*, 2012). Consistent with the different localizations of APP, γ-secretase activity is localized to the plasma membrane and to the endosomal/lysosomal system (Kaether *et al.*, 2002; Haass *et al.*, 2012). Intramembrane cleavage of CTFβ by γ-secretase results in the generation of AICD and Aβ. However, this final cleavage is not precise and probably takes place by stepwise proteolysis of the CTFβ, thus explaining the existence of Aβ peptides with various C-termini. It has been postulated that CTFβ is successively cleaved by γ-secretase at the ε-, ζ-, and finally at the γ-site resulting in the sequential generation of $Aβ_{48}$ and $Aβ_{49}$ as well as the AICD, followed by $Aβ_{45}$ and $Aβ_{46}$, and finally $Aβ_{39}$-$Aβ_{43}$ peptides (Qi-Takahara *et al.*, 2005; Haass *et al.*, 2012).

In contrast to the original idea that **Aβ** peptides are only generated under pathological conditions, Aβ is constitutively produced and secreted during normal cellular metabolism yet its physiological function is not fully understood (Haass *et al.*, 1992b; Brunholz *et al.*, 2012). Aβ forms containing 40 and 42 amino acids ($Aβ_{(1-40)}$ and $Aβ_{(1-42)}$) are predominantly produced but in addition various N- and C-terminally truncated Aβ species can be detected in brain, cerebrospinal fluid and plasma of both subjects with or without AD (Näslund *et al.*, 1994; Ida *et al.*, 1996). Aβ peptides can be found intra- and extracellularly as well as in soluble and insoluble forms as Aβ monomers readily accumulate into multimeric complexes ranging from dimers and trimers to high-molecular weight protofibrils and amyloid fibrils (Skovronsky *et al.*, 1998; LaFerla *et al.*, 2007). Toxicity and aggregation properties of Aβ peptides depend on their respective amino acid composition. For example, $Aβ_{42}$ species are more hydrophobic and fibrillogenic and exert greater neurotoxicity than $Aβ_{40}$ species (Burdick *et al.*, 1992; Jarrett *et al.*, 1993; Zhang *et al.*, 2002; Zou *et al.*, 2003; LaFerla *et al.*, 2007).

The **AICD** has been proposed to be involved in transcription (Cao and Südhof, 2001); however, only few putative AICD gene targets, e.g. APP and glycogen synthase kinase-3β, have been identified and data have been highly controversial (von Rotz *et al.*, 2004; Hébert *et al.*, 2006). Noteworthy, AICD can be further cleaved by caspases (reviewed in Bredesen *et al.*, 2010) or be metabolized by insulin degrading enzyme presumably precluding its translocation to the nucleus (Edbauer *et al.*, 2002).

Furthermore, intracellular **phosphorylation of APP** may influence APP processing and function. For example, phosphorylation of Thr668 (APP_{695} numbering) has been suggested to alter APP processing in favor of the amyloidogenic pathway (Lee *et al.*, 2003). This finding has been contested by Sano *et al.* who demonstrated that the substitution of Thr668 by alanine, which cannot be phosphorylated, has no effect of APP processing in transgenic mice (Sano *et al.*, 2006). Phosphorylation of Thr668 has also been suggested to be important for the binding of AICD to its interaction partner Fe65 and its subsequent translocation into the nucleus (Chang *et al.*, 2006); conversely, Ando et al. reported that phosphorylation of the same residue prevents AICD and Fe65 interaction (Ando *et al.*, 2001).

The non-amyloidogenic pathway

In the non-amyloidogenic pathway, APP is sequentially cleaved by α- and γ-secretases. Analogous to β-cleavage, α-cleavage results in the release of an N-terminal fragment termed sAPPα. The membrane-bound C-terminal stub, CTFα or C83, is further processed by γ-secretase releasing the small, non-amyloidogenic p3 fragment (3 kDa) and the AICD. The biological role of p3 is not yet known, but sAPPα has been suggested to be neuroprotective and to display trophic properties (Thornton *et al.*, 2006; Brunholz *et al.*, 2012).

α-secretase activity is displayed by various type I integral membrane proteins of the ADAM (a disintegrin and metalloprotease) family, including ADAM9, ADAM10, and ADAM17 (Buxbaum *et al.*, 1998; Koike *et al.*, 1999; Lammich *et al.*, 1999). To date it is still unclear which ADAM is most likely involved in AD and, in fact, ADAMs may be redundant as targeted disruption of different ADAMs has no effect on APP processing (Chow *et al.*, 2010; Haass *et al.*, 2012). Moreover, cells display constitutive as well as inducible α-secretase activity and different ADAMs have been suggested to be responsible for the two activities (Buxbaum *et al.*, 1998; Lammich *et al.*, 1999; Kuhn *et al.*, 2010). In neurons, ADAM10 appears to be the major constitutively active α-secretase (Kuhn *et al.*, 2010). ADAM10 proenzyme is enriched in the Golgi while the mature enzyme is localized mainly to the cell surface and in agreement with with this observation, the plasma membrane is the main site of α-cleavage (Sisodia *et al.*, 1992; Lammich *et al.*, 1999).

Since the α-cleavage site resides within the Aβ sequence (between Lys16 and Leu17), cleavage of APP by the α-secretase precludes Aβ generation (Esch *et al.*, 1990). It has been proposed that α- and β-secretase compete for APP substrate as modulation of one pathway reciprocally influences the other pathway. For example, Vassar *et al.* demonstrated that inhibition/overexpression of BACE1 results in increased/decreased α-cleavage of APP and Postina *et al.* showed that overexpression of ADAM10 reduces Aβ generation (Vassar *et al.*, 1999; Postina *et al.*, 2004). However, contradicting reports also exist showing no interrelation between these processing pathways (Dyrks *et al.*, 1994; Kuhn *et al.*, 2010).

1.3 O-GlcNAc and Alzheimer disease

Different lines of evidence suggest a potential role of protein O-GlcNAcylation in the pathogenesis of AD. O-GlcNAc and O-GlcNAc cycling enzymes OGT and OGA are highly expressed in the brain (Kreppel *et al.*, 1997; Heckel *et al.*, 1998; Cole and Hart, 2001; Gao *et al.*, 2001). O-GlcNAcylation is dependent on glucose flux through the HBP but glucose uptake is impaired in AD brain (Kalaria and Harik, 1989; Fukuyama *et al.*, 1994; Simpson *et al.*, 1994). Furthermore, key proteins implicated in AD pathogenesis, such as APP and tau are O-GlcNAcylated (Griffith *et al.*, 1995; Arnold *et al.*, 1996; Liu *et al.*, 2004).

Extensive studies have been performed to understand the role of tau O-GlcNAcylation and its implications in AD pathogenesis. While tau can be simultaneously modified by O-GlcNAc and O-phosphate, tau-enriched fractions from AD brains contain less O-GlcNAc when compared to control brains. Furthermore, abnormally phosphorylated tau isolated from AD brains is less O-GlcNAcylated than non-hyperphosphorylated tau (Robertson *et al.*, 2004; Liu *et al.*, 2004; 2009a). *In vitro* and *in vivo* studies demonstrated that modulation of global O-GlcNAcylation results in site-specific changes in tau phosphorylation and that increasing

O-GlcNAc levels reduces tau phosphorylation at some sites that are implicated in AD pathology (Liu *et al.*, 2004; 2009a; Yuzwa *et al.*, 2008). Furthermore, *in vivo* administration of a specific OGA inhibitor increased global and tau-specific O-GlcNAc modification and reduced the number of neurofibrillary tangles in the brains of tau transgenic mice (Yuzwa *et al.*, 2012). In agreement, site-specific O-GlcNAcylation of tau has been demonstrated to slow tau aggregation *in vitro* (Yuzwa *et al.*, 2012; 2014). In contrast, in a *C. elegans* model of neurodegeneration, increased O-GlcNAcylation had no effect on a severe tauopathy phenotype while decreased O-GlcNAcylation had positive effects (Wang *et al.*, 2012).

During the course of this work, other groups have also investigated the potential functions of APP´s O-GlcNAcylation and their results suggest that O-GlcNAcylation increases non-amyloidogenic processing of APP and/or reduces Aβ generation (Jacobsen and Iverfeldt, 2011; Kim *et al.*, 2013). However, in *C. elegans* expressing $A\beta_{(1-42)}$ in muscle, increased O-GlcNAcylation exacerbated Aβ toxicity and worsened the $A\beta_{(1-42)}$-induced paralysis phenotype (Wang *et al.*, 2012).

Taken together, these studies suggest an important role of O-GlcNAc in AD, yet the exact mechanisms by which (dysregulated) protein O-GlcNAcylation may contribute to the pathogenesis of AD remain to be elucidated.

1.4 Aim of this work

Since the discovery that APP and tau, which constitute the main components of AD´s most prominent pathological hallmarks, senile plaques and neurofibrillary tangles, are O-GlcNAcylated, many studies have suggested a role of O-GlcNAc in the pathogenesis of AD. However, the exact molecular mechanism(s) remain unclear. Contradicting data have been published on protein O-GlcNAcylation in AD, some studies demonstrating decreased O-GlcNAcylation in AD brain while others show unaltered or increased O-GlcNAc expression in AD. Furthermore, while the role of O-GlcNAcylation of tau has been investigated by different groups, the function of the O-GlcNAc modification of APP is not yet understood.

To gain a better understanding of the role of O-GlcNAcylation in the pathogenesis of AD, different aspects of AD pathology should be investigated in this work. In particular, potential effects of altered O-GlcNAc expression on the proteolytic processing of APP should be examined using APP overexpressing neuroblastoma cells. In addition, it was planned to improve a recently established *in vitro* OGT assay and to apply this assay to different proteins involved in AD pathology. A further aim was to analyze changes in O-GlcNAc and O-GlcNAc cycling enzymes in the brains of subjects with AD and age-matched controls.

2 Material

Experiments were performed in the laboratories of Prof. emer. Dr. B. Schmitz, Institute of Animal Sciences, Department Biochemistry, University of Bonn, Bonn (DE) and Prof. Dr. D. A. Butterfield, Department of Chemistry, University of Kentucky, Lexington, KY (US), therefore, sources of chemicals, buffer compositions, and methods may differ slightly.

2.1 Chemicals

Table 2: Chemicals

Chemical	Source
1,2-Dideoxy-2´-propyl-α-D-glucopyranoso-[2,1-D]-Δ2´-thiazoline (NButGT)	Kindly provided by D. J. Vocadlo, Simon Fraser University, Burnaby, BC (CA) (Macauley *et al.*, 2005)
10x Tris/Glycine/SDS (TGS) running buffer	Bio-Rad, Hercules, CA (US)
2,2´-Azino-bis-(3-ethylbenzothiazoline-6-sulfonic acid) (ABTS)	Sigma, Taufkirchen (DE)
2-Mercaptoethanol	Merck, Darmstadt (DE) Sigma-Aldrich, St. Louis, MO (US)
3-[(3-Cholamidopropyl)dimethylammonio]-1-propanesulfonate (CHAPS)	Merck, Darmstadt (DE) Sigma-Aldrich, St. Lious, MO (US)
5-Bromo-4-chloro-3-indolyl phosphate, p-toluidine salt (BCIP)	Thermo Fisher Scientific, Rockford, IL (US)
Acetic acid, 96%	Merck, Darmstadt (DE) Sigma-Aldrich, St. Loius, MO (US)
Acetonitrile (ACN)	Riedel-de Haen, Seelze (DE)
Acrylamide	Merck, Darmstadt (DE)
Adenosine 5´-monophosphate (5´-AMP)	Sigma-Aldrich, Steinheim (DE)
Agar	Difco, Detroit, MI (US)
Agarose	Roche, Grenzach-Whylen (DE)
Agarose for IEF	GE Healthcare, Uppsala (SE)
Alloxan	Sigma-Aldrich, Steinheim (DE)
Ammonium bicarbonat (NH_4HCO_3)	Merck, Darmstadt (DE)
Ammonium persulfate (APS)	Merck, Darmstadt (DE)
Ampicillin	Sigma, Taufkirchen (DE)
Aprotinin, from bovine lung	Sigma-Aldrich, Steinheim (DE)/St. Louis, MO (US)
Benzonase nuclease (25 U/ml)	Novagen, Darmstadt (DE)
Boric acid	Merck, Darmstadt (DE)
Bovine serum albumin (BSA)	Sigma-Aldrich, Steinheim (DE)/St. Louis, MO (US)
Bromophenol Blue	Merck, Darmstadt (DE) Sigma-Aldrich, St. Louis, MO (US)

Chemical	Source
Calcium chloride ($CaCl_2$)	Merck, Darmstadt (DE) Sigma-Aldrich, St. Louis, MO (US)
Chloroform	Merck, Darmstadt (DE)
Concanavalin A from *Canavalia ensiformis*, agaorose conjugate, Type VI, (ConA)	Sigma-Aldrich, St. Louis, MO (US)
Coomassie Brilliant Blue R-250	Serva, Heidelberg (DE)
D-Glucose	Sigma-Aldrich, Steinheim (DE)
Dimethyl sulfoxide (DMSO)	AppliChem, Darmstadt (DE)
Direct Blue 71	Sigma-Aldrich, Steinheim (DE)
Dithiothreitol (DTT)	Roth, Karlsruhe (DE)
Dulbecco´s Modified Eagle Medium high glucose (4.5 g/L) (DMEM-HG)	Invitrogen, Karlsruhe (DE)
Dulbecco´s Modified Eagle Medium low glucose (1 g/L) (DMEM-LG)	Invitrogen, Karlsruhe (DE)
Ethanol	Merck, Darmstadt (DE) Sigma-Aldrich, St. Louis, MO (US)
Ethidium bromide	Sigma-Aldrich, Steinheim (DE)
Ethylene glycol-bis(2-aminoethylether)-*N,N,N´,N´*-tetraacetic acid (EGTA)	Sigma-Aldrich, St. Louis, MO (US)
Ethylenediaminetetraacetic acid (EDTA)	Merck, Darmstadt (DE) Sigma-Aldrich, St. Louis, MO (US)
Fetal calf serum (FCS)	PAN Biotech, Aidenbach (DE)
GBX Developer	Kodak, Rochester (US)
GBX Fixer	Kodak, Rochester (US)
Glycerol	Roth, Karlsruhe (DE) Sigma-Aldrich, St. Louis, MO (US)
Glycine	Sigma-Aldrich, Steinheim (DE)/St. Louis, MO (US)
Hydrochloric acid (HCl)	KMF OptiChem, Lohmar (DE) Sigma-Aldrich, St. Louis, MO (US)
Hydrogen peroxide, 35% (H_2O_2)	Merck, Darmstadt (DE)
Imidazole	Sigma-Aldrich, Steinheim (DE)
Iodoacetamide	Merck, Hamburg (DE))
Isopropanol	KMF OptiChem, Lohmar (DE)
Isopropyl-β-D-thiogalactopyranoside (IPTG)	Biomol, Hamburg (DE)
Kanamycin	Sigma-Aldrich, Steinheim (DE)
Leupeptin	Sigma-Aldrich, Steinheim (DE)/St. Louis, MO (US)
L-Glutamine, 100x (200 mM)	Sigma, Taufkirchen (DE)
Lysozyme	Novagen, Darmstadt (DE)
Magnesium chloride ($MgCl_2$)	Merck, Darmstadt (DE) Sigma-Aldrich, St. Louis, MO (US)
Manganese (II) chloride ($MnCl_2$)	Sigma-Aldrich, St. Louis, MO (US)

Chemical	Source
Methanol	Merck, Darmstadt (DE)
Mineral oil	Sigma-Aldrich, Steinheim (DE)
N-(2-Hydroxyethyl)piperazine-N´-(2-ethane-sulfonic acid) (HEPES) solution, 1M, pH 7-7.6	Sigma-Aldrich, St. Louis, MO (US)
N,N,N´,N´-Tetramethylethylenediamine (TEMED)	Merck, Darmstadt (DE)
N-Acetyl-β-D-galactosamine	Sigma-Aldrich, St. Louis, MO (US)
N-Acetyl-β-D-glucosamine (GlcNAc)	Sigma-Aldrich, Steinheim (DE)/St. Louis, MO (US)
Neurobasal medium	Life Technologies, Darmstadt (DE)
Nickel-nitrolotriacetid acid (Ni-NTA) agarose	Qiagen, Hilden (DE)
Nitro blue tetrazolium (NBT)	Thermo Fisher Scientific, Rockford, IL (US)
N-N-Dimethylformamide (DMF)	Sigma-Aldrich, St. Louis, MO (US)
Octyl-β-D-glucopyranoside	Sigma-Aldrich, Steinheim (DE)
Penicillin-Streptomycin (P/S), 100x (10,000 I.U. Pen; 10,000 µg/ml Strep)	PAA, Cölbe (DE)
Pepstatin A	Sigma-Aldrich, Steinheim (DE)/St. Louis, MO (US)
Pharmalyte 3-10	GE Healthcare, Uppsala (SE)
Phenol Red	Merck, Darmstadt (DE)
Phenylmethanesulfonyl fluoride (PMSF)	Roth, Karlsruhe (DE) Sigma-Aldrich, St. Louis, MO (US)
Phorbol 12-myristate 13-acetate (PMA)	Calbiochem, Darmstadt (DE)
p-Nitrophenyl N-acetyl-β-D-glucosaminide (pNP-GlcNAc)	Sigma-Aldrich, St. Louis, MO (US)
Polyvinylpyrrolidone (PVP)	Sigma-Aldrich, Steinheim (DE)
Ponceau S	Sigma-Aldrich, Steinheim (DE)/St. Louis, MO (US)
Potassium chloride (KCl)	Merck, Darmstadt (DE)
Potassium phosphate monobasic (KH_2PO_4)	Merck, Darmstadt (DE)
Protease Inhibitor Cocktail	Sigma-Aldrich, Steinheim (DE)
Protein G Sepharose 4 Fast Flow	GE Healthcare, Uppsala (SE)
ReBlot Plus Strong Antibody Stripping Solution, 10x	EMD Millipore, Temecula, CA (US)
RIPA buffer	c-c-pro, Oberdorla (DE)
Rotiphorese Gel 40	Roth, Karlsruhe (DE)
Sodium acetate	Sigma, Taufkirchen (DE)
Sodium cacodylate trihydrate	Sigma-Aldrich, St. Louis, MO (US)
Sodium carbonate (Na_2CO_3)	Sigma-Aldrich, St. Louis, MO (US)
Sodium chloride (NaCl)	Merck, Darmstadt (DE) Sigma-Aldrich, St. Louis, MO (US)
Sodium dodecyl sulfate (SDS)	Roth, Karlsruhe (DE) Sigma-Aldrich, St. Louis, MO (US)

Chemical	Source
Sodium fluoride (NaF)	Sigma, Taufkirchen (DE)
Sodium hydroxide (NaOH)	T.J. Baker, Deventer (NL)
Sodium phosphate dibasic (Na_2HPO_4)	Merck, Darmstadt (DE) Sigma-Aldrich, St. Louis, MO (US)
Sodium phosphate monobasic (NaH_2PO_4)	Merck, Darmstadt (DE) Sigma-Aldrich, St. Louis, MO (US)
Sucrose	Sigma-Aldrich, Steinheim (DE)/St. Louis, MO (US)
Thiourea	Amersham Biosciences, Buckinghamshire (GB)
Trifluoroacetic acid (TFA)	Merck, Darmstadt (DE)
Tris(hydroxymethyl)aminomethane (Tris)	Merck, Darmstadt (DE) Bio-Rad, Hercules, CA (US)
Triton X-100	Serva, Heidelberg (DE)
Tryptone	Difco, Detroit, MI (US)
Tween 20	Sigma-Aldrich, Steinheim (DE)/St. Louis, MO (US)
Urea	Merck, Darmstadt (DE)
Uridine 5´diphosphate-N-acetylglucosamine (UDP-GlcNAc)	Sigma-Aldrich, Steinheim (DE)
Yeast Extract	Difco, Detroit, MI (US)
α-Cyano-4-hydroxy cinnamic acid (α-CHCA)	Sigma-Aldrich, Steinheim (DE)

2.2 Equipment

Table 3: Equipment

Equipment	Source
550 Sonic Dismembrator	Fisher Scientific, Rockford, IL (US)
ChemiDoc MP Imaging System	Bio-Rad, Hercules, CA (US)
Column XK 16	Pharmacia Biotech, Uppsala (SE)
Criterion Cell	Bio-Rad, Hercules, CA (US)
Dounce Tissue Grinder, 1 ml	Wheaton, Millville, NJ (US)
ELISA Reader Titertek PLUS MS2	ICN Biomedicals, Meckenheim (DE)
EPSON PERFECTION 4990 PHOTO Scanner	Epson, Suwa (JP)
Ettan IPGphor3	GE Healthcare, Freiburg (DE)
Glass homogenizer 863	Braun, Melsungen (DE)
Mini-PROTEAN 3 Cell	Bio-Rad, Hercules, CA (US)
Mini-Sub Cell GT Cell	Bio-Rad, Hercules, CA (US)
Multigel-Long System	Biometra, Göttingen (DE)
Peristaltic pump P-1	Pharmacia Biotech, Uppsala (SE)
Sonifier 250	Branson Ultrasonics, Danbury, CT (US)
Spectrophotometer Smart Spec Plus	Bio-Rad, Hercules, CA (US)

Equipment	Source
Speed Vac, Type SC110-240	Savant Instruments, Framingdale, NY (US)
Trans-Blot Semi Dry Transfer Cell	Bio-Rad, Hercules, CA (US)
Trans-Blot Turbo Blotting System	Bio-Rad, Hercules, CA (US)
Transilluminator UVsolo	Biometra, Göttingen (DE)

2.3 Software and databases

Table 4: Software and databases

Software and Databases	Source
ExPASy	Swiss Institute of Bioinformatics; www.expasy.org (Artimo *et al.*, 2012)
GraphPad Prism 5	GraphPad Software, San Diego, CA (US)
Image J 1.45s	National Institute of Health, Bethesda, MD (US)
Image Lab	Bio-Rad, Hercules, CA (US)
UniProt	The UniProt Consortium; www.uniprot.org (The UniProt Consortium, 2014)
YinOYang 1.2 Server	Center for Biological Sequence Analysis, Technical University of Denmark, Lyngby (DK); www.cbs.dtu.dk/services/YinOYang/ (Gupta and Brunak, 2002)

2.4 Working material

Table 5: Working material

Working material	Source
Amicon Ultra-15 Centrifigal Filter Devices	Merck Millipore, Cork (IE)
Cell and tissue culture flasks (75 cm^2)	Sarstedt, Nümbrecht (DE)
Cell scraper	Orange scientific, Braine-l´Alleud (BE)
Criterion TGX Precast gels	Bio-Rad, Hercules, CA (US)
Cryotubes	Nalge Nunc International, Rochester, NY (US)
Spectra/Por Dialysis Membrane, MWCO 3000	Roth, Karlsruhe (DE)
Express Capture Nickel Ccoated Plates	Express Biotech, Thurmont, MD (US)
Extra Thick Blot paper	Bio-Rad, Hercules, CA (US)
Filter paper 3 mm	Whatman, Dassel (DE)
IPG reswelling trays	GE Healthcare, Uppsala (SE)
Microtiter plates	Greiner, Nürtingen (DE)
Nitrocellulose membrane (0.2 µm)	Bio-Rad, Hercules, CA (US)
Nitrocellulose membrane Hybond ECL (0.3 µm)	GE Healthcare, Uppsala (SE)
Nunc CovaLink microtiter plates	Thermo Scientific, Karlsruhe (DE)

Working material	Source
Petri dishes	Corning, New York, NY (US)
Pipet Tips (various volumes)	Sarstedt, Nümbrecht (DE) Rainin, Oakland, CA (US)
Serological pipettes (various volumes)	Sarstedt, Nümbrecht (DE)
Tubes (various volumes)	Sarstedt, Nümbrecht (DE) Fisher Scientific, Rockford, IL (US)
Ultrafree-0.5 Centrifugal Filter Device	Millipore, Temecula, CA (US)
Vivaspin 6 (PES membrane: 30,000 MWCO)	Sartorius, Göttingen (DE)
X-Ray film CL-XPosure	Thermo Fisher Scientific, Rockford, IL (US)
Zeba Desalt Spin Columns	Pierce Biotechnology, Rockford, IL (US)

2.5 Kits and standards

Table 6: Kits and standards

Kit / Standard	Source
Clarity Western ECL Substrate	Bio-Rad, Hercules, CA (US)
DNA Clean and Concentrator 5	Zymo Research, Freiburg (DE)
GeneJET Plasmid Miniprep Kit	Fermentas, St. Leon-Rot (DE)
GeneRuler DNA Ladder Mix	Fermentas, St. Leon-Rot (DE)
Loading Dye Solution, 6x	Fermentas, St. Leon-Rot (DE)
Page Ruler Unstained Protein Ladder	Fermentas, St. Leon-Rot (DE)
PCR clean up kit	Seqlab, Göttingen (DE)
Pierce 660 nm Protein Assay Reagent	Thermo Fisher Scientific, Rockford, IL (US)
Pierce Bicinchoninic Acid Protein Assay Kit	Thermo Fisher Scientific, Rockford, IL (US)
Plasmid Midi Kit	Qiagen, Hilden (DE)
Precision plus protein all blue standards	Bio-Rad, Hercules, CA (US)
QIAquick Gel Extraction Kit	Qiagen, Hilden (DE)
SeeBlue Plus2 Prestained Standard	Invitrogen, Karlsruhe (DE)
SuperSignal West Dura Chemiluminescent Substrate	Thermo Fisher Scientific, Rockford, IL (US)
SuperSignal West Pico Chemiluminescent Substrate	Thermo Fisher Scientific, Rockford, IL (US)

2.6 Peptides

Table 7: Peptides

Peptide	Sequence / Molecular weight	Source
$A\beta_{(12-28)}$	VHHQKLVFFAEDVGSNK / 1955.2 Da	Bachem, Weil am Rhein (DE)
$A\beta_{(1-40)}$	DAEFRHDSGY EVHHQKLVFF AEDVGSNKGA IIGLMVGGVV / 4329.8 Da	Bachem, Weil am Rhein (DE)

Peptide	Sequence / Molecular weight	Source
cAPP1	KQYTSIHK / 1004.16 Da	Biomatik, Cambridge, ON (CA)
cAPP2	KVTPEERK / 986.14 Da	Biomatik, Cambridge, ON (CA)
cAPP3	RHLSKMQ / 899.09 Da	Biomatik, Cambridge, ON (CA)
cAPP4	ENPTYKFK / 1026.17 Da	Biomatik, Cambridge, ON (CA)
Cdk5 1 (J-1)	VFKAKNRETHEIG / 1528.74 Da	Biomatik, Cambridge, ON (CA)
Cdk5 2 (J-2)	EGVPSSALREICL / 1373.59 Da	Biomatik, Cambridge, ON (CA)
Cdk5 3 (J-3)	PYPMYPATTSLVN / 1453.69 Da	Biomatik, Cambridge, ON (CA)

2.7 Antibodies

Table 8: Primary antibodies

Primary antibodies	Characteristics	Source / Reference
4G8	Monoclonal mouse antibody, IgG Antigen: human Aβ, amino acids 17-24 Concentration: 1mg/ml	Covance, Emeryville, CA (US)
8E5	Monoclonal mouse antibody, IgG Antigen: human APP, amino acids 444-592 Concentration: 5.2 mg/ml	Elan Corporation plc, Dublin (IE)
AL28	Polyclonal rabbit antibody, IgG (serum) Antigen: C-terminus of OGT	kindly provided by S. Arnold, Johns Hopkins University, Baltimore, MD (US); Kreppel *et al.*, 1997
anti-actin	Polyclonal rabbit antibody, IgG Antigen: C-terminal actin fragment	Sigma-Aldrich, St. Louis, MO (US)
anti-GAPDH	Monoclonal mouse antibody, IgG Antigen: glyceraldehyde-3-phosphate dehydrogenase (GAPDH) Concentration: 1 mg/ml	Sigma-Aldrich, St. Louis, MO (US)
anti-GST	Monoclonal mouse antibody, IgG Antigen: Glutathione S-transferease (GST) from *Schistosoma japonicum* Concentration: 1 mg/ml	Novagen, Darmstadt (DE)
anti-His	Monoclonal mouse antibody, IgG Antigen: tetra histidine (His) Concentration: 0.2 µg/ml:	Qiagen, Hilden (DE)
anti-OGA	Polyclonal rabbit antibody, IgG Antigen: full length recombinant OGA	kindly provided by G. Crawford, Mercer University, Macon, GA (US) (Crawford *et al.*, 2008)
anti-OGT	Polyclonal rabbit antibody, IgG (serum) Antigen: full length recombinant OGT	kindly provided by G. Crawford, Mercer University, Macon, GA (US) (Crawford *et al.*, 2008)

Primary antibodies	Characteristics	Source / Reference
anti-sAPPβ	Polyclonal rabbit antibody, IgG Antigen: human sAPPβ-Wild Type Concentration: 0.2 mg/ml	Antibodies-online, Aachen (DE)
anti-β-actin	Monoclonal mouse antibody, IgG Antigen: N-terminal fragment of β-actin Concentration: 2 mg/ml	Sigma-Aldrich, St. Louis, MO (US)
C-8	Polyclonal rabbit antibody, IgG Antigen: C-terminus of human cyclin-dependent kinase 5 (cdk5) Concentration: 0.2 mg/ml	Santa Cruz Biotechnology, Heidelberg (DE)
CTD110.6	Monoclonal mouse antibody, IgM Antigen: O-GlcNAc-modified C-terminal domain of RNA-Polymerase II Concentration: 2 mg/ml	Sigma-Aldrich, Steinheim (DE)/St. Louis, MO (US) and kindly provided by G. W. Hart, Johns Hopkins University, Baltimore, MD (US)
D-20	Polyclonal goat antibody, IgG Antigen: C-terminus of nucleoporin 62 (Nup62) from *Rattus norwegicus* Concentration: 0.2 mg/ml	Santa Cruz Biotechnology, Heidelberg (DE)
JLA-20	Monoclonal mouse antibody, IgM Antigen: Actin	DSHB, Iowa City, IA (US)
RL2	Monoclonal mouse antibody, IgG Antigen: nuclear envelope proteins; detects O-GlcNAc Concentration: 2 mg/ml	Affinity Bioreagents, Golden, CO (US)
W0-2	Monoclonal mouse antibody, IgG Antigen: human Aβ, amino acids 5-8	Merck Millipore, Darmstadt (DE)

Table 9: Secondary antibodies

Secondary antibodies	Characteristics	Source / Reference
anti-goat-POD	Peroxidase (POD)-conjugated polyclonal donkey antibody against goat IgG	Dianova, Hamburg (DE)
anti-mouse-Cy5	Enhanced Chemiluminescence (ECL) Plex CyDye (Cy)5-conjugated goat antibody against mouse IgG	GE Healthcare, Pittsburgh, PA (US)
anti-mouse-POD	POD-conjugated polyclonal goat antibody against mouse IgG and IgM	Dianova, Hamburg (DE) Millipore, Temecula, CA (US)
anti-rabbit-AP	Alkaline Phosphatase (AP)-conjugated polyclonal goat antibody against rabbit IgG	Bio-Rad, Herkules, CA (US)
anti-rabbit-Cy5	ECL PLex Cy5-conjugated goat antibody against rabbit IgG	GE Healthcare, Pittsburgh, PA (US)
anti-rabbit-POD	POD-conjugated polyclonal goat antibody against rabbit IgG	Dianova, Hamburg (DE)

Secondary antibodies	Characteristics	Source / Reference
ECL anti-rabbit-POD	ECL POD-conjugated polyclonal goat antibody against rabbit IgG	GE Healthcare, Pittsburgh, PA (US)

2.8 Enzymes for molecular biology

For restriction analysis, restriction enzymes *Bam*HI and *Xho*I and their respective 10x buffers were used. Ligation was performed with T4 DNA ligase and 10x ligase buffer. All enzymes and buffers for molecular biology were from Fermentas, St. Leon-Rot (DE).

2.9 Plasmids

pBJG1-ncOGT

pBJG1 is a modified pET24b vector, its generation as well as generation of pBJG1-ncOGT containing the cDNA of human ncOGT has been described (Gross *et al.*, 2005). Plasmid was kindly provided by S. Walker, Harvard Medical School, Boston, MT (US). pBJG1 plasmid allows for the expression of recombinant proteins with a C-terminal His_8-tag.

pBJG1-hNCAM180cyt

The generation of pBJG1-hNCAM180cyt in our lab has been described (Wobst *et al.*, 2012).

pBJG1-Nup62

The generation of pBJG1-Nup62 plasmid is described in this work. Briefly, cDNA of Nup62 from *Rattus norwegicus* lacking its stop codon was cloned into pBJG1 vector using *Bam*HI and *Xho*I restriction enzymes. Plasmid map is provided in Appendix A.

pGex-2TK-Cdk5

The generation of pGex-2TK-Cdk5 has been described (Sharma *et al.*, 1999a). Plasmid was kindly provided by H. C. Pant, National Institute of Health, Bethesda, MD (US). pGex plasmid contains a gene encoding for GST from *Schistosoma japonicum* allowing for the expression of N-terminal GST fusion proteins.

pGex-4T-1-CK2α

The generation of pGex-4T-1-CK2α has been described (Kim *et al.*, 2006). Plasmid was kindly provided by Y. G. Yu, Kookmin University, Seoul (KR).

2.10 Biological material

Bacterial strains

Two different strains of *Escherichia coli* (*E. coli*) were used. Molecular biology methods were performed in *E. coli* XL1-Blue (Bullock *et al.*, 1987); strain was kindly provided by K. H. Scheidtmann, University of Bonn. Protein expression was performed in *E. coli* BL21 (DE3) (Studier and Moffatt, 1986).

Cell line

Human neuroblastoma SH-SY5Y cells were stably transfected with the cDNA of human APP_{695} to obtain SH-SY5Y-APP_{695} cells (Parkin *et al.*, 2007). Cell line was kindly provided by E. T. Parkin, School of Health and Medicine, Lancaster University, Lancaster (UK).

Human brain samples

Frozen inferior parietal lobule (IPL) and cerebellar samples were obtained from the Sanders-Brown Center on Aging, University of Kentucky, Lexington, KY (US). Biodata was kindly provided by T. P. Shannon and E. Abner, University of Kentucky. Clinical and pathological information on samples used in this work are listed in Appendix B.

2.11 Solutions

All buffers and solutions are prepared with deionized (DI) water unless indicated otherwise.

2.11.1 Commonly used solutions

Phosphate bufferes saline (PBS) 10x

1.5 M	NaCl
80 mM	Na_2HPO_4
17 mM	NaH_2PO_4

PBST

0.1 % (v/v) Tween 20
in PBS 1x

Aprotinin

10 mg/ml	Aprotinin
in PBS 1x	

Pepstatin A

1 mg/ml Pepstatin A
in acetic acid:methanol (1:10)

Leupeptin

10 mg/ml	Leupeptin

PMSF

100 mM PMSF
in ethanol

2.11.2 Cell culture media and other solutions for cell culture

Cell culture medium
10 % (v/v) FCS
0.5 % (v/v) P/S
in DMEM-HG

Media for cell treatments
1 % (v/v) L-Glutamine
in neurobasal medium

Hank´s Balanced Salt Solution (HBSS$^-$) 10x
54 mM KCl
4.4 mM KH_2PO_4
1.37 M NaCl
4.23 mM Na_2HPO_4
55.5 mM D-Glucose
0.3 mM Phenol Red
pH 7.2-7.4, sterile filtered

NButGT stock solution
0.88 mM NBuGT
in DMEM-LG; sterile filtered

Alloxan stock solution
500 mM Alloxan
in neurobasal medium; sterile filtered

EDTA/HBSS$^-$
5 mM EDTA
in 1x HBSS$^-$; sterile filtered

PMA stock solution
10 µM PMA
in DMSO; sterile filtered

2.11.3 Solutions for bacterial culture

LB medium
10 g/l NaCl
10 g/l Tryptone
5 g/l Yeast extract
pH 7.0; autoclaved

Ampicillin stock solution
50 mg/ml Ampicillin
sterile-filtered

LB agar
15 g/l Agar
in LB medium; autoclaved

Kanamycin stock solution
30 mg/ml Kanamycin
sterile filtered

2.11.4 Solutions for molecular biology

TBE buffer 10x
1 M Tris
0.83 M Boric acid
10 mM EDTA

TE buffer
10 mM Tris
1 mM EDTA
pH 8.0; sterile filtered

2.11.5 Solutions for protein biochemistry

2.11.5.1 Solutions for the expression and analysis of recombinant proteins

PBS-L

1 mM	DTT
1 mM	EDTA
1 mg/ml	Lysozyme
25 U/ml	Benzonase nuclease

in PBS 1x

PBS-Triton

1 % (v/v)	Triton X-100

in PBS 1x

PBS equilibration buffer

1 mM	EDTA
1 mM	DTT

in PBS 1x

Urea lysis buffer

8 M	Urea
100 mM	NaH_2PO_4
10 mM	Tris HCl, pH 8.0
1:1000	Aprotinin
1:1000	Leupeptin
1:100	Pepstatin A
1:100	PMSF

protease inhibitors added freshly

Urea equilibration buffer

8 M	Urea
100 mM	NaH_2PO_4
10 mM	Tris HCl, pH 8.0

2.11.5.2 Solutions for the preparation of cell culture lysates and human brain samples

RIPA lysis buffer

0.1 M	GlcNAc
1:100	PMSF

in RIPA buffer

protease inhibitor is added freshly

2D lysis buffer

6 M	Urea
2 M	Thiourea
4 % (w/v)	CHAPS
1 % (w/v)	DTT
1 % (v/v)	Pharmalyte 3-10
1 % (v/v)	Protease Inhibitor Cocktail

in 0.1 M GlcNAc

Isolation buffer

0.32 M	Sucrose
20 mM	HEPES
2 mM	EDTA
2 mM	EGTA
0.1 M	GlcNAc

pH 7.4

4 µg/ml	Leupeptin
4 µg/ml	Pepstatin A
5 µg/ml	Aprotinin
0.2 mM	PMSF

protease inhibitors added freshly

2.11.5.3 Solutions for determination of protein concentrations

BSA for Pierce 660 nm Protein assay

50 mg/ml	BSA

BSA for Bicinchoninic Acid Protein assay

2 mg/ml	BSA

2.11.5.4 Solutions for immunoprecipitation (IP)

Sodium phosphate buffer
10 mM NaH_2PO_4 is added to 10 mM Na_2HPO_4 until buffer reaches pH 7.2

$A\beta_{12-28}$ stock solution

50 µM	$A\beta_{12-28}$

in IP wash buffer

RIPA wash buffer

1 M	NaCl
10 mM	EDTA
40 mM	NaF
0.2 % (v/v)	Triton X-100

in sodium phosphate buffer, pH 7.0-7.2

IP wash buffer

10 mM	Tris HCl, pH 8.0
150 mM	NaCl
0.1 % (v/v)	Triton X-100

2.11.5.5 Solutions for electrophoretic separation of proteins using polyacrylamide gels

Solutions for SDS polyacrylamide gel electrophoresis (SDS-PAGE)

4x sample buffer

0.25 M	Tris HCl, pH 6.8
40 % (v/v)	Glycerol
20 % (v/v)	2-Mercaptoethanol
12 % (w/v)	SDS
0.25 % (w/v)	Bromophenol Blue

4x sample buffer for human brain samples

0.2 M	Tris HCl, pH 6.8
40 % (v/v)	Glycerol
20 %(v/v)	2-Mercaptoethanol
8 % (w/v)	SDS
0.01 % (w/v)	Bromophenol Blue

Acrylamide solution

75 %	Rotiphorese Gel 40

Running buffer 10x

0.25 M	Tris
1.918 M	Glycine
35 mM	SDS

Separation gel buffer

1 M	Tris HCl, pH 8.8

Stacking gel buffer

1 M	Tris HCl, pH 6.8

Buffers and solutions for two-dimensional SDS-PAGE (2D SDS-PAGE)

Rehydration solution

7 M	Urea
2 M	Thiourea
2 % (w/v)	CHAPS
0.5 % (v/v)	Pharmalyte 3-10
20 mM	DTT
0.01 % (w/v)	Bromophenol Blue

in 0.1 M GlcNAc

Sample preparation solution for cup loading

7 M	Urea
2 M	Thiourea
4 % (w/v)	CHAPS
2 %	Pharmalyte 3-10 (v/v)
40 mM	DTT

in 0.1 M GlcNAc

4x Separation gel buffer

1.5 M	Tris HCl, pH 8.8
0.04 % (w/v)	SDS

4x Stacking gel buffer

0.5 M	Tris HCl, pH 6.8
0.04 % (w/v)	SDS

Equilibration solution

6 M	Urea
0.1 mM	EDTA
50 mM	Tris HCl, pH 6.8
30 % (v/v)	Glycerol
6 % (w/v)	SDS
0.01 % (w/v)	Bromophenol Blue

Overlay agarose

0.5 % (w/v) Agarose for IEF
in 1x running buffer

2.11.5.6 Solutions for staining of proteins in gels

Destaining/fixing solution

10 % (v/v)	Acetic acid
30 % (v/v)	Ethanol

Coomassie staining solution

2 g Coomassie Brilliant Blue R-250
in 1 L destaining/fixing solution

2.11.5.7 Solutions for Western blot and immunodetection of proteins

Transfer buffer

39 mM	Glycine
48 mM	Tris
0.0375 % (w/v)	SDS
20 % (v/v)	Ethanol

Transfer buffer for human brain samples

192 mM	Glycine
30 mM	Tris
20 % (v/v)	Methanol

AP buffer

0.1 M	Tris
0.1 M	NaCl
5 mM	$MgCl_2$
pH 9.5	

AP developer solution

66 µl NBT solution
33 µl BCIP solution
in 10 ml AP buffer

NBT solution

30 mg	NBT
70 %(v/v)	DMF
in 1 ml	

Stripping solution

0.2 M	Glycine
0.5 M	NaCl
pH 2.8	

BCIP solution

50 mg	BCIP
in 1 mL	DMF

Chemiluminescence solution

Luminol/Enhancer reagent
and Peroxide reagent (1:1)

Wash buffer

150 mM	NaCl
3 mM	NaH_2PO_4
17 mM	Na_2HPO_4
0.04 % (v/v)	Tween 20

2.11.5.8 Solutions for staining of proteins on membranes

Direct Blue stock solution

0.1 % (w/v)	Direct Blue 71

Direct Blue staining solution

8 % (v/v)	Direct Blue stock solution
40 % (v/v)	Ethanol
10 % (v/v)	Acetic acid

Ponceau S staining solution

0.3 % (w/v)	Ponceau S
10 % (v/v)	Acetic acid

2.11.5.9 Solutions for OGT assays

OGT buffer (2x)

50 mM	Tris
2 mM	DTT
25 mM	$MgCl_2$
pH 7.4	

BSA solution

1 mg/mL	BSA

UDP-GlcNAc solution

100 mM	UDP-GlcNAc
in 25 mM	5´-AMP

Developer

0.05 M	NaH_2PO_4
0.1 M	Sodium acetate
pH 4.2 (with glacial acetic acid)	

ABTS solution

9.5 ml	Developer
0.5 ml	2 % (w/v) ABTS
10 µl	H_2O_2 (added freshly)

2.11.5.10 Solutions for OGA activity assay

ConA wash solution

1 M	NaCl
5 mM	$MgCl_2$
5 mM	$MnCl_2$
5 mM	$CaCl_2$

ConA equilibration solution

5 mM	$MnCl_2$
5 mM	$CaCl_2$
in isolation buffer without EDTA, EGTA, and GlcNAc	

OGA buffer (10x)

500 mM	Sodium cacodylate, pH 6.4
500 mM	N-acetylgalactosamine
3 %	BSA (w/v)

3 Methods

3.1 Cell culture

All cell culture experiments are performed in SY5Y-APP cells.

3.1.1 Cultivation of cells

Cell cultures are maintained at 37°C in a humidified atmosphere of 5 % CO_2 and 95 % air. Cells are grown in culture flasks and medium is changed every two to three days. Upon reaching 80 % to 90 % confluence, cells are split into subcultures. Therefore, cell culture medium is removed and cells are rinsed with 10 ml $HBSS^-$. Cells are detached from the bottom of the flask by the addition of 1 ml 5 mM EDTA/$HBSS^-$ and gentle tapping on the side of the flask. Detached cells are suspended in 10 ml cell culture medium, transferred into a 15 ml tube and centrifuged for 7 minutes at 170 x g at room temperature. Supernatant is discarded; cells are resuspended in 1 ml fresh cell culture medium and diluted into flasks containing fresh cell culture medium.

3.1.2 Freezing and thawing of cells

Cells are removed from flasks as described above. After centrifugation, cell pellet is resuspended in 900 µl cell culture medium and transferred into a cryotube. 100 µl DMSO are added and intermixed gently. Cells are stored at -80°C or in liquid nitrogen.

Cells are thawed by adding cell culture medium directly into the cryotube and transferring the resulting suspension into a 15 ml tube containing 9 ml cell culture medium. After centrifugation at 170 x g for 7 minutes at room temperature, supernatant is discarded. Cells are resuspended in 1 ml cell culture medium and transferred into flasks containing fresh cell culture medium. Medium is changed after 24 hours.

3.1.3 Treatment of cells

For different treatments, cells are grown to 80 % confluence. Cell culture medium is removed and cells are rinsed with $HBSS^-$. All treatments are performed for 24 hours in fresh neurobasal medium supplemented with 1 % L-glutamine. Treatments of cells include 30 µM NButGT, 5 mM Alloxan, and 80 nM PMA as well as controls treated with equal volumes of the appropriate vehicle.

3.2 Bacterial culture

3.2.1 Cultivation of *E. coli*

Using a sterilized inoculating loop, *E. coli* bacteria are streaked onto an agar plate containing the respective antibiotic. Plates are incubated for 16 hours at 37°C and then stored at 4°C. For overnight cultures, a single clone is picked from the agar plate and incubated in 5 ml bacterial medium containing the proper antibiotic at 220 rpm for 16 hours at 37°C. Larger cultures are prepared by 1:50 dilution of overnight cultures into fresh culture medium and incubation at 220 rpm at 37°C until the appropriate cell density is reached. Untransformed bacteria are cultivated without antibiotics; for bacteria containing pGex plasmids, 50 µg/ml ampicillin is added to LB medium; for bacteria containing pBJG1 plasmids, 30 µg/ml kanamycin is added.

3.2.2 Heat shock transformation

50 µl competent bacteria are mixed with 50-100 ng plasmid DNA or the entire ligation preparation (see 3.3.5) and incubated on ice for 15-30 minutes. Heat shock is performed by placing the tubes into a water bath (42°C) for 1 minute prior to cooling of the tubes on ice for 2 minutes. 450 µl LB medium are added and bacteria are grown for 30-60 minutes at 220 rpm and 37°C. Afterwards, 50-100 µl of transformation culture is spread on agar plates containing the appropriate antibiotic and plates are incubated for 16 hours at 37°C.

3.3 Molecular biology

3.3.1 Plasmid preparation

Analytical plasmid preparation is performed using GeneJET Plasmid Miniprep Kit according to the manufacturer´s instructions. Isolated DNA is stored at -20°C.

Preparative plasmid preparation is performed using Plasmid Midi Kit according to the manufacturer´s instructions for very low copy plasmids with the following change. pBJG1 is a low copy plasmid, therefore, instead of the instructed 500 ml only 250 ml culture medium are used. Isolated DNA is stored at -20°C.

3.3.2 Estimation of DNA concentration and purity

Sample is diluted 1:100 in DI water and absorption is measured at 260 and 280 nm. OD_{260} of 1 equals a DNA concentration of 50 µg/ml. The ratio of the absorbance measured at 260 nm

and at 280 nm provides information on the purity of the sample and should be 1.8-1.9 for sequencing.

3.3.3 Restriction analysis

Plasmid pBJG1-hNCAM180cyt is digested successively with restriction enzymes *Bam*HI and *Xho*I according to the manufacturer´s instructions. After each digest, DNA is purified with DNA Clean and Concentrator 5 Kit according to the manufacturer´s instructions. Double-digested and purified DNA is subjected to agarose gel electrophoresis.

3.3.4 Agarose gel electrophoresis

0.8 % agarose gels are prepared by melting 0.4 g agarose in 50 ml TBE buffer. After cooling to approximately 60°C, 2 µl ethidium bromide are added to the solution and the gel is cast. Upon hardening, gel is immersed in TBE buffer and samples along with DNA ladder mix are combined with 6x loading dye and loaded onto the gel. Agarose gel is run at 80 V for 1-1.5 hours and gel image is acquired with a UV transilluminator. For ligation, DNA is quantified by comparing the band thickness to the DNA ladder bands. If necessary, bands of interest are excised from the gel and gel extraction is performed using QIAquick Gel Extraction Kit according to the manufacturer's instructions. For ligation, DNA is eluted with DI water instead of TE buffer.

3.3.5 Ligation

Generation of Nup62 insert is described elsewhere (Balzen, 2010). Briefly, using vector pExpress-1 containing the cDNA of Nup62 from *Rattus norwegicus*, Nup62 insert was prepared by deleting the stop codon and adding *Bam*HI and *Xho*I restriction sites by polymerase chain reaction. Digested Nup62 insert was kindly provided by S. Balzen (Institute of Animal Sciences, University of Bonn). pBJG1 vector and Nup62 insert, both digested with *Bam*HI and *Xho*I, are mixed 1:3 and 1:6 and ligation is performed with T4 DNA ligase for 16-40 hours at 16°C. Preparations are transformed into *E. coli* XL1 Blue and tested for successful ligation by restriction analysis and agarose gel electrophoresis.

3.3.6 Sequencing

Using the standard primers T7 and T7term, sequencing is performed by Eurofins MWG Operon (Ebersberg, DE).

3.4 Protein biochemistry

3.4.1 Expression of recombinant proteins and bacterial cell lysis

Expression of recombinant proteins is performed in *E. coli* BL21 (DE3). An overnight culture is diluted 1:50 in fresh LB medium containing the appropriate antibiotics and cells are grown at 220 rpm and 37°C until an OD_{600} of 0.6-0.8 is reached. In *E. coli* transformed with pBJG1 or pGex plasmids protein expression is induced by the addition of IPTG.

For **Nup62** expression, IPTG is added to a final concentration of 0.5 mM and expression is performed for 6 hours at 37°C and 220 rpm. Bacterial culture is centrifuged for 30 minutes at 3,000 x g and 4°C and pellet is stored at -20°C or processed directly. Pellets are suspended in 1/20 of the original culture volume in urea lysis buffer and 1 ml aliquots are sonicated on ice (4 pulses of 2 seconds), centrifuged 20 minutes at 15,000 x g and 4°C, and resulting supernatant is stored at -20°C. For negative controls, untransformed bacteria are grown and lysed in parallel.

For **CK2α** expression, IPTG is added to a final concentration of 0.5 mM and expression is performed for 3 hours at 37°C and 220 rpm. Bacterial culture is centrifuged for 30 minutes at 3,000 x g at 4°C and pellet is stored at -20°C or processed directly. Lysis is performed as described above for Nup62.

For **OGT** expression, bacterial culture is cooled to room temperature and protein expression is induced with 0.2 mM IPTG. OGT is expressed for 4 hours at 20°C and 220 rpm. Bacterial culture is centrifuged for 30 minutes at 3,000 x g at 4°C and pellet is stored at -20°C or processed directly. Pellets are suspended in 1/20 of the original culture volume in PBS-L and incubated for 30 minutes at room temperature on a shaker. Cells are subjected to 10 freeze-thaw cycles using liquid nitrogen for freezing and lukewarm water for thawing. Samples are transferred into a chilled glass homogenizer and subjected to 20 strokes and 1 ml aliquots are sonicated on ice (4 pulses of 2 seconds), centrifuged at 20,000 x g for 30 minutes at 4°C, and resulting supernatant is stored at -80°C. For negative controls, untransformed bacteria are grown and lysed in parallel.

Cdk5 expression, lysis and purification were performed as described elsewhere (Strempel, 2010). Isolated cdk5 was kindly provided by N. Strempel (Institute of Animal Sciences, University of Bonn).

GST expression, lysis and purification were performed as described elsewhere (Sabrowski, 2012). Isolated GST was kindly provided by J. Sabrowski (Institute of Animal Sciences, University of Bonn).

3.4.2 Purification of recombinant proteins

His_8-tagged proteins can be purified by Ni-NTA affinity chromatography. Therefore, column is packed with Ni-NTA agarose, final bed volume is 15 ml. Equilibration and washing is performed at a constant flow rate of 75 ml/h; for sample application and elution flow rate is reduced to 50 ml/h. All flow-through is collected in various fractions for further analysis. Prior to storage in PBS at 4°C, column is washed with 90 ml DI water.

For **Nup62** purification, affinity chromatography is performed at room temperature to prevent urea crystallization. Column is equilibrated with 60 ml urea equilibration buffer. Nup62 lysate is centrifuged for 10 minutes at 20,000 x g at 4°C and imidazole is added to a final concentration of 2 mM before sample is applied to the column. Column is washed with 60 ml urea equilibration buffer containing 20 mM imidazole and Nup62 is eluted with 60 ml urea equilibration buffer containing 250 mM imidazole. Elution fractions containing Nup62 as determined by SDS-PAGE and Coomassie staining are pooled and subjected to dialysis and/or concentrated using Amicon Ultra-15 Centrifigal Filter Devices or Vivaspin 6 concentrators according to the manufacturer´s instructions.

OGT purification is performed as described above with minor changes. In general, PBS equilibration buffer is used instead of urea equilibration buffer. After sample application, column is washed with PBS equilibration buffer containing 250 mM NaCl and 40 mM imidazole and OGT is eluted with PBS equilibration buffer containing 250 mM NaCl and 250 mM imidazole. Elution fractions containing OGT as determined by SDS-PAGE and Coomassie staining are pooled, concentrated and elution buffer is exchanged to 2x OGT buffer using an Ultrafree-0.5 Centrifugal Filter Device according to the manufacturer´s instructions.

3.4.3 Dialysis of affinity-purified Nup62

Prior to use, dialysis membranes are washed in DI water to remove storage solution. Sample is filled into the membrane and both ends are sealed off. For small volumes, sample is filled into an Eppendorf tube which is sealed with dialysis membrane. Dialysis takes place under constant stirring by placing the membrane into 100-fold sample volume of buffer. Affinity-purified Nup62 is successively dialyzed for 2 hours each against 6 M, 4 M, and 2 M urea buffer. Triton X-100 is added to the sample in a final concentration of 1 % and sample is dialyzed against PBS overnight at 4°C. Sample aliquots are stored at -20°C.

3.4.4 Harvest of conditioned medium and cell lysis

Conditioned medium for immunoblot analyses is harvested and centrifuged at 500 x g for 7 minutes to remove cell debris. Supernatant is transferred into 1.5 ml tubes containing protease inhibitors and samples are stored immediately at -80°C.

For RIPA lysis, culture flasks are placed on ice, cells are washed with ice-cold PBS and chilled RIPA lysis buffer is added to the cells. The cells are scraped off the bottom of the culture flask and transferred into a 1.5 ml tube. Samples are incubated on ice for 30 minutes with occasional mixing. Lysates are centrifuged at 12,300 x g for 30 minutes, resulting supernatant is transferred into a new tube and stored at -80°C. Alternatively, cells can be detached from flasks as described in 3.1.1. Sample is then transferred into a 1.5 ml tube, centrifuged for 7 minutes at 200 x g. RIPA lysis buffer is added to the cell pellet and lysis is continued as described above.

For 2D analyses, cells are lysed in chilled 2D lysis buffer. Cells are detached from flasks as described in 3.1.1. Cells are transferred into a 1.5 ml tube, centrifuged for 7 minutes at 200 x g and supernatant discarded. 500 µl 2D lysis buffer are added and sample is mixed briefly. Sample is then sonicated three times for 1 second each, centrifuged for 1 hour at 20,000 x g and 4°C; the resulting supernatant is aliquoted and immediately stored at -80°C.

3.4.5 Preparation of human brain samples

All steps are performed on ice. Frozen IPL and cerebellar samples are thawed and homogenized in ice-cold isolation buffer using a glass homogenizer. For **homogenates**, samples are diluted 1:4 with isolation buffer and sonicated twice for 10 seconds each at 20 % power using a 550 Sonic Dismembrator. After centrifugation for 10 minutes at 1,000 x g and 4°C, supernatant is stored at -80°C. For subcellular fractionation, samples are homogenized and centrifuged for 10 minutes at 1,000 x g and 4°C. Supernatant (crude cytosolic fraction) is transferred into a new tube and centrifuged again for 10 minutes at 16,090 x g and 4°C. The resulting supernatant represents the **cytosolic fraction**. All samples are stored at -80°C.

3.4.6 Determination of protein concentration

In samples from cell or bacterial culture, determination of protein concentration is performed with Pierce 660 nm Protein Assay while Pierce Bicinchoninic acid Protein Assay Kit is used for the analysis of human brain samples. Both assays are performed according to the manufacturer´s instructions using BSA for the standard curve.

3.4.7 Immunoprecipitation (IP)

For **APP-IP**, per sample 25 µl Protein G-Sepharose are incubated with 2.5 µl 8E5 antibody for 30 minutes on ice. Sample (250 µg RIPA cell lysate) is added and incubated on an end over end rotator for 16 hours at 4°C. The following day, IP preparation is centrifuged for 1 minute at 3,000 x g and 4°C, supernatant is discarded and beads are washed three times with 500 µl RIPA wash buffer and one time with 300 µl DI water. 4x sample buffer is diluted 1:1 with DI water and 40 µl 2x sample buffer are added to the beads. Sample is heated for 5 minutes at 94°C, centrifuged for 2 minutes at 6,000 x g, and supernatant is subjected to SDS-PAGE (see 3.4.8).

OGT-IP is performed as described above with minor changes. Briefly, Protein G-Sepharose is incubated with 5 µl AL28 antibody and 1 ml OGT lysate is added and incubated for 16 hours at 4°C. The following day, beads are washed three times with 1 ml PBS containing 1 mM DTT and 1 mM EDTA and one time with 1 ml DI water. After centrifugation and removal of the supernatant, beads (with bound OGT) can be used for OGT assay.

Aβ-IP procedure is based on previously published protocols (Uljon *et al.*, 2000; Öckl, 2007) with minor changes. Per sample, 20 µl Protein G-Sepharose are incubated with 2.5 µl 4G8 antibody for 30 minutes on ice. Triton X-100 is added to conditioned media to a final volume of 0.1 %. 1 ml sample is added to the beads and incubated for 16 hours at 4°C. Fresh neurobasal medium is used as a negative control and a positive control is included where 1 µl 1 µM $A\beta_{(12-28)}$ is added to the sample. The following day, IP preparations are centrifuged for 1 minute at 10,000 x g and 4°C, supernatant is discarded and beads are washed twice with 1 ml IP wash buffer, three times with 1 ml 25 mM NH_4HCO_3 and one time with 1 ml DI water. After the last wash, beads are centrifuged again to remove residual liquid. To elute bound material, 50 µl 0.1 % TFA are added to the beads, mixed briefly and centrifuged. Supernatant is transferred into a new tube and elution step is repeated. Further analysis was carried out by B. Gehrig (Institute of Biochemistry and Molecular Biology, University of Bonn). Briefly, eluate is lyophilized and resolved in 10 µl 0.1 % TFA. Sample is co-crystallized with equal volumes of matrix (saturated α-CHCA in 50 % ACN/0.1 % TFA) onto the sample probe. Sample is air-dried and analyzed by matrix-assisted desorption/ionization time-of-flight (MALDI-TOF) MS. Instrument (Autoflex III Smartbeam) and software (FlexControl Version 3.3 (Build 108) and FlexAnalysis Version 3.3 (Build 89)) are from Bruker Daltonik, Bremen (DE).

3.4.8 Electrophoretic separation of proteins using polyacrylamide gels

3.4.8.1 SDS-PAGE

Composition of gels is listed in Table 10, volumes are sufficient for two gels. APS and TEMED are added shortly before casting the gels and solution in mixed gently. Separation gel is cast between the glass plates of a casting cassette and overlaid with isopropanol. Upon polymerization, isopropanol is discarded, stacking gel is cast on top of the separation gel, and sample well comb is applied. After polymerization, gel apparatus is assembled, running chamber is filled with 1x running buffer, and the sample well comb is removed. Samples are mixed with 4x sample buffer, heated for 5 minutes at 95°C and centrifuged briefly before being loaded onto the gel next to a protein standard. 0.75 mm thick gels are run at 15 mA per gel; 1 and 1.5 mm thick gels are run at 15 mA per gel for 15 to 30 minutes, then current is increased to 20 mA per gel. Gels are run until the blue dye front reaches the end of the separation gel. After the run is completed, gel apparatus is disassembled and gels are immersed in fixing solution for Coomassie staining (3.4.9) or in transfer buffer for Western blot transfer (3.4.10).

Table 10: Composition of separation and stacking gels for SDS-PAGE

Gel component	Separation gel (8 %)	Separation gel (10 %)	Stacking gel
Acrylamide solution	4 ml	5 ml	1.5 ml
1 M Tris HCl pH 8.8	5.6 ml	5.6 ml	-
1 M Tris HCl pH 6.8	-	-	1.3 ml
DI water	5.25 ml	4.25 ml	7.15 ml
10 % (w/v) SDS	150 µl	150 µl	150 µl
20 % (w/v) APS	30 µl	30 µl	30 µl
TEMED	15 µl	15 µl	15 µl

3.4.8.2 2D SDS-PAGE

For 2D SDS-PAGE, proteins are first separated on immobilized pH gradients (IPGs) by isoelectric focusing (IEF) and then separated by SDS-PAGE. IEF is performed on self-made IPGs (11cm, pH 4-7 or pH4-9; Westermeier, 2005).

Chloroform-methanol precipitation

Cell lysates are thawed on ice and adjusted to 100 µg protein per 100 µl with 2D lysis buffer. Successively, 300 µl methanol, 75 µl chloroform, and 200 µl DI water are added, the sample is mixed briefly after each step. Sample is centrifuged for 5 minutes at 15,000 x g at 4°C and supernatant is removed without disturbing the interphase. 225 µl methanol are added, the sample mixed briefly and/or incubated for 5 minutes in an ultrasonic water bath to dissolve

the interphase. Sample is centrifuged for 5 minutes at 15,000 x g at 4°C and supernatant is removed. The pellet is air dried and then resolubilized in 100 µl sample preparation solution.

IPG rehydration

Per IPG, 200 µl rehydration solution are pipetted into an IPG tray and IPG is placed gel side facing down into the solution. Strips are overlaid with 2 ml mineral oil and IPGs are rehydrated overnight at room temperature.

IEF

108 ml mineral oil is added to the tray in the IPGphor3 and rehydrated IPGs are placed into the slots with the gel side facing up and the acidic end on the anode. Filter paper wicks, pre-wetted with 50 µl DI water, are placed on both ends of the IPG and the electrodes are applied. Sample cups are positioned on top of the IPGs, 1 cm from the basic end of the strip at the cathode. 100 µl of sample are added into the sample cup. IEF is performed at 20°C with current limited to maximal 50 µA per IPG. IEF protocol used for sample cup loading is listed in Table 11. After IEF run, excess mineral oil is removed and IPGs are stored at -80°C.

Table 11: IEF program

Step and voltage mode	Voltage (V)	Step duration (h:min)	Volt hours (Vh)
1 Step and Hold	500	1:00	500
2 Gradient	1000	1:00	750
3 Gradient	6000	2:00	7000
4 Step and Hold	6000	0:30	3000
Total		4:30	11250

Equilibration of IPGs

IPGs are thawed for 5 minutes in 2 ml equilibration solution. Solution is discarded and IPGs are incubated for 15 minutes in 2 ml equilibration solution containing 1 % DTT followed by 15 minutes in 2 ml equilibration solution with 4.8 % iodoacetamide.

SDS-PAGE

Composition of gels is listed in Table 12, volumes are sufficient for two gels. APS and TEMED are added shortly before casting the gels and solution is mixed gently. Separation gel and stacking gel (1 ml) are cast as described above. Upon polymerization of the stacking gel, isopropanol is replaced by 1x running buffer and equilibrated IPG is placed on top of the gel. Running buffer is discarded and IPG is fixed with overlay agarose. Gel apparatus is assembled, running chamber is filled with 1x running buffer and gels are run at 15 mA per gel for 20 minutes, then current is increased to 30 mA per gel. Gel run is stopped when the blue

dye front reaches the bottom of the gel, gel apparatus is disassembled and gels are immersed in transfer buffer for subsequent Western blot transfer (3.4.10).

Table 12: Composition of separation and stacking gels for 2D SDS-PAGE

Gel component	Separation gel (7.5 %)	Stacking gel
Acrylamide solution	7.5 ml	1 ml
4x separation gel buffer	7.5 ml	-
4x stacking gel buffer	-	2.5 ml
DI water	15 ml	6.5 ml
20 % (w/v) APS	75 µl	30 µl
TEMED	15 µl	20 µl

3.4.8.3 SDS-PAGE using precast gels

Proteins from human brain samples are separated using 4-15 % or 8-16 % Criterion TGX Precast gels. Excess storage solution is rinsed off with DI water, gels are placed in Criterion Cell and 1x TGS running buffer is added. Samples (50 µg homogenates or 25 µg cytosolic fractions) are mixed with 4x sample buffer, heated for 5 minutes at 95°C, and centrifuged briefly before application onto the gel next to protein standard. Gels are run at 80 V for 10 minutes, voltage is then increased to 120 V and gels are run until the blue dye front reaches the end of the gel. After completion of the run, gel apparatus is disassembled and gels are immersed in transfer buffer for subsequent Western blot transfer (3.4.10).

3.4.8.4 Bicine/Tris/urea SDS-PAGE

Bicine/Tris/urea SDS-PAGE is performed as described elsewhere (Klafki *et al.*, 1996).

3.4.9 Coomassie staining of proteins in gels

Gels are incubated in destaining/fixing solution for 15 minutes. Destaining/fixing solution is removed and staining solution is added for 1 hour. Staining solution is removed and destaining/fixing solution is added and exchanged repeatedly until the background is clear and protein bands or spots are clearly visible.

3.4.10 Western blot

For semi-dry Western blot, polyacrylamide gels are incubated for 15 minutes in transfer buffer; filter papers and nitrocellulose membrane are only shortly incubated in transfer buffer. Blot sandwich is built as follows: three filter papers, nitrocellulose membrane, gel, three filter papers. Excess transfer buffer and air bubbles are removed by gentle rolling on each layer of

filter paper with a flexible roll. Western blots are run at 1 mA/cm^2 for 90 minutes. For transfer of proteins from bicine/Tris/urea gels, Western blot is run at 1 mA/cm^2 for 60 minutes. For transfer of proteins from precast gels, one extra-thick blot paper is used instead of three filter papers and Western blot is performed at 25 V for 30 minutes using the Trans-Blot Turbo Transfer System.

3.4.11 Immunodetection of proteins on membranes

Cell and bacterial culture experiments and experiments involving human brain samples were performed in different labs using slightly different protocols for immunological detection of proteins, therefore both procedures are described below. Dilutions of primary and secondary antibodies are listed in Table 13.

3.4.11.1 Immunodetection of proteins from cell or bacterial culture experiments

Membranes are incubated in blocking solution (1 % PVP/PBST) for 1 h at room temperature. Primary antibody is diluted in 0.1 % PVP/PBST, added to the membranes, and incubated overnight at 4°C. Membranes are washed three times for 5 minutes each in PBST prior to 1 hour incubation with POD-conjugated secondary antibodies diluted in 0.1 % PVP/PBST at room temperature. Membranes are washed four times with PBST and two times with PBS (5 minutes per wash). Membranes are placed inside an autoradiography cassette and chemiluminescence solution (Thermo Fisher Scientific) is added to the membrane (100 µl/lane). For signal detection X-ray film is placed on top of the membrane (exposure time depends on signal intensity). X-ray films are then incubated for 1 minute in GBX developer, rinsed shortly in water and incubated for 2 minutes in GBX fixer. Dry X-ray films are scanned and image analysis is performed using ImageJ software.

3.4.11.2 Immunodetection of proteins from human brain samples

Membranes are incubated in blocking solution (3 % BSA in wash buffer) for 1.5 hours at room temperature. Primary antibody is diluted in blocking solution and membranes are incubated overnight at 4°C. Membranes are washed three times for 5 minutes each in wash buffer prior to 1 hour incubation with secondary antibodies diluted in wash buffer at room temperature. Membranes are washed one time for 5 and two times for 10 minutes with wash buffer. If Cy5-conjugated secondary antibodies are used, antibody incubation and the following wash steps are performed protected from light. Signal detection method depends on the secondary antibody used. When using Cy5-conjugated antibodies, signals are detected with the appropriate fluorescent laser. When using POD-conjugated antibodies, signals are detected chemiluminescently with chemiluminescence solution (Bio-Rad)

according to the manufacturer´s instructions. Exposure time depends on signal intensity. When using AP-conjugated antibodies, signals are detected colorimetrically by incubation of the membrane with AP developer solution. Developing time depends on signal intensity; upon reaching the desired signal intensity, membranes are rinsed with DI water and dried overnight at room temperature before scanning. All images are acquired with the ChemiDoc MP imaging system and image analysis is performed using Image Lab Software.

Table 13: Primary and secondary antibody dilutions

Primary antibody	Dilution
8E5	1:5,000
AL28	1:10,000
anti-actin	1:4,000
anti-GAPDH	1:30,000
anti-GST	1:10,000
anti-His	1:8,000
anti-OGA	1:1,000
anti-OGT	1:500
anti-sAPPβ	1:100
anti-β-actin	1:4,000
C-8	1:30,000
CTD110.6	1:2,000-1:4,000
D-20	1:12,000
JLA-20	1:4,000
W0-2	1:4,000

Secondary antibody	Dilution
anti-goat-POD	1:25,000
anti-mouse-Cy5	1:2,500
anti-mouse-POD (Dianova)	1:40,000
anti-mouse-POD (Millipore)	1:100,000
anti-rabbit-AP	1:10,000
anti-rabbit-Cy5	1:2,500
anti-rabbit-POD	1:15,000
ECL anti-rabbit-POD	1:20,000

3.4.12 Removal of antibodies from membranes

Membranes are stripped of bound antibodies by incubation with stripping solution for 5 minutes or by using ReBlot Plus Strong Antibody Stripping Solution according to the manufacturer´s instructions. After rinsing twice with PBS or wash buffer membranes can be reprobed as described in 3.4.11 or membranes can be stained as described in 3.4.13.

3.4.13 Staining of proteins on membranes

For reversible **Ponceau S staining** after Western blot transfer, membranes are briefly rinsed with DI water before incubation with Ponceau S staining solution for 1 minute. Staining solution is removed and membranes are rinsed repeatedly with DI water until the background is destained and proteins are visible. For complete destaining, membranes are incubated for 5 minutes in 60°C warm PBS or rinsed with wash buffer.

For **Direct Blue staining**, membranes are incubated in Direct Blue staining solution for 5 minutes, rinsed with DI water and air-dried.

3.5 OGT activity assays

3.5.1 OGT assay on the membrane

For OGT assay on the membrane, sample containing the protein of interest is subjected to SDS-PAGE and Western blot transfer as described in 3.4.8 and 3.4.10. Nup62 lysate is included as a positive control, negative controls include untransformed *E. coli* BL21 (DE3) lysate and GST lysate. Membrane is blocked in 1 % PVP/PBST for 1 hour at room temperature, rinsed with PBS and then incubated with OGT in OGT assay buffer (1 ml/lane; Table 14) for 2 hours at 37°C under gentle agitation (100 rpm). As another negative control, assay is also performed with buffer containing untransformed *E. coli* BL21 (DE3) lysate instead of OGT lysate. After incubation, membrane is rinsed with PBS and O-GlcNAc signals are detected as described in 3.4.11.

Table 14: OGT assay buffer

Buffer components	Volume
2x OGT buffer	500 µl
BSA (1 mg/ml)	10 µl
UDP-GlcNAc solution	10 µl
OGT lysate or lysate from untransformed *E. coli* BL21 (DE3)	100 µg
0.1M GlcNAc	Ad 1 ml

3.5.2 ELISA-based OGT assay

All incubations take place under gentle agitation (100 rpm) and all wash steps consist of three washes with 300 µl PBS each; all measurements are carried out in duplicates. Express capture Ni-coated plates are washed and wells are incubated with 100 µl sample for 1 hour at room temperature. After washing, wells are blocked with 100 µl 1 % BSA/PBS for 1 hour at room temperature. Wells are washed, OGT in 100 µl OGT assay buffer (Table 14) is added and OGT assay is performed for 2 hours at 37°C. After washing, wells are incubated with primary antibody diluted in 100 µl 1 % BSA/PBS overnight at 4°C. CTD110.6 or RL2 antibodies are diluted 1:150 and 1:125, respectively. After washing, wells are incubated with secondary antibodies (anti-mouse-POD) diluted 1:200 in 100 µl 1 % BSA/PBS for 1 hour at room temperature. After a final wash step, 100 µl ABTS developer solution is added. The developing process is stopped by the addition of 100 µl 0.6 % SDS solution and absorbance is measured at 405 nm. Negative controls include assays without sample, without OGT and

without primary antibody. As a positive control, OGT assay on the membrane is run in parallel using the same preparation of OGT in OGT assay buffer.

3.5.3 OGT assay with peptides

OGT is immunoprecipitated as described in 3.4.7. Peptides are diluted in OGT assay buffer for peptides (Table 15; final peptide concentration is 2-2.5 mM) and solution is added to Protein G-Sepharose beads containing immobilized OGT. OGT assay is performed for 2 hours at 37°C under gentle agitation. Afterwards, beads are pelleted by centrifugation at 5,000 x g for 1 minute and supernatant is immediately stored at -20°C. Further analysis is carried out with B. Gehrig (Institute of Biochemistry and Molecular Biology, University of Bonn). Briefly, O-GlcNAc-modified peptides are labeled with the Click-iT O-GlcNAc Enzyme Labeling and Click-iT Protein Analysis Detection Kits (Invitrogen, Eugene, OR (US)) according to the manufacturer´s instructions and biotin-labeled peptides are purified on Monomeric Avidin Ultralink Resin (Thermo Fisher Scientific, Rockford, IL (US)) before samples are subjected to MALDI-TOF MS analysis.

Table 15: OGT assay buffer for peptides

Buffer components	Volume
2x OGT buffer	50 µl
BSA (1 mg/ml)	1 µl
UDP-GlcNAc solution	10 µl
0.1M GlcNAc	Ad 100 µl

3.6 OGA activity assay

OGA activity assay is performed as described elsewhere (Zachara *et al.*, 2011). Briefly, brain samples are homogenized in 300 µl ice-cold isolation buffer without EGTA, EDTA and GlcNAc. Samples are centrifuged at 4°C for 10 minutes at 1,000 x g and supernatant representing the crude cytosolic fraction is used for further analysis. Per sample, 100 µl ConA agarose is centrifuged for 5 minutes at 679 x g at 4°C to remove storage buffer. ConA agarose is washed with 500 µl ConA wash solution and equilibrated with 500 µl equilibration solution. Prior to sample application, equilibration solution is removed by centrifugation. To bind interfering acidic hexosaminidases, samples are incubated with ConA agarose under constant shaking for 30 minutes at 4°C. After centrifugation for 5 minutes at 679 x g, supernatants are desalted using Zeba Desalt Spin Columns according to the manufacturer´s instructions and protein concentration is determined as described in 3.4.6. Microtiter plates are placed on ice and assay components are added as listed in Table 16. A negative control without sample (blank) is included. Reactions are incubated in duplicates for 2-2.5 hours at

37°C and stopped by the addition of 100 µl 500 mM Na_2CO_3. Absorbance is read at 405 nm, blank is subtracted from all sample values and OGA activity is calculated using the following equation:

$$mM\ of\ GlcNAc\ released = A400 / (17.4 \times 10\ mM^{-1} \cdot cm^{-1} \times pathlength)$$

The molar extinction coefficient for pNP is 17.4 × 10 $mM^{-1} \cdot cm^{-1}$ at pH 10; path length for 200 µl in a 96-well plate is 0.71 cm; one enzyme unit represents the amount of enzyme catalyzing the release of 1 µmol/min of pNP from pNP-GlcNAc (Zachara *et al.*, 2011).

Table 16: OGA assay buffer

Buffer components	Volume
Sample	25 µg
10x OGA buffer	10 µl
pNP-GlcNAc (100 mM)	2 µl
DI water	Ad 100 µl

3.7 Statistical Analysis

All statistical analyses are performed using GraphPad Prism 5. Comparison of two groups is performed by unpaired t-test. Comparison of more than two groups is performed by one-way ANOVA followed by Tukey´s Multiple Comparison Test. Possible relationships of two factors are assessed by Pearson correlation followed by computation of two-tailed p-value. Data are presented as mean ± standard deviation (SD) or mean ± standard error of the mean (SEM); statistical significance is considered at $p < 0.05$.

4 Results

The experiments performed in this work can be divided into three distinct parts: O-GlcNAc modulation in SY5Y-APP cells, implementation of different *in vitro* OGT assays, and the analysis of O-GlcNAc and O-GlcNAc cycling enzymes in the progression of AD. Therefore results will be presented and discussed individually.

4.1 O-GlcNAc modulation in SY5Y-APP cells

The effects of O-GlcNAc modulation on APP were investigated in human neurobloastoma SH-SY5Y cells that had been stably transfected with cDNA of human wild-type APP_{695} (termed SY5Y-APP from here on; Parkin *et al.*, 2007). To modulate O-GlcNAcylation, SY5Y-APP cells were treated with the specific OGA inhibitor **NButGT** or OGT inhibitor **Alloxan** (Konrad *et al.*, 2002; Macauley *et al.*, 2005). In addition, indirect O-GlcNAc modulation was achieved by treatment of the cells with **PMA**, a protein kinase C activator (Gonzales *et al.*, 1987). In accordance with the proposed “yin-yang” relationship of O-GlcNAc and phosphorylation (see 1.1.2), PMA has previously been shown to decrease O-GlcNAc in the detergent-insoluble cytoskeleton-associated fraction of cerebellar neurons (Griffith and Schmitz, 1999). Treatments of SY5Y-APP cells for 24 hours with 30 µM NButGT, 5 mM Alloxan, and 80 nM PMA were selected based on pretests (data not shown); the applied dosages are in agreement with previous reports using N2a (murine neuroblastoma cells) or SH-SY5Y cells (Gollner, 2001; Tritz, 2010; Jacobsen and Iverfeldt, 2011). To investigate potential effects of O-GlcNAc modulation on expression and proteolytic processing of APP, after treatments, conditioned media and RIPA cell lysates were analyzed by SDS-PAGE and Western blot. To further characterize APP´s O-GlcNAcylation, APP was immunoprecipitated in a subset of experiments or samples were subjected to 2D SDS-PAGE.

4.1.1 Treatment effects on global and APP-specific O-GlcNAcylation

For analysis of **global O-GlcNAcylation**, cell lysates (15-25 µg) were subjected to 10 % SDS-PAGE and Western blot analysis. After O-GlcNAc detection with CTD110.6 antibody, membranes were stained with Direct Blue (data not shown) and O-GlcNAc signals were normalized to total protein levels. Results of the control treatments (Dulbecco´s Modified Eagle Medium low glucose (DMEM-LG) for Alloxan and NButGT or dimethyl sulfoxide (DMSO) for PMA treatments) were set to 100 % and results were converted to % control. Values of three (for Alloxan and PMA) or six (for NButGT) individual experiments were combined for densitometric analysis.

As depicted in Figure 5, NButGT treatment significantly increased **global O-GlcNAcylation** (321 ± 62 %; p = 0.005) while Alloxan had no effect on O-GlcNAcylation (109 ± 32 %). However, it was noted that in contrast to the pretests, Alloxan treatment markedly increased O-GlcNAcylation in one trial while it decreased O-GlcNAcylation in the others when compared to the control (169, 61, and 96 %).

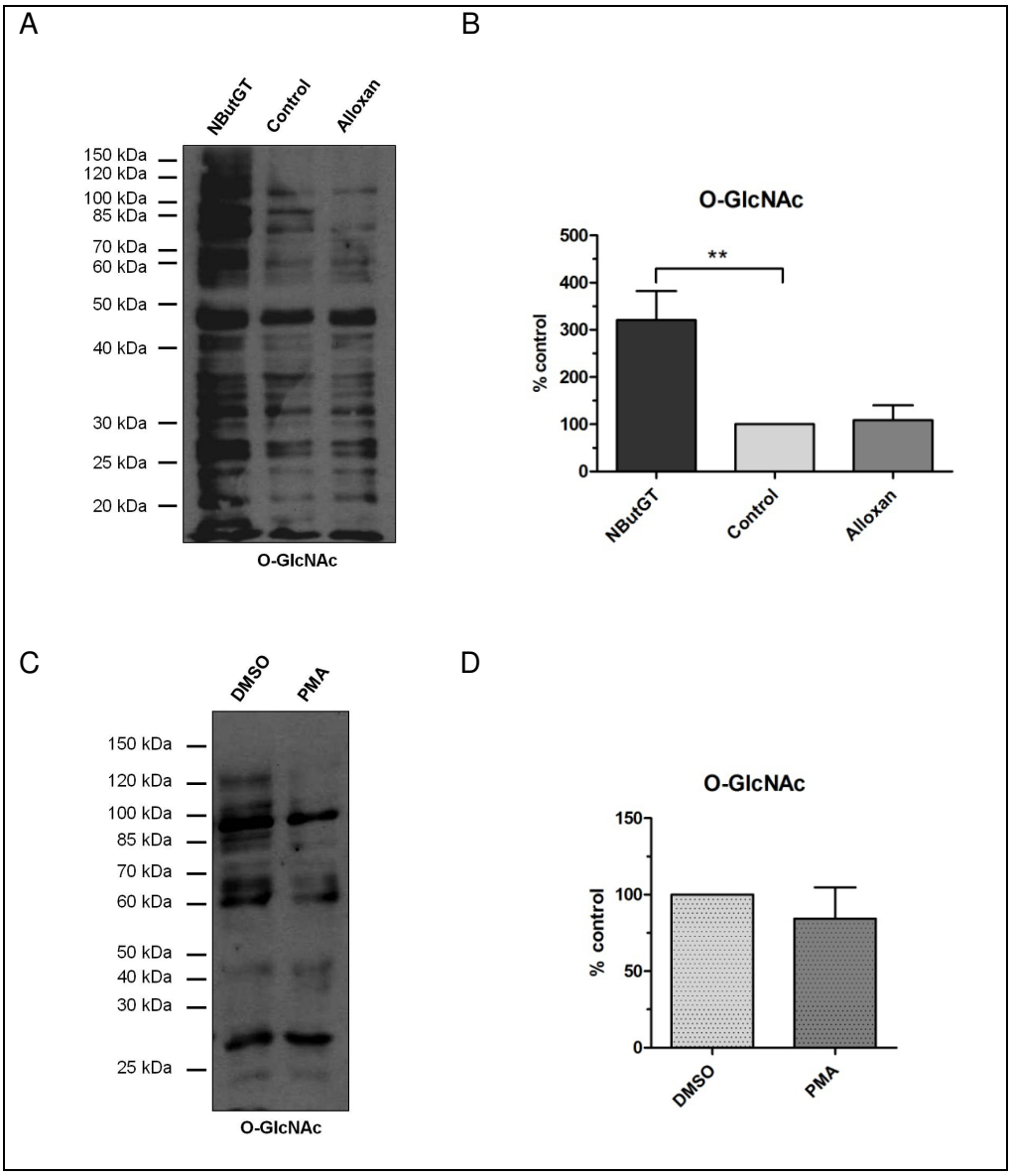

Figure 5: Effects of NButGT, Alloxan or PMA on global O-GlcNAcylation

SY5Y-APP cells were treated for 24 hours with 30 µM NButGT, 5 mM Alloxan or 80 nM PMA. **(A)** Representative Western blot and **(B)** densitometric quantification of O-GlcNAc signals from cell lysates after treatment with NButGT or Alloxan. **(C)** Representative Western blot and **(D)** densitometric quantification of O-GlcNAc signals from cell lysates after treatment with PMA. Global O-GlcNAcylation was normalized to total protein loading determined by Direct Blue staining. Control treatments (DMEM-LG medium or DMSO) were set to 100 % and results were converted to % control. Results of three to six individual experiments were combined and are presented as mean ± SEM. **p < 0.01.

PMA treatment slightly decreased O-GlcNAcylation but changes were not significant (84 ± 21 %; p = 0.5). In addition, as described for Alloxan treatment, PMA effects on global O-GlcNAcylation were contradictory. While PMA treatment decreased O-GlcNAcylation in two experiments, it increased it in the third (65, 62, and 125 %).

To analyze potential effects of NButGT and Alloxan treatments on **APP-specific O-GlcNAcylation**, APP was immunoprecipitated using 8E5 antibody prior to SDS-PAGE and Western blot analysis. Membranes were probed for O-GlcNAc, stripped and then reprobed for APP with 8E5 antibody and O-GlcNAc signals were normalized to APP signals. IP was performed three times and one representative result is shown in Figure 6. Both NButGT and Alloxan increased O-GlcNAcylation of APP (164 ± 15 % and 148 ± 39 %, respectively) but only after NButGT treatment did this increase show statistical significance (p = 0.01). Noteworthy, the lower APP band at approximately 110 kDa, was O-GlcNAc-modified. An additional O-GlcNAc signal was detected just below 100 kDa which corresponded to an additional lower-molecular weight APP band that was only visible after prolonged exposure times (data not shown). The nature of this band is unclear but it is conceivable that it may arise due to proteolysis of APP during cell lysis despite the addition of protease inhibitors.

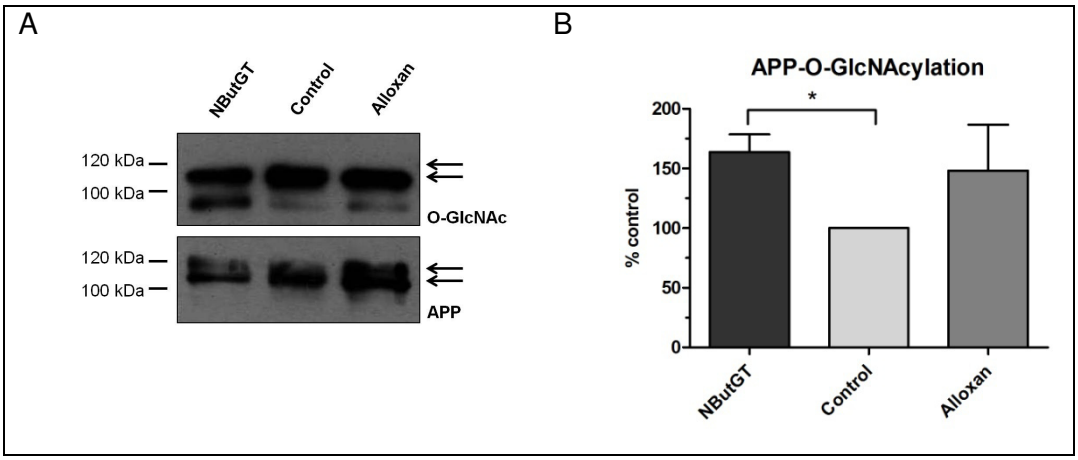

Figure 6: Effects of NButGT or Alloxan treatment on APP-specific O-GlcNAcylation

SY5Y-APP cells were treated for 24 hours with 30 µM NButGT or 5 mM Alloxan. **(A)** Representative Western blot and **(B)** densitometric analysis of O-GlcNAcylation of immunoprecipitated APP. Membranes were probed for O-GlcNAc and APP and O-GlcNAc signals were normalized to APP signals. Results of control treatment (DMEM-LG medium) were set to 100 % and results were converted to % control. Results of three individual experiments were combined and are presented as mean ± SEM. *p < 0.05. Arrows indicate mature (top) and immature (bottom) APP.

To further characterize O-GlcNAcylation of APP, untreated cell lysates were subjected to 2D SDS-PAGE prior to immunoblot analysis. In contrast to passive rehydration loading where no APP could be detected (data not shown), cathodic sample cup loading allowed for APP detection although sample separation was not satisfactory. Still, membranes were probed for O-GlcNAc, stripped and then reprobed with 8E5 antibody for APP (Figure 7). Results indicate that only a small subpopulation of APP is O-GlcNAc-modified and, in contrast to the results of APP-IP experiments, O-GlcNAcylation seems to occur mainly on the mature form of APP. The experiment was repeated three times with similar results (data not shown).

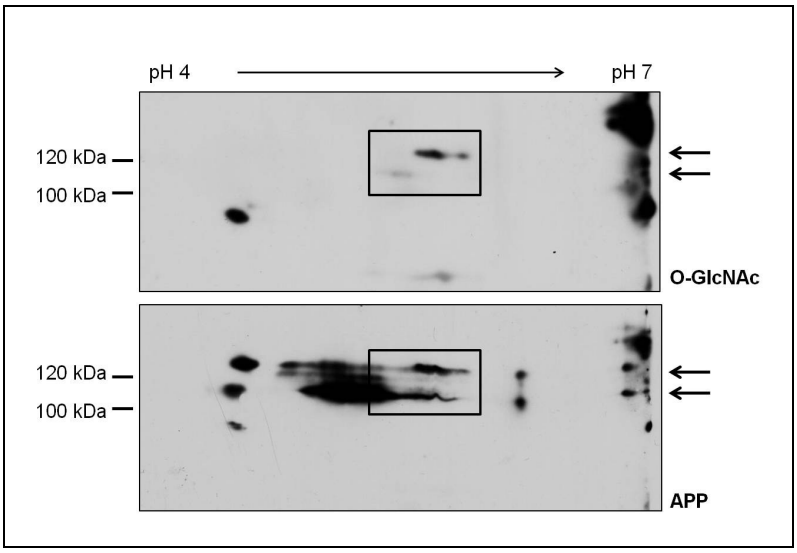

Figure 7: 2D analysis of O-GlcNAcylation of APP

Representative Western blot of O-GlcNAc and APP expression after 2D SDS-PAGE. Untreated SY5Y-APP cells were lysed in 2D lysis buffer, 100 µg of sample were loaded onto IPGs by cathodic sample cup loading and subjected to first dimension separation by IEF on self-made IPGs (pH 4-7). After second dimension SDS-PAGE and Western blot transfer, membrane was first probed for O-GlcNAc, stripped and then reprobed for APP. The black boxes point out overlapping APP and O-GlcNAc signals; arrows indicate the position of mature (top) and immature (bottom) APP forms.

4.1.2 Treatment effects on expression and processing of APP

For analysis of **APP expression**, cell lysates (15-25 µg) were subjected to SDS-PAGE and Western blot. APP and actin were probed for with 8E5 and JLA-20 antibodies, respectively, and APP signals were normalized to actin signals. As illustrated in Figure 8, NButGT slightly decreased APP expression but this effect was not significant (82 ± 14 %; $p = 0.2$). Furthermore, while Alloxan had no effect on APP expression (92 ± 6 %), PMA markedly increased APP expression but due to high variation and/or small sample number, this increase was not statistically significant (181 ± 43 %; $p = 0.13$).

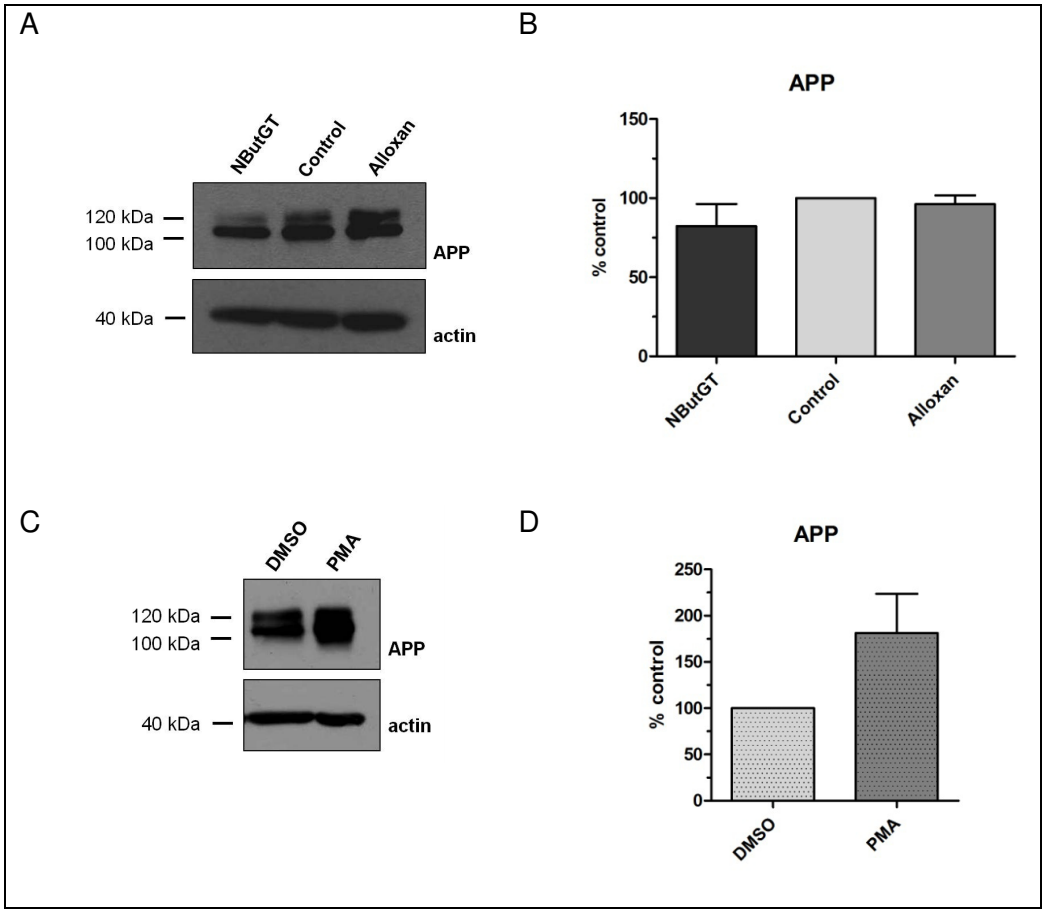

Figure 8: Effects of NButGT, Alloxan or PMA on APP expression

SY5Y-APP cells were treated for 24 hours with 30 µM NButGT, 5 mM Alloxan or 80 nM PMA. **(A)** Representative Western blot and **(B)** densitometric quantification of APP signals from cell lysates after treatment with NButGT or Alloxan. **C)** Densitometric quantification and **D)** representative Western blot of APP signals from cell lysates after treatment with PMA. APP levels were normalized to actin signals, control treatments (DMEM-LG medium or DMSO) were set to 100 % and results were converted to % control. Results of three to six individual experiments were combined and are presented as mean ± SEM.

APP processing by secretases produces various APP fragments (see 1.2.3.2). To investigate whether O-GlcNAc modulation affected the amount and/or composition of Aβ peptides, **Aβ** was analyzed by different methods (bicine/Tris/urea SDS-PAGE, Aβ-IP and MALDI-TOF MS). However, in contrast to the included positive control (synthetic $A\beta_{(1-40)}$ or $A\beta_{(12-28)}$) no endogenous Aβ could be detected (Western blot data not shown; exemplary MS results are included in Appendix C).

To analyze sAPP fragments, 50 µl of conditioned media were subjected to SDS-PAGE and Western blot transfer. **sAPPα** was detected with W0-2 antibody and ,in a subset of experiments, **sAPPβ** was analyzed with anti-sAPPβ antibodies. As identical volumes of conditioned medium were loaded onto SDS-PAGE independent of protein concentration in lysates, sAPPα and sAPPβ signals were normalized to total sAPP signals as detected with 8E5 antibody raised against the N-terminus of APP. Results are illustrated in Figure 9 and

show that NButGT treatment had no effect on sAPPα secretion (96 ± 15 %). In contrast, both Alloxan and PMA treatments induced a strong increase of sAPPα signals in conditioned medium. While the change in sAPPα level was not quite significant after Alloxan treatment (178 ± 51 %; p = 0.05) it was so after PMA treatment (197 ± 19 %; p = 0.008).

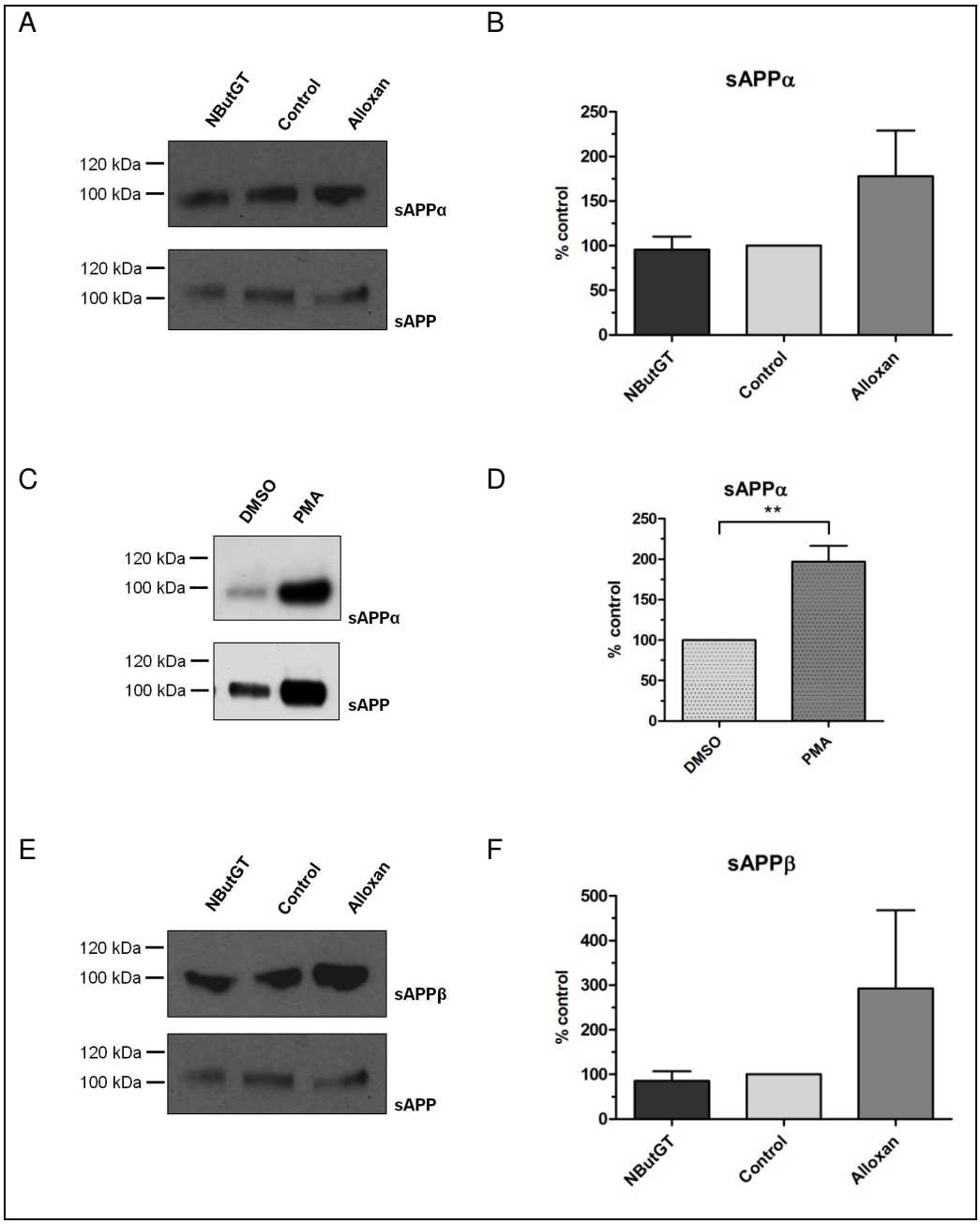

Figure 9: Effects of NButGT, Alloxan or PMA on APP secretion

SY5Y-APP cells were treated for 24 hours with 30 µM NButGT, 5 mM Alloxan or 80 nM PMA. **(A)** Representative Western blot and **(B)** densitometric quantification of sAPPα signals from conditioned medium after treatment with NButGT or Alloxan. **(C)** Representative Western blot and **(D)** densitometric quantification of sAPPα signals from conditioned medium after treatment with PMA. **(E)** Representative Western blot and **(F)** densitometric quantification of sAPPβ signals from conditioned medium after treatment with NButGT or Alloxan. sAPPα and sAPPβ signals were normalized to sAPP signals, control treatments (DMEM-LG medium or DMSO) were set to 100 % and results were converted to % control. Results of three to six individual experiments were combined and are presented as mean ± SEM. **p < 0.01.

Only in a subset of experiments (n = 3) sAPPβ was analyzed. NButGT treatment slightly decreased sAPPβ levels in conditioned medium, but results were inconsistent and not significant (85 ± 22 %; p = 0.5). In contrast, Alloxan treatment markedly increased sAPPβ secretion, however, individual results within the group varied extremely (70 to 640 %) and changes were not significant (293 ± 176 %; p = 0.3).

4.1.3 Summary

In summary, NButGT significantly increased global and APP-specific O-GlcNAcylation ($p < 0.01$ and $p < 0.05$, respectively) but had no significant effects on APP expression and secretion. Alloxan treatment had inconsistent effects on global O-GlcNAcylation and unexpectedly, elevated APP-specific O-GlcNAcylation, albeit not significantly. While Alloxan did not influence APP expression, it increased both sAPPα and sAPPβ levels in conditioned media although these changes were also not significant. PMA treatment had no significant effects on global O-GlcNAcylation or APP expression. However, PMA resulted in significantly augmented sAPPα secretion ($p < 0.01$); APP-specific O-GlcNAcylation and sAPPβ levels were not analyzed. Unfortunately, treatment effects on Aβ quantity and/or peptide composition could not be analyzed. Lastly, 2D SDS-PAGE and Western blot analysis revealed that only a subpopulation of APP is O-GlcNAc-modified.

4.2 Implementation of *in vitro* OGT assays

For the design and development of different OGT assays, nuclear pore protein Nup62 was chosen as a substrate because it has been described to be extensively O-GlcNAc-modified and our group and others have repeatedly demonstrated *in vitro* O-GlcNAcylation of Nup62 (Lubas *et al*., 1995; Strempel, 2010).

4.2.1 ELISA-based OGT assay

Recombinant Nup62 used in earlier OGT assays was expressed mainly in inclusion bodies and strong denaturing agents were necessary for its solubilization (Balzen, 2010; Strempel, 2010), therefore, optimizing of Nup62 expression and lysis conditions was attempted prior to the refinement of *in vitro* OGT assays.

Cloning, expression, and purification of Nup62

Plasmid pBJG1-Nup62 was generated by subcloning the cDNA encoding Nup62 from *Rattus norwegicus* into pBJG1 as described in 3.3.3 and 3.3.5. Successful ligation was confirmed by restriction analysis and agarose gel electrophoresis and additional sequencing revealed no

mutations in the Nup62 sequence (data not shown). In order to express soluble Nup62, various expression conditions (20-37°C; 0.1-1.0 mM IPTG; 1-24 hours) were tested, however, recombinant Nup62 proved to be insoluble in PBS and PBS-Triton (data not shown). For further analyses, expression conditions producing high yields of Nup62 (37°C, 0.5 mM IPTG, 6 hours) were chosen and a different approach for recovery of native Nup62 was applied. Bacterial pellet was lysed in urea lysis buffer and His_8-tagged Nup62 was isolated by affinity chromatography using Ni-NTA agarose. Purification process was monitored by SDS-PAGE and Western blot and probing for Nup62 with specific antibodies confirmed successful purification (data not shown). To allow for refolding of denatured protein, fractions containing isolated Nup62 were pooled and subjected to gradual dialysis against three buffers containing decreasing concentrations of urea and finally, after addition of Triton X-100 to the sample, against PBS. Monitoring of the dialysis process by SDS-PAGE and Western blot analysis revealed decreasing Nup62 solubility with each dialysis step (data not shown). Final concentration of renatured Nup62 in PBS-Triton was 1 µg/ml.

Establishment of ELISA-based OGT assays

One aim of this work was to establish an ELISA-based non-radioactive OGT assay using Nup62 as a substrate. Pretests with denatured as well as renatured samples were performed to confirm binding of His_8-tagged Nup62 to Ni-coated microtiter plates (data not shown).

Results of OGT assay using renatured Nup62

The procedure of ELISA-based OGT assay is described in 3.5. Briefly, affinity-purified and dialyzed (renatured) Nup62, along with equal volumes of PBS-Triton as a negative control, were incubated in Ni-coated microtiter plates. After blocking, wells were incubated with OGT for 2 hours at 37°C. Negative controls containing untransformed *E. coli* BL21 (DE3) lysate instead of OGT were included. After incubation with primary and POD-conjugated secondary antibodies, O-GlcNAc signals were detected with ABTS solution and absorbance was measured at 405 nm. As a positive control, OGT assay on the membrane was run in parallel using the same preparation of OGT and detection of Nup62-specific O-GlcNAcylation proved that the assay was functioning (data not shown). Colorimetric development of ELISA-based OGT assay revealed O-GlcNAc-positive signals in the wells incubated with Nup62, OGT and CTD110.6 antibody; however, even after prolonged developing times, signal intensities were very weak (OD_{405} < 0.3). Furthermore, secondary antibody controls without CTD110.6 antibody as well as the negative controls without Nup62 or OGT showed weak signals, too. To determine if signals in the negative controls were due to unspecific binding of CTD110.6 antibody, OGT assay was repeated with RL2 antibody but signal detection lead to similar results. Mean OD_{405} values of preparations containing all components (Nup62, OGT and

primary antibody) were set to 100 % and all values were converted to % control. Results of three individual experiments were combined and are shown in Figure 10A.

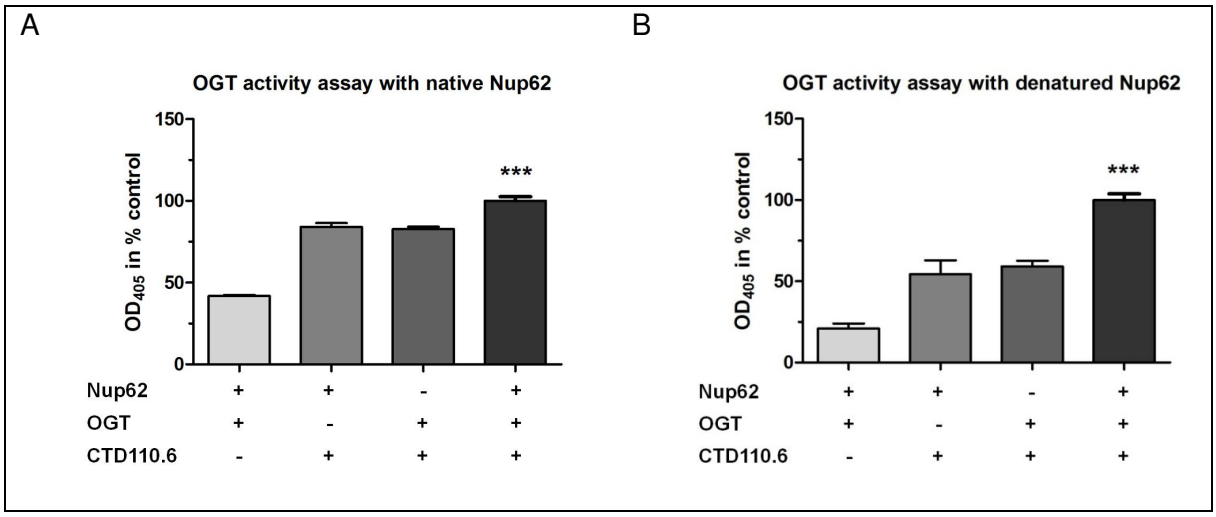

Figure 10: ELISA-based OGT assays with Nup62

OGT assay was performed with affinity-purified and dialyzed (renatured) Nup62 **(A)** or with denatured Nup62 **(B)**. His_8-tagged Nup62 or negative controls (PBS-Triton or lysate of untransformed *E. coli* BL21 (DE3)) were coated into the wells of Ni-coated microtiter plates, incubated with or without OGT, and O-GlcNAc modification was detected with CTD110.6 and anti-mouse-POD antibodies. Secondary antibody controls without CTD110.6 antibody were included. After colorimetric development with ABTS solution, absorbance was measured at 405 nm. Mean values of the preparation including Nup62, OGT and CTD110.6 were set to 100 % and values were converted to % control. Results of three individual assays were combined and data are shown as mean ± SEM. *** $p < 0.0001$.

Results of OGT assay using denatured Nup62

The same assay as described above was also performed with denatured Nup62. According to the manufacturer´s instructions, wells of Ni-coated microtiter plates were incubated with 100 µg of Nup62 lysate; lysate of untransformed *E. coli* BL21 (DE3) was included as a negative control. Detection at 405 nm revealed stronger signals after shorter incubation times (OD_{405} = 0.5 - 2.0, up to 30 minutes) when compared to the OGT activity assays using renatured Nup62 (OD_{405} = 0.2 - 0.3, up to 90 minutes) but negative controls were still not blank. Mean OD_{405} values of the preparations including Nup62, OGT and CTD110.6 antibody were set to 100 % and all values were converted to % control. The results of three individual experiments were combined and are shown in Figure 10B.

In both OGT assays, using native or denatured Nup62 as a substrate, signals of the negative controls were significantly lower than the signals in the actual assay preparation ($p < 0.0001$) indicating successful O-GlcNAcylation of Nup62.

4.2.2 OGT assay on the membrane

Cdk5 has been shown to be O-GlcNAcylated in N2a and SY5Y-APP cells (Kellersmann, 2003; Nowak, 2011). To confirm and further characterize the O-GlcNAcylation of cdk5, OGT assay on the membrane was performed as described in 3.5.1. Briefly, affinity-purified GST-tagged cdk5 was subjected to SDS-PAGE and Western blot transfer. Untransformed *E. coli* BL21 (DE3) and Nup62 lysates were included as controls to monitor assay performance. After blocking, membranes were incubated with OGT for 2 hours at 37°C and O-GlcNAc signals were detected with CTD110.6 antibody. Membranes were stripped and reprobed with antibodies against Nup62, GST or cdk5. OGT assay with cdk5 was performed four times and O-GlcNAc-positive signals at the apparent molecular weight of GST-tagged cdk5 (57 kDa) could be detected in two of the four trials. In one assay, no cdk5 O-GlcNAc signals could be detected at all and in one assay O-GlcNAc detection lead to negative signals at the cdk5 band (data not shown). Figure 11 illustrates one exemplary result showing successful O-GlcNAcylation of cdk5.

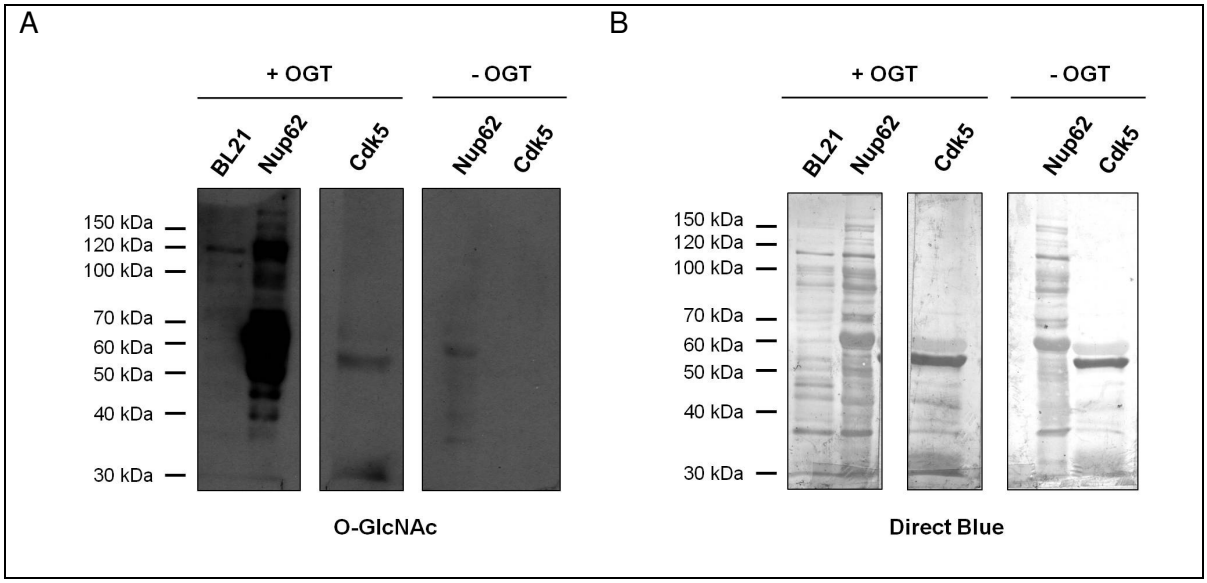

Figure 11: OGT assay with cdk5

Affinity-purified GST-tagged cdk5 along with untransformed *E. coli* BL21 (DE3) and Nup62 lysates were subjected to SDS-PAGE and Western blot transfer. After blocking, membrane was incubated for 2 hours at 37°C with (+) or without (-) OGT. **(A)** Membrane was probed for O-GlcNAc with CTD110.6 and anti-mouse-POD antibodies and signals were detected after 1 hour exposure to X-ray film. **(B)** After signal detection, proteins were stained with Direct Blue. BL21: untransformed *E. coli* BL21 (DE3) lysate; Nup62: Nup62 lysate; cdk5: affinity-purified GST-tagged cdk5.

Affinity-purified GST showed no O-GlcNAc-positive signals, demonstrating that GST is not O-GlcNAc-modified in this assay (data not shown) and thus indicating that O-GlcNAc signals detected at the apparent molecular weight of GST-cdk5 arise from the transfer of O-GlcNAc moieties to cdk5 and not to the GST-tag. O-GlcNAcylation of Nup62 could be detected and

secondary antibody controls (data not shown) as well as negative controls without OGT remained blank indicating functioning assay. However, after incubation with the more sensitive SuperSignal West Dura Chemiluminescent Substrate and longer exposure times weak signals could be detected in untransformed *E. coli* BL21 (DE3) negative controls and in the preparations without OGT (Figure 11A). After Direct Blue staining of the proteins, it was noted that a weaker band was present just above the cdk5 band (Figure 11B). The identity of this band is not clear as it did not react with antibodies against GST or cdk5 (data not shown) and it did not react with CTD110.6 antibody when probed for O-GlcNAc.

O-GlcNAc signals of cdk5 were much weaker than those of Nup62 and could only be detected after long exposure times (1-10 minutes for Nup62 compared to 1-2 hours for cdk5). To determine if this difference was cdk5-specific, OGT assay was repeated with GST-tagged CK2α (apparent molecular weight: 71 kDa; Figure 12B) as OGT activity assays using CK2α peptides as substrate have been described (McClain *et al.*, 2002). OGT assay on the membrane was performed as described above and probing with CTD110.6 antibody confirmed O-GlcNAcylation of CK2α (Figure 12A). While comparison of Direct Blue stained membranes showed high expression levels of recombinant GST-tagged CK2α (Figure 12C), CK2α´s O-GlcNAc signals were considerably weaker than Nup62´s O-GlcNAc signals. In contrast to cdk5 samples, Nup62 and CK2α samples were prepared identically, suggesting that differences in the strength of O-GlcNAc modification may be inherent to the protein analyzed. OGT assay with CK2α was repeated and yielded the same results.

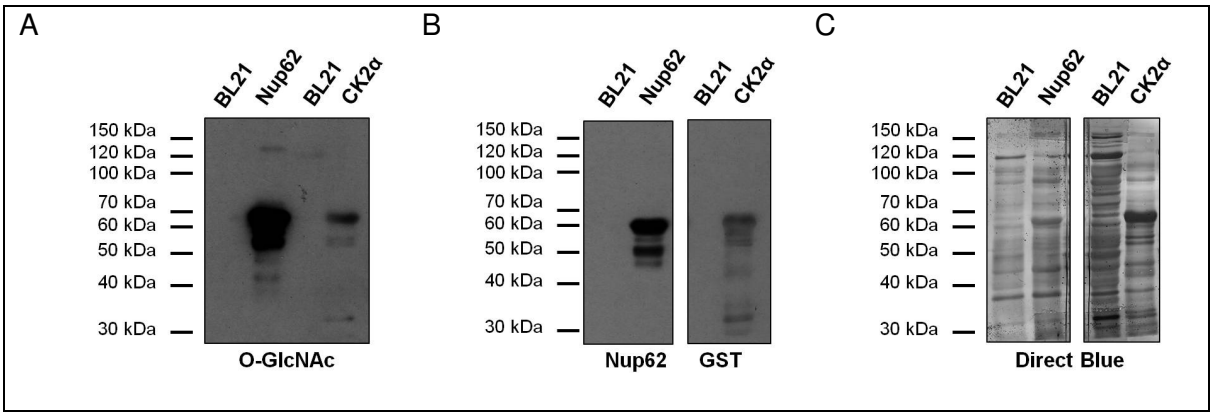

Figure 12: OGT assay with CK2α

GST-tagged CK2α along with untransformed *E. coli* BL21 (DE3) and Nup62 lysates were subjected to SDS-PAGE and Western blot transfer. After blocking, membrane was incubated for 2 hours at 37°C with OGT. **(A)** Membrane was probed for O-GlcNAc with CTD110.6 and anti-mouse-POD antibodies. **(B)** Membrane was stripped and reprobed with antibodies against Nup62 or GST. **(C)** After signal detection, membrane was stained with Direct Blue. BL21: untransformed *E. coli* BL21 (DE3) lysate; Nup62: Nup62 lysate; CK2α: GST-CK2α lysate; GST: glutathione S-transferase.

4.2.3 OGT activity assay with affinity-purified OGT

Additionally, to test if active OGT could be isolated, recombinantly expressed, His_8-tagged OGT was affinity-purified with Ni-NTA agarose as described in 3.4.2. Purified OGT was dialyzed against 2x OGT buffer prior to OGT assay and, using Nup62 as a substrate, OGT assay on the membrane was performed as described above. Probing for O-GlcNAc demonstrated that affinity-purification of OGT did not eliminate the enzyme´s activity as O-GlcNAc modification of Nup62 could be detected (data not shown).

4.2.4 OGT assay with APP and cdk5 peptides

To further characterize O-GlcNAcylation of APP and cdk5, the identification of the O-GlcNAc-bearing residue(s) on these proteins was attempted. As O-GlcNAc is found intracellularly, only the cytoplasmic domain of APP was of interest for *in vitro* O-GlcNAcylation studies. To simplify matters, only small synthetic peptides were supposed to be used for the *in vitro* OGT assay. Various peptides containing all five serine/threonine residues of AICD as well as different cdk5 peptides were purchased; peptide sequences are listed in Table 7. Selection criteria for cdk5 peptides have been described elsewhere (Novak, 2011). Briefly, two peptides included potential O-GlcNAcylation sites as determined by *in silico* O-GlcNAc analysis (Ser46, Thr245, Thr246, Ser247). A third cdk5 peptide included Ser26 which has been suggested to be potentially O-GlcNAc-modified (Godenschweger, 2007). OGT assay with peptides is described in 3.5. Briefly, OGT was immunoprecipitated and peptides were incubated with immobilized OGT for 2 hours at 37°C to allow *in vitro* O-GlcNAcylation. In accordance with a recent report analyzing O-GlcNAcylation of tau and peptides thereof, UDP-GlcNAc concentration in the OGT assay preparations was increased to 10 mM (Smet-Nocca *et al.*, 2011). Afterwards, beads were pelleted by centrifugation and the supernatant was examined by MS with B. Gehrig (Institute of Biochemistry and Molecular Biology, University of Bonn). Briefly, using commercially available kits, O-GlcNAc moieties were first labeled with azide-modified galactose and then, via “click reaction”, with a biotin-labeled alkyne (Invitrogen, 2007a; b). Biotin-labeled O-GlcNAcylated peptides were purified by avidin-biotin affinity chromatography and MALDI-LIFT-TOF/TOF analysis was applied for the identification of O-GlcNAc sites (Suckau *et al.*, 2003). However, while peptides could be identified, no O-GlcNAc was detected (data acquisition by B. Gehrig; data not shown).

4.2.5 Summary

In summary, ELISA-based OGT activity assay was successfully implemented with Nup62 as a substrate. *In vitro* O-GlcNAcylation of cdk5 was demonstrated albeit O-GlcNAc signals were weaker than for other proteins tested. Whether *in vitro* O-GlcNAcylation of APP and

cdk5 peptides was unsuccessful or could not be detected with the herein applied techniques is unclear at this point but experiments are ongoing in other groups. Lastly, it was shown that affinity-purification of His_8-tagged OGT does not abolish the enzyme´s activity.

4.3 O-GlcNAc and O-GlcNAc-cycling enzymes in the progression of AD

In this work, samples from two different brain areas, IPL and cerebellum, of subjects with AD and age-matched controls were examined for potential changes in O-GlcNAcylation. While the IPL, a subregion of the cortex, has been shown to be severely affected by AD (Greene *et al.*, 2010), the cerebellum is often used as a control because it is less affected in AD (Braak *et al.*, 1989). Samples from subjects with amnestic mild cognitive impairment (MCI), a transitional state between normal aging and early AD (Petersen, 2004), were included in this work to study possible changes in O-GlcNAcylation in the progression of AD. Full data on all cases are provided in Appendix B, a summarized version of the clinical and pathological information can be found in Table 17 and Table 18.

Table 17: Summary of clinical and pathological information of IPL cases

Group	n	Gender	Age at death	PMI (h)	Braak stage***	MMSE score***
C	12	9 F; 3 M	84.9 ± 5.3	3.1 ± 2.3	0-II	28.8 ± 1.1
MCI	10	5 F; 5 M	89.1 ±5.3	3.6 ± 2.3	III-V	24.0 ± 3.8
AD	13	9 F; 4 M	84.1 ± 5.8	3.2 ± 0.8	V-VI	12.7 ± 7.7

C: control; MCI: mild cognitive impairment; AD: Alzheimer disease; F: female; M: male; Age at death (in years); PMI: post-mortem interval (in hours); MMSE: Mini-Mental State Examination. All data are provided as mean ± SD. One-way ANOVA was performed and parameters which differed significantly between the groups are marked with asterisks. ***p < 0.0001.

Table 18: Summary of clinical and pathological information of cerebellum cases

Group	n	Gender	Age at death*	PMI (h)	Braak stage***	MMSE score***
C	8	4 F; 4 M	81.8 ± 5.4	3.7 ± 2.7	I-II	28.8 ± 1.2
MCI	8	4 F; 4 M	90.0 ±5.6	3.8 ± 2.5	III-V	24.4 ± 4.1
AD	8	4 F; 4 M	84.8 ± 5.8	3.2 ± 0.8	V-VI	11.7 ± 8.7

C: control; MCI: mild cognitive impairment; AD: Alzheimer disease; F: female; M: male; Age at death (in years); PMI: post-mortem interval (in hours); MMSE: Mini-Mental State Examination. All data are provided as mean ± SD. One-way ANOVA was performed and parameters which differed significantly between the groups are marked with asterisks. *p < 0.05; ***p < 0.0001.

In the progression of AD, neurofibrillary changes occur in a predictable spaciotemporal pattern and therefore, upon post-mortem analysis of the brain, six stages can be distinguished (I-VI) with stages V and VI corresponding with the clinical presentation of AD

(Braak and Braak, 1991; 1997). These stages, now known as Braak stages, were used to gather brain samples into the respective groups. Furthermore, patients and healthy volunteers underwent testing of coginitive function by Mini-Mental State Examination (MMSE), and, if available, MMSE scores were included for AD, MCI and control cases. Maximum MMSE score is 30 and the lower the score, the more likely it is that patients suffer from cognitive impairment (Folstein *et al.*, 1975).

Statistical comparison of samples from subjects with amnestic MCI, AD and age-matched controls revealed that Braak stages as well as MMSE scores were significantly different between the three groups ($p < 0.0001$). Within the IPL samples, age at death showed no differences between the groups. Within the cerebellar samples, age at death was significantly different ($p = 0.02$), however, post-test proved significant differences only when comparing MCI and control cases. Post-mortem interval (PMI) did not differ between any of the groups and, furthermore, it was noted, that more IPL samples were obtained from female subjects with AD and age-matched controls.

4.3.1 Analysis of IPL samples from subjects with AD

Brain samples were homogenized and submitted to subcellular fractionation as described in 3.4.5. Due to the large number of samples, samples were run on multiple precast gels with at least three samples per group and gel. Membranes were probed for O-GlcNAc and actin as a loading control as described in 3.4.11 and O-GlcNAc signals were normalized to loading control signals. Mean values of control samples were set to 100 % and % control values of different blots were combined for statistical analysis.

Pre-incubation of CTD110.6 antibody with 0.1 M GlcNAc almost completely prevented signal detection in IPL homogenates and cytosolic fractions confirming the antibody´s specificity against O-GlcNAcylated proteins (data not shown).

In IPL, cytosolic **O-GlcNAcylation** was significantly augmented in AD samples when compared to age-matched controls (119 ± 8 %; $p = 0.04$; Figure 13A,B). Noteworthy, O-GlcNAc signals showed great inter- and intra-group variations. Particularly O-GlcNAc signals at approximately 75, 50 and 27 kDa (indicated by the arrows in Figure 13A) differed greatly within the AD group and were therefore analyzed separately.

As shown in Figure 13C-E, the 75 kDa O-GlcNAc band is significantly decreased in AD while the O-GlcNAc signals at 50 kDa and 27 kDa are both increased in AD when compared to age-matched controls, however, these changes are not quite significant (75 kDa: 44 ± 7 %; $p < 0.01$; 50 kDa: 147 ± 23 %; $p = 0.07$; 25 kDa: 158 ± 27 %; $p = 0.07$). Identities and functions of these differentially O-GlcNAcylated proteins remain to be elucidated.

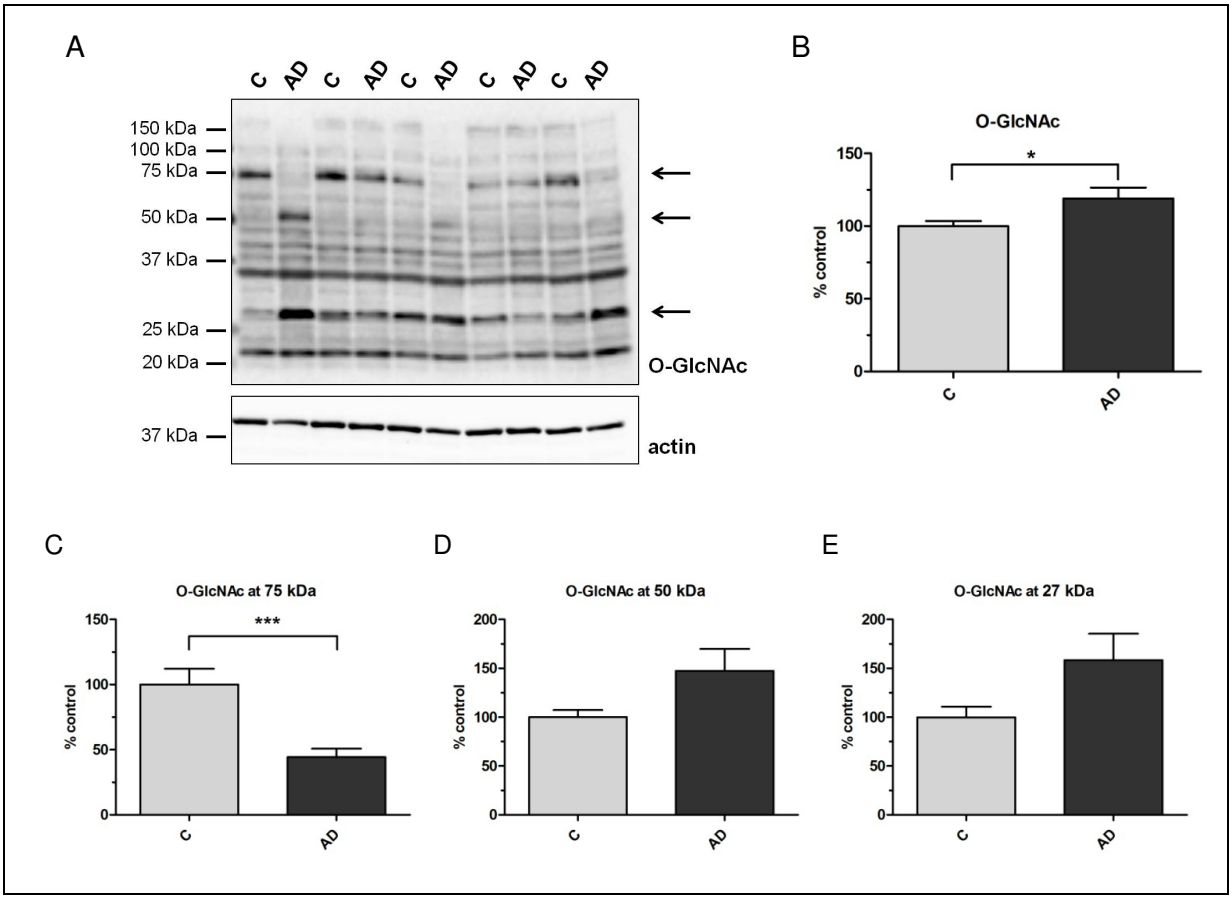

Figure 13: O-GlcNAc expression in IPL cytosolic fractions from subjects with AD and age-matched controls

(A) Representative Western blot of cytosolic fractions of IPL samples from subjects with AD and age-matched controls. Membrane was probed for O-GlcNAc with CTD110.6 and anti-mouse-POD antibodies before probing for the loading control with anti-actin and anti-rabbit-Cy5 antibodies. Arrows indicate O-GlcNAc signals at approximately 75, 50 and 27 kDa which display great variations and were therefore further analyzed. Densitometric quantification of total **(B)** or band-specific **(C-E)** O-GlcNAc signals in the cytosolic fraction of IPL samples from subjects with AD and age-matched controls. O-GlcNAc signals were normalized to actin signals, mean values of controls were set to 100 % and results were converted to % control. Data from three Western blot analyses were combined, and are shown as mean ± SEM (n = 12-13). C: control; AD: Alzheimer disease; *$p < 0.05$; ***$p < 0.001$.

For analysis of **OGA and OGT expression**, brain sample homogenates were subjected to SDS-PAGE and Western blot transfer and membranes were probed for OGA and actin as a loading control. Acquired OGA signals were normalized to loading controls, mean values of control samples were set to 100 % and % control values of different blots were combined for statistical analysis. When compared to age-matched controls, OGA expression was significantly decreased in IPL samples from subjects with AD (75 ± 8 %; $p = 0.04$; Figure 14). Probing for OGA also revealed a second albeit weaker signal at approximately 75 kDa which is not present in the secondary antibody control (data not shown). While the identity of this additional band is not entirely clear, its analysis demonstrated no difference between subjects with AD and age-matched controls (data not shown).

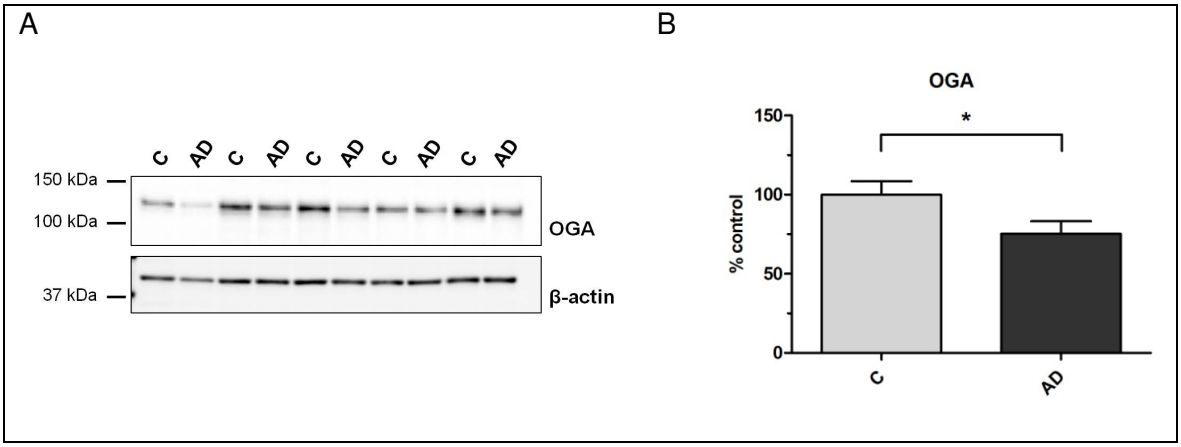

Figure 14: OGA expression in IPL samples of AD subjects and age-matched controls

(A) Representative Western blot and **(B)** densitometric quantification of OGA expression in IPL sample homogenates from subjects with AD and age-matched controls. Membranes were probed with anti-OGA and ECL anti-rabbit-POD antibodies before probing for the loading control with anti-β-actin and anti-mouse-Cy5 antibodies. OGA signals were normalized to actin signals, mean values of control samples were set to 100 % and results were converted to % control. Data from three Western blot analyses were combined and are shown as mean ± SEM (n = 12-13). C: control; AD: Alzheimer disease; ECL: enhanced chemiluminescence; *p < 0.05.

After OGA detection, membranes were stripped and reprobed for OGT with AL28 and anti-rabbit-AP antibodies. Colorimetric development revealed a band at approximately 105 kDa. In general, signal intensity was weak. However, prolonging development time resulted in the appearance of multiple additional bands, all of which were not present in the secondary antibody control (data not shown). Only the band at approximately 105 kDa was analyzed and signals were normalized to loading controls. Mean values of control samples were set to 100 % and % control values of different blots were combined for statistical analysis. As shown in Figure 15, when compared to age-matched controls, OGT expression was unchanged in AD (103 ± 5 %; p = 0.74).

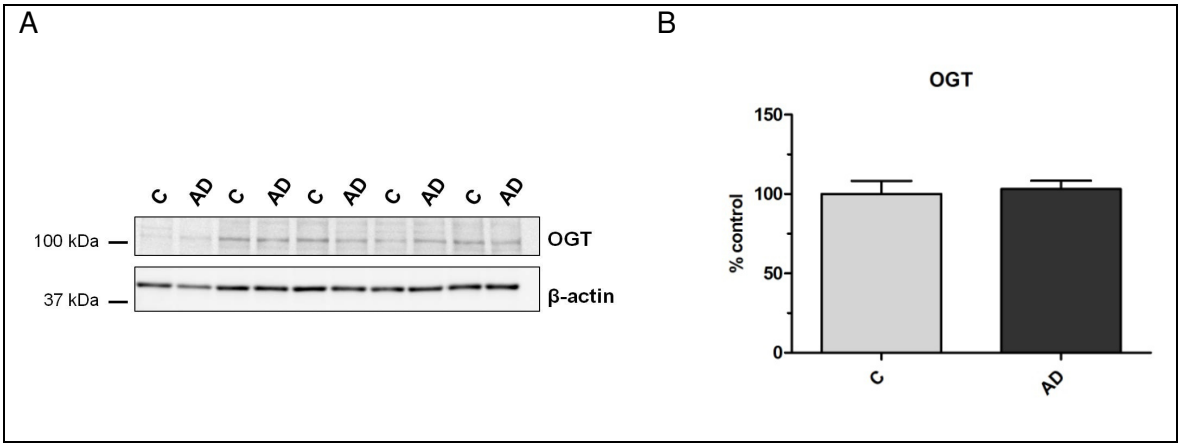

Figure 15: OGT expression in IPL samples of AD subjects and age-matched control

(A) Representative Western blot and **(B)** densitometric quantification of OGT expression in IPL sample homogenates from subjects with AD and age-matched controls. After probing for OGA and the loading control, membranes were stripped and reprobed for OGT with AL28 and anti-rabbit-AP antibodies. OGT signals were normalized to loading controls, mean values of control samples were set to 100 % and

results were converted to % control. Data from three Western blot analyses were combined and are shown as mean ± SEM (n = 12). C: control; AD: Alzheimer disease.

In a subset of samples, **OGA activity** was investigated by OGA activity assay as described in 3.6. Briefly, crude cytosolic fractions were prepared from IPL samples, interfering hexosaminidases were removed by incubation with ConA agarose and samples were desalted. Assay was performed in microtiter plates and samples as well as blanks were prepared in duplicates. Samples were incubated with the synthetic OGA substrate pNP-GlcNAc in OGA assay buffer for 2-2.5 hours at 37°C. OGA cleavage product pNP was monitored spectrophotometrically at OD_{405} and mean values of the duplicates were used for further analysis. Mean absorption of blanks was subtracted from the samples and GlcNAc release was then calculated as described elsewhere (Zachara *et al.*, 2011). Results (in µM) were divided by the assay incubation time (in minutes) to calculate enzyme activity units. OGA activity assay was repeated with more samples and, after separate calculations, the results from both assays were combined (individual results of the two OGA activity assays are included in Appendix D).

Statistical analysis revealed a significant reduction in OGA activity in IPL samples from subjects with AD when compared to age-matched controls (p = 0.01; Figure 16A). However, after normalization of OGA activity to OGA expression in the respective sample, no difference in OGA activity was found between the two groups (p = 0.96; Figure 16B).

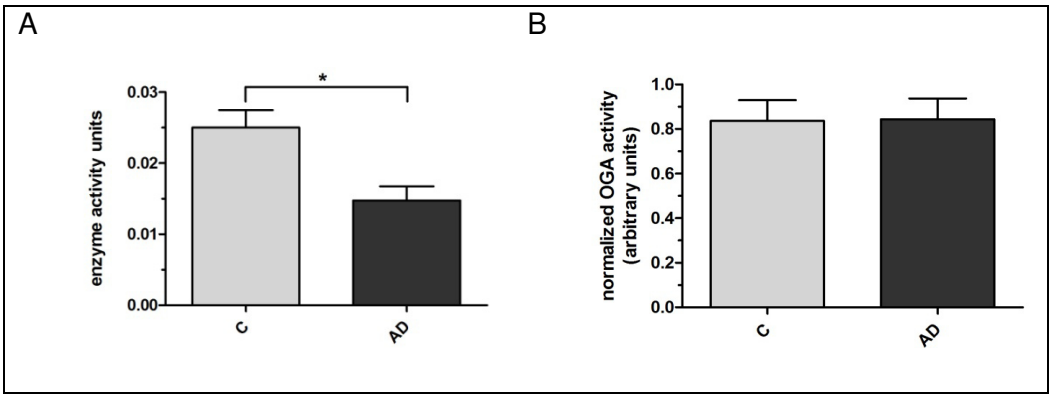

Figure 16: OGA activity in IPL samples from AD subjects and age-matched controls

(A) OGA activity in IPL samples from subjects with AD and age-matched controls was measured as cleavage of pNP-GlcNAc. Crude cytosolic fractions were prepared, interfering hexosaminidases were removed by incubation with ConA agarose and samples were desalted. Samples were incubated with the synthetic OGA substrate pNP-GlcNAc in OGA assay buffer and absorbance of free pNP was detected at 405 nm. Results of two individual experiments were combined for a total of n = 5; data are shown as mean ± SEM enzyme activity units where one unit represents the amount of enzyme catalyzing the release of 1 µmol/min of pNP from pNP-GlcNAc. **(B)** OGA enzyme activity units were normalized to OGA expression (as % control) in the respective IPL sample homogenates and results are presented in arbitrary units as mean ± SEM (n = 5). C: control; AD: Alzheimer disease; *p < 0.05.

4.3.2 Analysis of IPL samples from subjects with MCI

O-GlcNAc levels in cytosolic fractions from IPL samples of subjects with MCI were slightly but not significantly increased when compared to controls (112 ± 9 %; p = 0.23; Figure 17).

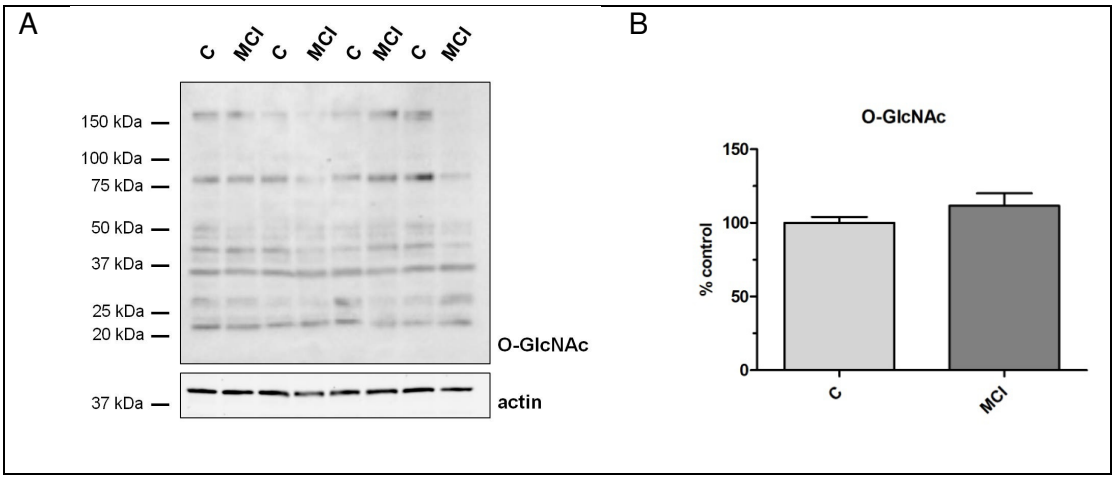

Figure 17: O-GlcNAc expression in IPL cytosolic fractions of control and MCI subjects

(A) Representative Western blot and **(B)** densitometric quantification of O-GlcNAc expression in cytosolic fractions of IPL samples from MCI and control subjects. Membrane was probed for O-GlcNAc with CTD110.6 and anti-mouse-POD antibodies before probing for the loading control with anti-actin and anti-rabbit-Cy5 antibodies. O-GlcNAc signals were normalized to actin signals, mean values of controls were set to 100 % and results were converted to % control. Data from two Western blot analyses were combined and are shown as mean ± SEM (n = 10). C: control; MCI: mild cognitive impairment.

As illustrated in Figure 18, **OGA expression** was unaltered when comparing samples from amnestic MCI and control subjects (109 ± 11 %; p = 0.62).

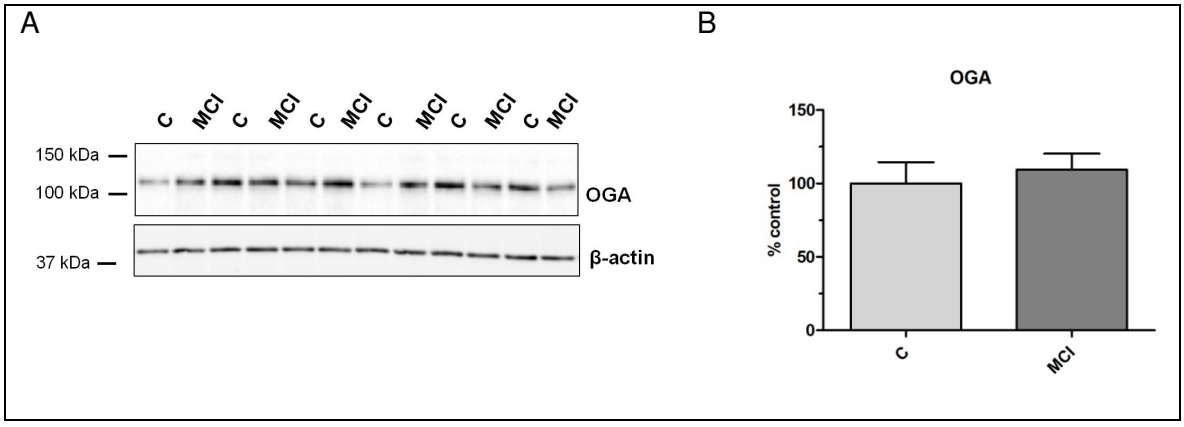

Figure 18: OGA expression in IPL samples of control and MCI subjects

(A) Western blot and **(B)** densitometric quantification of OGA signals in IPL sample homogenates from control and MCI subjects. Membranes were probed with anti-OGA and ECL anti-rabbit-POD antibodies before probing for the loading control with anti-β-actin and anti-mouse-Cy5 antibodies. OGA signals were normalized to β-actin signals, mean value of controls was set to 100 % and results were converted to % control. Data are shown as mean ± SEM (n = 6). C: control; MCI: mild cognitive impairment; ECL: enhanced chemiluminescence.

After OGA detection, membranes were stripped and reprobed for OGT. **OGT expression** was unaltered in MCI samples when compared to controls (104 ± 7 %; p = 0.85; Figure 19).

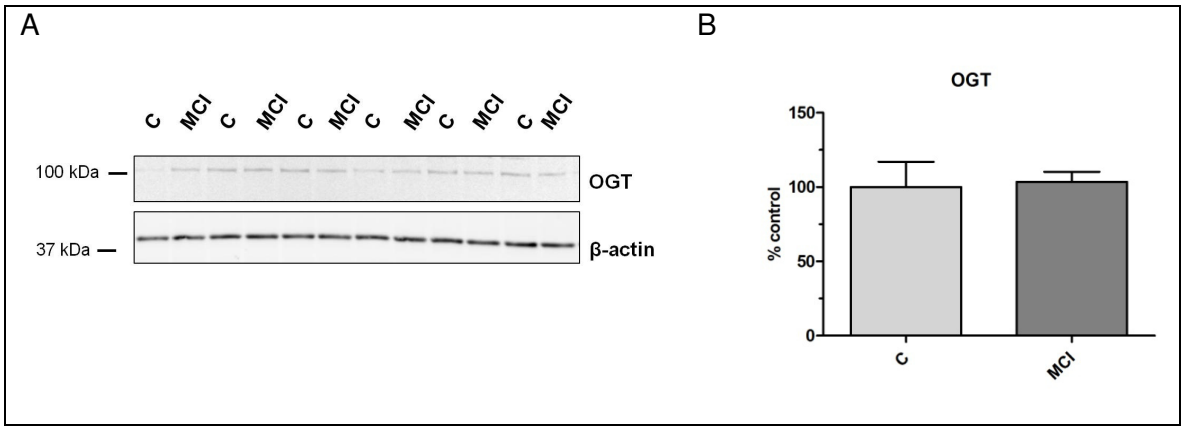

Figure 19: OGT expression in IPL samples of control and MCI subjects

(A) Western blot and **(B)** densitometric quantification of OGT expression in IPL sample homogenates from control and MCI subjects. After probing for OGA and loading control, membranes were stripped and reprobed for OGT with AL28 and anti-rabbit-AP antibodies. OGT signals were normalized to the loading controls, mean value of controls was set to 100 % and results were converted to % control. Data are shown as mean ± SEM (n = 6). C: control; MCI: mild cognitive impairment.

4.3.3 Analysis of cerebellar samples from subjects with MCI and AD

Cerebellar samples were subjected to SDS-PAGE and Western blot and membranes were probed for O-GlcNAc and actin as a loading control as described above. However, densitometric analysis demonstrated a significant decrease of cytosolic actin expression in the cerebellum of subjects with AD (data not shown). Cytosolic GAPDH expression, in constrast, was unaltered when comparing cerebellar samples from subjects with AD and age-matched controls. Therefore, cytosolic O-GlcNAc expression was normalized to GAPDH signals in cerebellar samples.

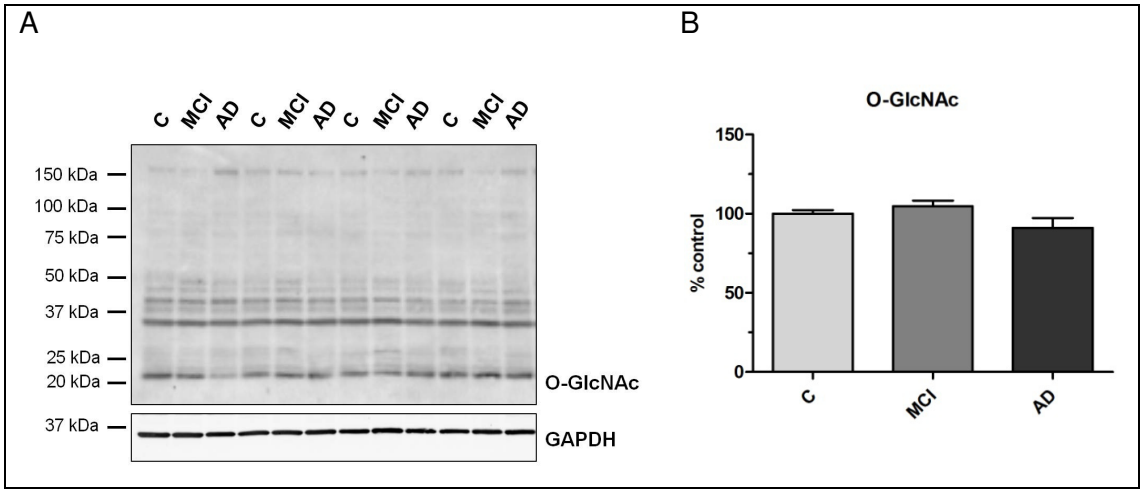

Figure 20: O-GlcNAc expression in the cytosolic fraction of cerebellar samples

(A) Representative Western blot and **(B)** densitometric quantification of O-GlcNAc signals in cytosolic fractions of cerebellum samples from control, MCI, and AD subjects. Membrane was probed for O-GlcNAc with CTD110.6 and anti-mouse-POD antibodies before probing for the loading control with anti-GAPDH and anti-mouse-Cy5 antibodies. O-GlcNAc signals were normalized to GAPDH signals, mean values of controls were set to 100 % and results were converted to % control. Data from two Western blot analyses were combined and are shown as mean ± SEM (n = 8). C: control; MCI: mild cognitive impairment; AD: Alzheimer disease.

As shown in Figure 20, there were no significant differences in cytosolic **O-GlcNAcylation** between the three groups, however, O-GlcNAc expression was slightly decreased in AD (MCI: 105 ± 4 %; AD: 91 ± 6 %; p = 0.10;). Interestingly, O-GlcNAc signal pattern in cerebellum seemed to differ from that in IPL (see Figure 13).

Cerebellar **OGA expression** was also unaltered between the three groups (Figure 21). Although OGA expression seemed slightly increased in subjects with MCI and decreased in subjects with AD when compared to age-matched controls, these differences were not significant (MCI: 108 ± 15 %; AD: 82 ± 12 %; p = 0.36).

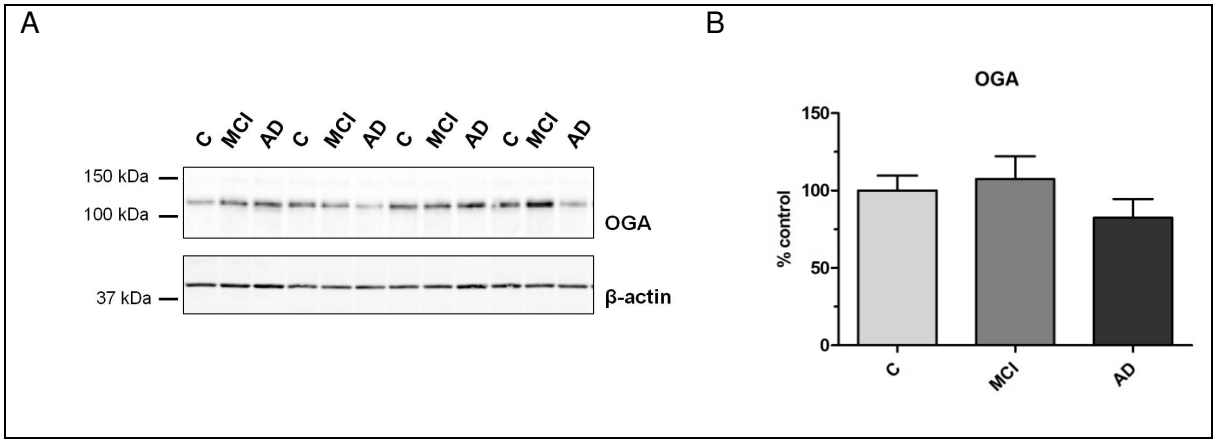

Figure 21: OGA expression in the cerebellum

(A) Representative Western blot and **(B)** densitometric quantification of OGA expression in cerebellar sample homogenates from control, MCI and AD subjects. Membranes were probed with anti-OGA and ECL anti-rabbit-POD antibodies before probing for the loading control with anti-β-actin and anti-mouse-Cy5 antibodies. OGA signals were normalized to β-actin signals, mean values of controls were set to 100 % and results were converted to % control. Data from two Western blot analyses were combined and are shown as mean ± SEM (n = 8). C: control; MCI: mild cognitive impairment; AD: Alzheimer disease; ECL: enhanced chemiluminescence.

After OGA detection, membranes were stripped and reprobed for OGT. As illustrated in Figure 22, **OGT expression** in the cerebellum seemed to decrease with the progression of AD, however this trend was not significant (MCI: 98 ± 4 %; AD: 82 ± 7 %; p = 0.09).

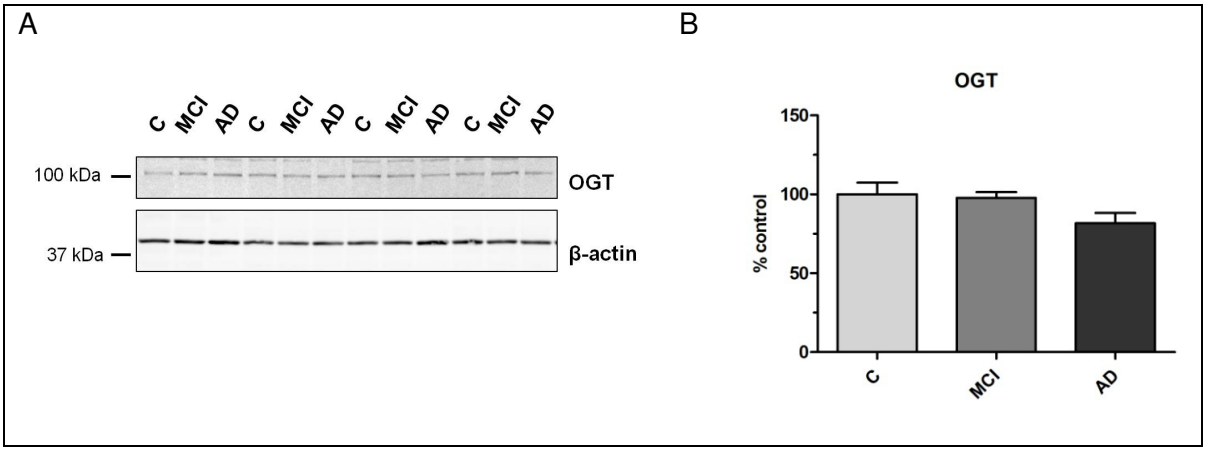

Figure 22: OGT expression in the cerebellum

(A) Representative Western blot and **(B)** densitometric quantification of OGT expression in cerebellar sample homogenates from control, MCI and AD subjects. After probing for OGA and loading controls, membranes were stripped and reprobed for OGT with AL28 and anti-rabbit-AP antibodies. OGT signals were normalized to the loading controls and signals were converted to % control. Data from two Western blot analyses were combined and data are shown as mean ± SEM (n = 8). C: control; MCI: mild cognitive impairment; AD: Alzheimer disease.

4.3.4 Correlation studies

Analysis of potential correlations in IPL samples

Correlation analyses of IPL samples from subjects with AD and age-matched controls (Figure 23) demonstrated an inverse relationship between cytosolic O-GlcNAcylation and OGA levels. This relationship could not be detected when comparing IPL samples from control and MCI subjects. In AD and MCI samples, cytosolic O-GlcNAc levels correlated inversely with MMSE scores but no significant correlation of O-GlcNAc with Braak stage was detected. Furthermore, OGA and OGT protein levels were positively correlated in IPL samples.

Analysis of potential correlations in the cerebellum

No relationship was found between cytosolic O-GlcNAcylation expression and OGA levels in the cerebellum but interestingly, O-GlcNAc correlated positively with OGT levels ($r = 0.55$; $p < 0.01$; data not shown). As demonstrated in IPL samples, also in the cerebellum, OGA and OGT levels were positively correlated in control, MCI and AD samples ($r = 0.46$; $p = 0.02$; data not shown).

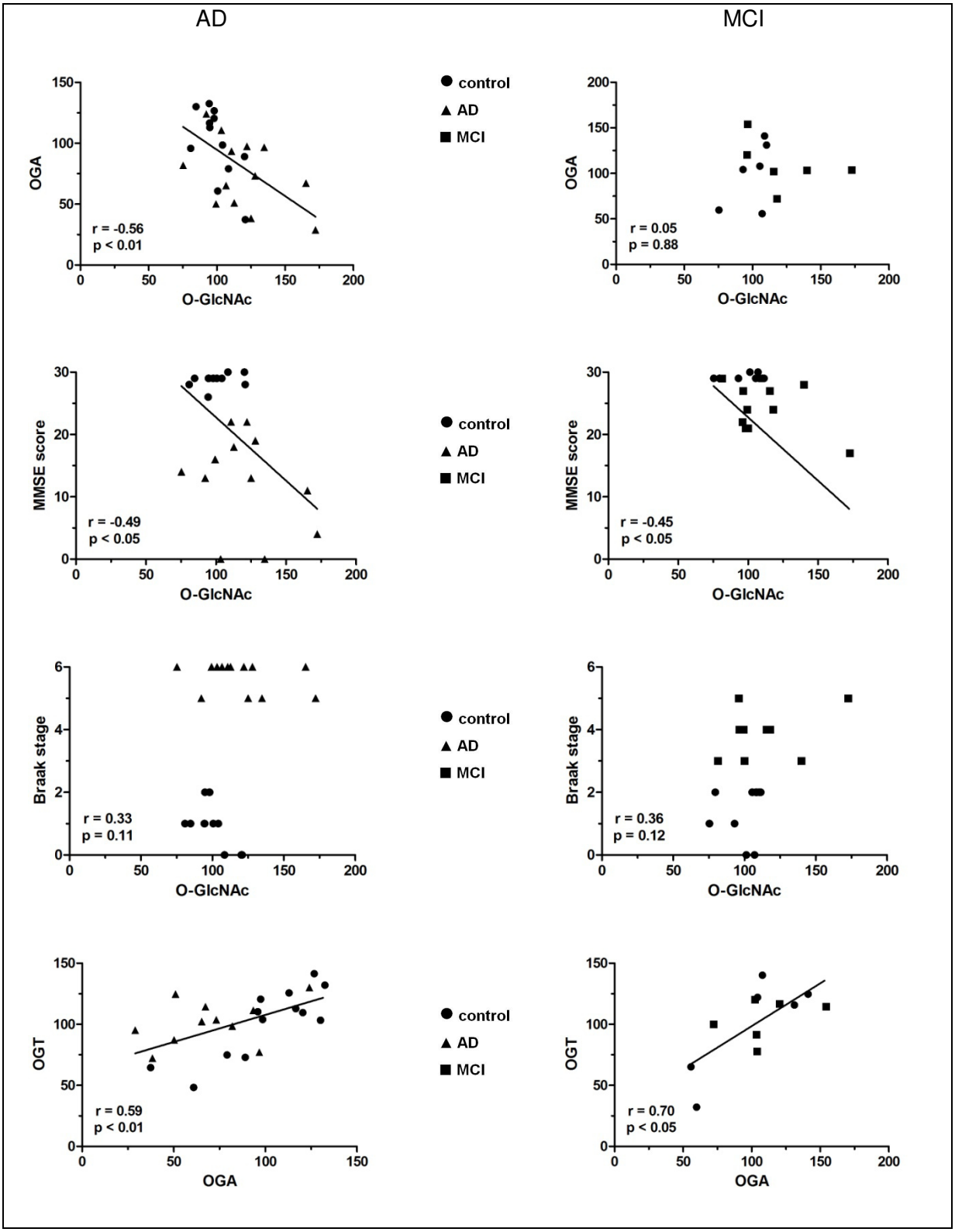

Figure 23: Analysis of potential correlations between various factors in IPL samples

Correlation analyses were performed between various factors in IPL samples from control and MCI or AD subjects. Global cytosolic O-GlcNAc levels as well as OGA and OGT protein levels were determined by Western blot analyses. OGA and OGT signals as well as MMSE scores and Braak stages were then plotted against the corresponding O-GlcNAc or OGA signals. For visualization, a linear regression line is included in the graphs where Pearson correlation reached significance ($p < 0.05$). r: Pearson correlation coefficient; MMSE: Mini-Mental State Examination; C: control; AD: Alzheimer Disease; MCI: mild cognitive impairment.

4.3.5 Summary

In summary, increased cytosolic O-GlcNAc and decreased OGA expression and activity was observed in IPL samples from subjects with AD when compared to age-matched controls. In AD IPL samples, augmented O-GlcNAcylation correlated with reduced OGA expression. OGT expression was unaltered in AD when compared to age-matched controls. Furthermore, augmented O-GlcNAcylation seemed to correlate with increased disease severity as indexed by decreasing MMSE scores and increasing Braak stages. In IPL samples from subjects with amnestic MCI, expression of O-GlcNAc, OGA, and OGT were not significantly altered when compared to samples from control subjects. Also cerebellar samples from subjects with AD or MCI showed no significant differences in O-GlcNAcylation or OGA and OGT expression when compared to controls.

5 Discussion

Below, the results of O-GlcNAc modulation in SY5Y-APP cells, implementation of *in vitro* OGT assays and analysis of O-GlcNAcylation and O-GlcNAc cycling enzymes in the progression of AD are discussed separately. When relevant, the applied methods are reviewed including their strengths and weaknesses and potential future directions are proposed. Lastly, the results obtained in this thesis and by others previously are combined in a comprehensive overview.

5.1 Effects of O-GlcNAc modulation on APP processing

Potential effects of O-GlcNAc modulation on APP processing were tested in SH-SY5Y cells stably transfected with APP_{695} cDNA. APP-overexpressing cells were chosen based on a recent report demonstrating that detection of endogenous sAPPβ and Aβ was not possible in conditioned media of untransfected SH-SY5Y cells (Harris *et al.*, 2009).

5.1.1 OGA inhibition by NButGT

Modulation of O-GlcNAc levels was achieved by treatment of the cells with NButGT, a cell permeable, highly selective OGA inhibitor (Macauley *et al.*, 2005). As expected, inhibition of OGA significantly increased global O-GlcNAcylation. Consistent with a previous report (Jacobson and Iverfeldt, 2011), OGA inhibition also significantly increased APP-specific O-GlcNAcylation. Interestingly, NButGT treatment had no significant effects on APP expression or its processing by α- or β-secretases (analyzed as sAPPα/β). These results stand in contrast to previous reports using a different inhibitor of OGA, O-(2-Acetamido-2-deoxy-D-glucopyranosylidene)amino-N-phenylcarbamate (PUGNAc). After treatment with PUGNAc for 1 hour, sAPPα level in conditioned medium from murine N2a cells expressing human APP_{695} was slightly augmented (Kellersmann, 2003); in SH-SY5Y cells, this increase was highly significant after 24 hours of treatment (Jacobson and Iverfeldt, 2011). Unfortunately, both studies did not analyze sAPPβ levels, however, Jacobsen and Iverfeldt report reduced $Aβ_{40}$ concentration in conditioned medium after PUGNAc treatment (Kellersmann, 2003; Jacobson and Iverfeldt, 2011). Possible reasons for the observed discrepancies may include the use of different cell lines and wild-type versus transfected cells, different sample preparation and/or ways of presenting the results as well as the use of different OGA inhibitors.

Both overexpression of APP_{695} and the use of different cell lines have been demonstrated to influence APP processing. Comparison of sAPPα and sAPPβ levels from mock and APP_{695}-cDNA transfected SH-SY5Y cells suggested altered APP processing in APP-overexpressing

cells. In SY5Y-APP cells, sAPPα secretion was increased about 1.5-fold while the level of sAPPβ in conditioned media increased more than 35-fold when compared to mock transfected cells. Furthermore, Belyaev and coworkers compared APP processing in different cell lines (human embryonic kidney cells (HEK293), N2a and SH-SY5Y) that had been transfected with the cDNA of wild-type APP and found that especially sAPPβ levels differed greatly between the cell lines (Belyaev *et al.,* 2010). These results indicate that studies analyzing APP processing in different cell lines and especially when working with APP overexpressing cells may not be comparable.

The contradicting results of OGA inhibition on APP processing may also arise from different sample preparation and/or ways of presenting the results. Kellersmann seeded the same number of cells for various treatments and upon analysis, loaded equal volumes of conditioned medium onto polyacrylamide gels. Comparison of the signals of secreted APP fragments (total sAPP and sAPPα) was performed without any further normalization (Kellersmann, 2003). In agreement with Kellersmann, in this work, equal volumes of conditioned medium were subjected to SDS-PAGE and Western blot analysis. However, since conditioned medium was harvested several days after seeding of the cells, and to account for potential differential effects of the treatments on cell viability and growth rates, sAPPα/β signals were normalized to total sAPP secretion. In contrast, in the study by Jacobsen and Iverfeldt, conditioned medium was applied to the gels in different volumes but corresponding to the same protein amount of the lysates (Jacobsen and Iverfeldt, 2011).

The aforementioned discrepancies may also be the consequence of the use of different OGA inhibitors as PUGNAc and NButGT may have diverse effects. In contrast to NButGT which is highly specific for OGA (Macauley *et al*., 2005), PUGNAc additionally inhibits other glucoside hydrolases and shows no selectivity for OGA over lysosomal β-hexosaminidases (Horsch *et al*., 1991; Dong and Hart, 1994; Macauley *et al*., 2005). Furthermore, PUGNAc leads to decreased growth rates and viability of different cell lines and has been shown to cause insulin resistance in adipocytes (Slawson *et al*., 2005; Macauley *et al*., 2008; 2010). Consequently, results obtained using PUGNAc need to be interpreted critically and with regards to possible off-target effects. NButGT, as used in this work, should be preferred to PUGNAc for future cell culture studies.

5.1.2 Effects of Alloxan and PMA

In contrast to OGA, OGT inhibition is more challenging due to the lack of specific and commercially available inhibitors. Alloxan was the first OGT inhibitor described although it is mainly used as a diabetogenic compound in diabetes research (Konrad *et al*., 2002; Lenzen, 2008). Despite previous results showing decreased O-GlcNAcylation of APP in SH-SY5Y

cells after treatment with 1 mM Alloxan (Jacobsen and Iverfeldt, 2011), in this work, a higher Alloxan concentration (5 mM) was used based on pretests demonstrating that lower concentrations did not reduce global O-GlcNAcylation. Conversely, Alloxan has also been shown to inhibit OGA (Lee *et al.*, 2006). In fact, Alloxan may exert differential effects based on its concentration since 1 mM Alloxan was sufficient for complete inhibition of OGT, but at least 5 mM Alloxan were necessary for significant inhibition of recombinant OGA (Konrad *et al.*, 2002; Lee *et al.*, 2006). Furthermore, Alloxan induces the generation of reactive oxygen species and may thereby indirectly influence protein O-GlcNAcylation as O-GlcNAc expression has been demonstrated to increase in response to oxidative stress (Zachara *et al.*, 2004; Lenzen, 2008). Although Alloxan treatment successfully decreased O-GlcNAcylation in pre-tests (data not shown) and has been used to inhibit OGT (Dehennaut *et al.*, 2007; Jacobsen and Iverfeldt, 2011; Gurel *et al.*, 2014), in this work, Alloxan exerted inconsistent effects on global O-GlcNAcylation and, unexpectedly, increased APP´s O-GlcNAcylation. In retrospect, since Alloxan dose-dependently inhibits both OGT and OGA (Konrad *et al.*, 2002; Lee *et al.*, 2006; Ranuncolo *et al.*, 2012), a different method of OGT inhibition should have been preferred.

Cells were further treated with PMA, an activator of protein kinase C (Gonzales *et al.*, 1987), but also the influence of PMA on global O-GlcNAcylation was inconsistent. In agreement with the proposed “yin-yang” relation of O-GlcNAcylation and phosphorylation, PMA treatment has previously been shown to (indirectly, via the induction of protein kinase C) decrease O-GlcNAcylation in primary cerebellar neurons (Griffith and Schmitz, 1999). Interestingly, this reduction was significant only in the detergent-insoluble cytoskeletal fraction while PMA had no effect on O-GlcNAcylation in the detergent-soluble fraction (Griffith and Schmitz, 1999). Results in this work may have been clearer, if the same fractionation had been performed. Independent of its (indirect) effects on O-GlcNAcylation, PMA has been demonstrated to alter APP processing in favor of α-secretase cleavage (Hung *et al.*, 1993; Qiu *et al.*, 2001). In agreement, in this work, the only reproducible effect of PMA treatment was significantly increased sAPPα secretion. Furthermore, protein kinase C, amongst other kinases, has been shown to phosphorylate both APP and PS1 (Gandy *et al.*, 1988; Seeger *et al.*, 1997) which may consequently have biased the observed effects on APP processing.

Based on the inconsistent results of Alloxan treatment on global O-GlcNAcylation in combination with its described side effects as well as the multiple consequences of activation of protein kinase C by PMA a discussion of the obtained results seems unreasonable. Whether the observed changes in APP processing were in fact the consequences of altered O-GlcNAcylation or whether they were attributable to off-target effects is not known. The use of a more specific mode of OGT inhibition might have clarified these questions.

In parallel to this work, Vocadlo *et al.* have implemented a “Trojan horse strategy” to generate cellular OGT inhibitors: modified metabolic UDP-GlcNAc precursors (GlcNAc derivates with the ring oxygen replaced by sulfur (5S)) were processed normally through the HBP but the resulting UDP-5SGlcNAc was found to inhibit OGT *in vitro* and in cell culture (Gloster *et al.*, 2011). This method of OGT inhibition appears to be highly suitable for future studies investigating the influence of decreased O-GlcNAcylation on the processing of APP. Alternatively, OGT expression can be knocked down by RNA interference (Robinson *et al.*, 2007; Ranunculo *et al.*, 2012).

5.1.3 O-GlcNAcylation of APP

To further characterize the O-GlcNAc modification of APP, APP was immunoprecipitated or separated by 2D gel electorophoresis prior to analysis by Western blot. APP-IP experiments indicated that the lower molecular weight band at approximately 110 kDa corresponding to the immature form of APP_{695} was O-GlcNAc-modified (Figure 6). This is in agreement with a previous report investigating the O-GlcNAcylation of APP in AD brain (Werner, 2004). Interestingly and in accordance with the “yin-yang” hypothesis, this result is further corroborated by the finding that immature APP_{695} is not phosphorylated in rodent brain (Oishi *et al.*, 1997; Iijima *et al.*, 2000). In contrast, Western blot analysis after 2D SDS-PAGE pointed towards O-GlcNAcylation of mature APP. So far no explanation for this discrepancy has been found. It should be noted that sample preparation for 2D SDS-PAGE differs greatly from that for IP and subsequent SDS-PAGE as buffers have to be adjusted for IEF (urea instead of RIPA lysis buffer) and proteins are enriched by chloroform-methanol precipitation. 2D analysis further revealed that only a subpopulation of APP is O-GlcNAc-modified and this subpopulation is more basic than the majority of APP. In contrast to negatively charged phosphate groups, O-GlcNAc moieties are uncharged, thus their addition does not affect the protein´s net charge. The observed shift in charge implies that O-GlcNAcylated APP may be less phosphorylated. Whether upregulation of O-GlcNAc results in decreased APP phosphorylation remains to be elucidated.

5.1.4 Analysis of Aβ peptides

As described in the Introduction (see 1.2.3), Aβ peptides of various lengths and characteristics are generated under physiological and pathophysiological conditions. According to the “β-amyloid cascade hypothesis”, Aβ deposition was long thought to be the causative agent in AD pathogenesis (Hardy and Higgins, 1992; see Figure 24). However, this model has been contested by the discovery of pronounced AD pathology, including high abundance of senile plaques, in cognitively normal patients (Davis *et al.*, 1999).

In fact, not the number of senile plaques but the levels of $A\beta_{40}$ and $A\beta_{42}$ peptides were found to correlate with cognitive decline (Näslund *et al.*, 2000). Compared to non-demented controls, AD brains contain more soluble Aβ peptides and in addition, a substantial degree of Aβ peptides is N-terminally truncated (Lue *et al.*, 1999; Sehlin *et al.*, 2012). Increasing evidence indicates that soluble oligomers are the toxic form of Aβ and noteworthy, Aβ oligomerization begins intracellularly (Walsh *et al.*, 2000; Wirths *et al.*, 2004). Furthermore, intracellular Aβ accumulation precedes extracellular amyloid deposition in the brains of subjects with AD or Trisomy 21 (Gouras *et al.*, 2000; Mori *et al.*, 2002). Based on these and other studies, a modified β-amyloid cascade hypothesis has been suggested in which the intraneuronal accumulation of Aβ marks the first pathological alteration in AD brain (Wirths *et al.*, 2004; Figure 24).

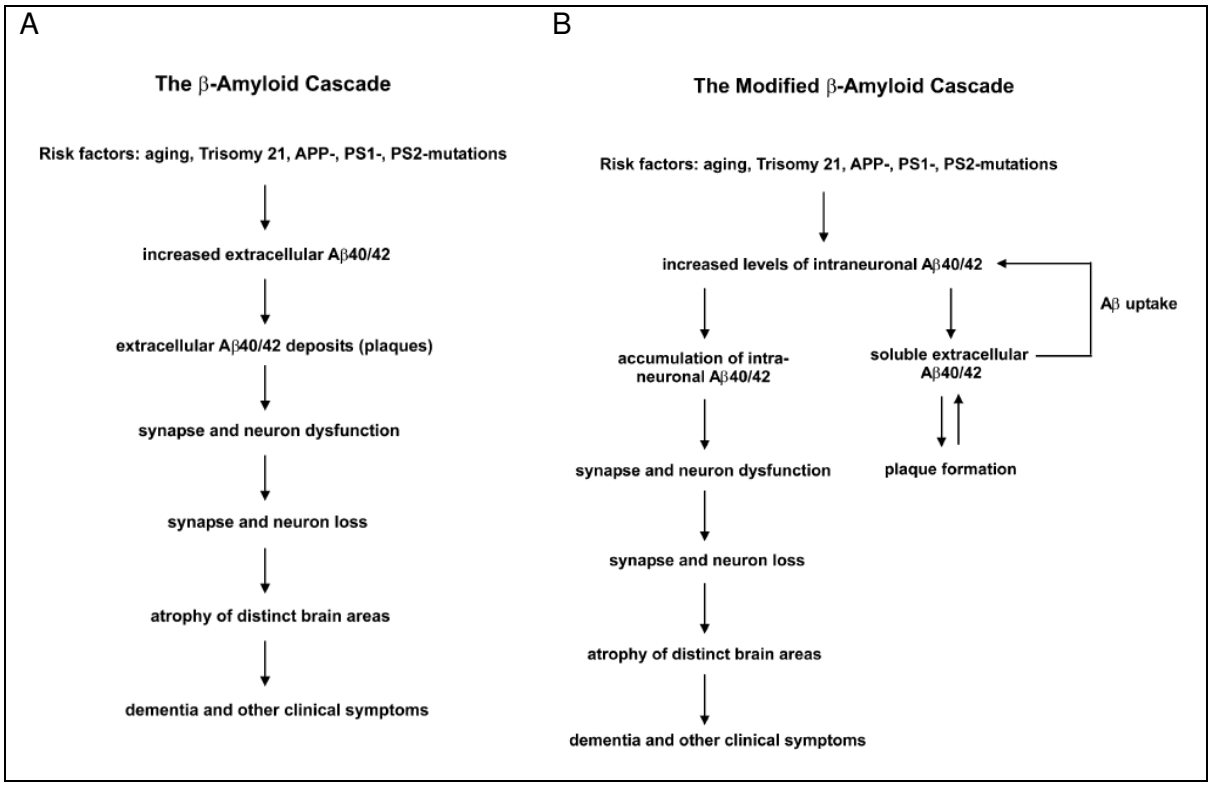

Figure 24: The β-amyloid cascade (Wirths *et al.*, 2004)

Comparison of **(A)** the original β-amyloid cascade hypothesis according to Hardy and Higgins (1992) and **(B)** the modified β-amyloid cascade hypothesis by Wirths *et al.*, 2004. APP: amyloid precursor protein; PS1: presenilin 1; PS2: presenilin 2.

Intra- and extracellular (soluble) Aβ was supposed to be analyzed to determine whether O-GlcNAc modulation had an effect on the quantity and/or composition of Aβ species. Aβ levels should be quantified by Western blot analysis after bicine/Tris/urea SDS-PAGE. This electrophoretic system was originally designed for the separation and detection of peptides and small proteins with molecular weights ranging from 1 to 100 kDa and has been successfully used for the separation and detection of Aβ peptides (Wiltfang *et al.*, 1991;

Klafki *et al.*, 1996). In this work, however, no endogenous Aβ could be detected, not even after enrichment by IP. This was not due to methodical errors since synthetic $Aβ_{(1-40)}$ could be detected with Aβ-specific antibodies (data not shown). For the analysis of Aβ by Western blot, some studies describe boiling of the nitrocellulose membrane for 5 minutes in PBS prior to blocking and antibody incubation (Ida *et al.*, 1996; Sastre, 2010). In this work, membranes were routinely incubated in warm PBS to increase signal sensitivity (based on Swerdlow *et al.*, 1986). Whether Aβ detection could have been improved by boiling of the membranes was not tested.

Next, a different technique was applied for the analysis of Aβ peptides. Using MALDI-TOF MS, the detection of as little as 1 nM (corresponding to 450 pg/ml) of $Aβ_{(1-42)}$ has been described (Wang *et al.*, 1996). Furthermore, MALDI-TOF MS allows for the characterization of Aβ signatures in biological matrices such as conditioned media or cerebrospinal fluid (Wang *et al.*, 1996; Portelius *et al.*, 2006). To concentrate sample, secreted Aβ was immunoprecipitated prior to MS analysis (Uljon *et al.*, 2000; Öckl, 2007), but Aβ signals could only be observed for positive controls where synthetic $Aβ_{(12-28)}$ was added to the sample. The included detergent further complicated signal detection as it produced a specific pattern of peaks that interfere with MS analysis (Keller *et al.*, 2008). Omitting detergent or exchanging Triton X-100 for octyl-β-D-glucopyranoside ameliorated the problem of signal interference, but endogenous Aβ remained undetectable (data not shown).

Based on its hydrophobic character, Aβ may adsorb to or aggregate in sample tubes, further reducing the concentration of (soluble) Aβ in the samples. To decrease potential adsorption to sample vials, specific LoBind Tubes (Eppendorf, Hamburg (DE)) were utilized for sample preparation and storage; also 1 % BSA was included in the samples based on a report showing that the presence of BSA significantly improved peptide recovery from different glass or plastic wares (Goebel-Stengel *et al.*, 2011). Unfortunately, despite different variations of the protocol detection of endogenous Aβ remained unsuccessful and therefore, the potential effects of O-GlcNAc modulation on Aβ peptides could not be analyzed.

During the course of this work, elevated O-GlcNAcylation of APP (by PUGNAc treatment) was demonstrated to decrease the concentration of $Aβ_{40}$ in conditioned medium of SH-SY5Y cells (Jacobsen and Iverfeldt, 2011). However, potential effects on $Aβ_{42}$ as well as on intracellular Aβ pools were not analyzed.

5.2 OGT assays

5.2.1 Implementation of an ELISA-based OGT assay

For the development and implementation of *in vitro* OGT assays, recombinantly expressed His_8-tagged Nup62 was chosen as a substrate. Nup62 was lysed in urea buffer, affinity-purified and denatured protein was then allowed to refold by the stepwise removal of urea (based on Lubas *et al.*, 1995). Despite the fact that increasing amounts of Nup62 precipitated with each dialysis step, a small amount of Nup62 remained soluble and could be used for the implementation of an ELISA-based OGT assay. After adsorption of native (refolded) or denatured Nup62 to the wells of a microtiter plate, *in vitro* OGT assay was performed with recombinant OGT. O-GlcNAcylation of Nup62 could be detected with O-GlcNAc-specific antibodies proving successful implementation of the ELISA-based OGT assay.

Comparison of the results of OGT assays with native and denatured Nup62 clearly demonstrated stronger O-GlcNAc signals when using denatured protein which may have been due to the low final concentration of refolded Nup62. Also, denatured proteins may expose additional O-GlcNAc sites that, due to tertiary or quaternary structure, may otherwise not have been accessible for OGT. It should be noted however, that the final three-dimensional structure of refolded Nup62 may differ significantly from that of the native protein. Moreover, *in vitro* O-GlcNAcylation of isolated proteins may not represent *in vivo* conditions as both OGT and protein substrates could have interaction partners that may facilitate or impede O-GlcNAcylation *in vivo*. Nevertheless, this assay can provide a first indication for potential O-GlcNAcylation of a protein of interest.

The incubation of negative controls lacking either Nup62 or OGT with O-GlcNAc-specific antibodies produced weak background signals indicating a small degree of unspecific binding of both the CTD110.6 and the RL2 antibody. To circumvent this problem, a different detection method may be applied. Commercially available Click-iT kits take advantage of the copper-catalyzed cycloaddition or “click reaction” between an azide and an alkyne (Rostovtsev *et al.*, 2002; Invitrogen, 2007a). Similar to the labeling of O-GlcNAc with [^{3}H]galactose which is catalyzed by galactosyltransferase, O-GlcNAc moieties can be labeled with azide-modified galactose using a mutant β-1,4-galactosyltransferase. Via the click reaction, the azide then reacts with a differentially labeled alkyne (e.g. biotin- or dapoxyl-alkyne) forming a stable triazole conjugate (Ramakrishnan and Qasba, 2002; Khidekel *et al.*, 2003; Invitrogen, 2007b). Biotin-labeled O-GlcNAc can be detected with Streptavidin-POD; alternatively, dapoxyl-labeled O-GlcNAc can be quantified spectrophotometrically. Recently, a similar OGT assay has been described where, instead of UDP-GlcNAc, UDP-N-azidoacetylglucosamine (UDP-GlcNAz) was included as the sugar donor. The resulting

GlcNAz-modification of OGT substrate (Nup62 and CK2α) was then demonstrated with RL2 antibody or, after click reaction using TAMRA-conjugated alkyne, with anti-TAMRA antibody (Kim *et al.*, 2014).

A great advantage of ELISA-based assays is that a multitude of different proteins or peptides can be analyzed simultaneously for possible O-GlcNAcylation. Furthermore, characterization of OGT has been difficult based on the lack of sensitive, quick and economical assays as common OGT activity assays involve the measurement of [^{3}H]GlcNAc incorporation into peptides or proteins (e.g. Haltiwanger, 1990; Marshall *et al.*, 2003; Cheung and Hart, 2008; Liu *et al.*, 2012). The assay described in this work may circumvent the need for expensive isotopes for the analysis of OGT activity. In addition, using affinity-purified recombinant OGT, this assay may facilitate rapid screening of potential OGT inhibitors. Whether this ELISA-based OGT assay can be applied for quantitative purposes remains to be investigated but it certainly provides a promising tool for the future.

5.2.2 *In vitro* O-GlcNAcylation of cdk5

Data from our group strongly suggests that cdk5 is O-GlcNAcylated (Kellersmann, 2003; Schmitt, 2009; Nowak, 2011). Cdk5, amongst others, phosphorylates APP as well as tau and appears to be implicated in AD pathogenesis (Ando *et al.*, 2001; Cruz and Tsai, 2004). For further characterization, *in vitro* O-GlcNAcylation of recombinant cdk5 was performed. OGT assay on the membrane demonstrated very weak O-GlcNAc signals on cdk5 when compared to Nup62. Weaker O-GlcNAcylation was also detected when the OGT assay was performed with CK2α. This phenomenon has also been observed by others and can be explained by *in silico* O-GlcNAc analysis (Gupta and Brunak, 2002; Lazarus *et al.*, 2006). In contrast to Nup62 which contains seventy potential O-GlcNAc sites, CK2α and cdk5 contain only ten and four potential O-GlcNAc sites, respectively. The number of sites per protein which are effectively O-GlcNAc-modified in this *in vitro* assay is not known. Nonetheless, the results obtained using Nup62, cdk5 and CK2α as substrates indicate that, in addition to qualitative investigation, the OGT assay on the membrane may potentially provide crude quantitative information on the O-GlcNAc content of proteins of interest.

Whether cdk5 is actually O-GlcNAcylated *in vivo* as well as potential consequences of this modification on cdk5´s physiological function or its dysregulation in AD remain to be elucidated. Cdk5 requires the binding of the regulatory protein p35 or its truncated version p25 for its catalytic activity and cdk5´s activity is further increased by phosphorylation at Ser159 (Lew *et al.*, 1994; Tsai *et al.*, 1994; Sharma *et al.*, 1999b). O-GlcNAcylation of cdk5 is predicted on Ser46, Thr245, Thr246, and Ser247 but not on Ser159 (see Appendix E). It

could therefore be speculated that O-GlcNAcylation may not play a direct role in the regulation of cdk5 activity.

5.2.3 Analysis of O-GlcNAcylation of APP and cdk5 peptides

O-GlcNAc site mapping is important for functional analysis as knowledge of the exact modification site(s) would allow for point mutations to further explore the role of O-GlcNAcylation in different cellular pathways. In this work, the identification of potential O-GlcNAc sites on APP and cdk5 peptides was attempted by MS analysis after *in vitro* O-GlcNAcylation. Unfortunately, O-GlcNAc could not be detected on the substrate peptides. *In vitro* OGT assay was successfully performed using different protein substrates (see 4.2.2) and our group and others have demonstrated that immunoprecipitated OGT is able to O-GlcNAc-modify Nup62 (Marshall *et al.*, 2003; Okuyama and Marshall, 2003; Strempel, 2010); furthermore, a similar method has been recently applied to modify tau and tau peptides (Smet-Nocca *et al.*, 2011). It may therefore be speculated that not OGT assay performance but the subsequent sample preparation and/or analysis by MS impeded the detection of O-GlcNAc moieties on the peptides.

O-GlcNAc analysis by MS still poses a great challenge. O-GlcNAc is a dynamic, substoichiometric modification and only a small percentage of a protein may be O-GlcNAcylated at any point in time. For example, as little as 0.1 GlcNAc residue/protein molecule were found on different OGT constructs *in vitro* and only 2 % of synapsin IIa is O-GlcNAcylated in adult rat brain cortex (Kreppel and Hart, 1999; Rexach *et al.*, 2010). Furthermore, the glycosidic bond is labile and susceptible to cleavage during MS.

To circumvent these problems in O-GlcNAc detection, different precautionary measures should be applied when anylzing O-GlcNAc. Global O-GlcNAcylation can be increased by inhibition of OGA and/or activation of the HBP. Furthermore, enrichment of O-GlcNAcylated proteins/peptides prior to MS analysis is highly recommended because ionization of O-GlcNAcylated peptides is suppressed in the presence of unmodified peptides (Wang and Hart, 2008; Ma and Hart, 2014). This effect is particularly pronounced in MALDI-MS. Still, successful O-GlcNAc site mapping has been demonstrated with MALDI-TOF MS/MS (Matsuura *et al.*, 2008; Hoffmann *et al.*, 2012). Enrichment or purification of O-GlcNAcylated peptides can be performed by lectin weak affinity chromatography or by the binding of biotin-labeled O-GlcNAc peptides to streptavidin (see click reaction in 5.2.1).

The combination of electrospray ionization- or MALDI-MS with different fragmentation techniques has greatly advanced O-GlcNAc site mapping. Nevertheless, O-GlcNAc detection is still difficult as not all fragmentation methods preserve the modification, e.g. high-energy collision dissociation (HCD) usually results in the loss of the O-GlcNAc group prior to peptide

fragmentation (Chalkley and Burlingame, 2001; Ma and Hart, 2014). Substitution of the labile O-glycosidic bond with a stable, MS-compatible bond by mild β-elimination and Michael addition of DTT (BEMAD) can circumvent this problem (Wells *et al.*, 2002b). Also, the combination of MS with electron capture dissociation (ECD) or electron transfer dissociation (ETD) enables O-GlcNAc site mapping. Under these conditions peptide backbone fragmentation occurs without concomitant cleavage of the glycosidic bond and thus the addition of O-GlcNAc to serine or threonine residues can be detected as a mass increment of m/z = 203 (Mikesh *et al.*, 2006; Myers *et al.*, 2013; Ma and Hart, 2014).

In this work, yet another MS technique, MALDI-LIFT-TOF/TOF was applied for O-GlcNAc site mapping (Suckau *et al.*, 2003). This method has been previously used to identify site(s) of O-glycosylation on short glycopeptides demonstrating that, similar as under ETD or ECD conditions, fragmentation occurs preferably at the peptide bond without affecting the glycosidic bond (Kurogochi *et al.*, 2004). Furthermore, our group has successfully used this technique for the identification of the position of O-GlcNAc on a synthetic O-GlcNAcylated peptide (Förster *et al.*, 2012). Prior to MS analysis, separation of O-GlcNAc-modified and unmodified peptides was performed by chemoenzymatic tagging with azide-modified galactose and alkyne-biotin and subsequent enrichment of biotin-labeled O-GlcNAc peptides by avidin affinity chromatography. Unfortunately, derivatized O-GlcNAc is still not 100 % stable under MALDI-LIFT conditions and can still be lost during ionization and, despite the aforementioned precautionary measures, O-GlcNAc site mapping in APP and cdk5 peptides was not successful in this work.

This project is still being pursued by B. Gehrig (Institute of Biochemistry and Molecular Biology, University of Bonn) and Dr. J. Ma (Department of Biological Chemistry, Johns Hopkins University). *In vitro* OGT assay with APP and cdk5 peptides was repeated and samples were subjected to tandem MS analysis (HCD/ETD or BEMAD/HCD). Preliminary results indicate O-GlcNAcylation of Ser5 of cAPP1 (corresponding to Ser655 of APP_{695}) as well as Ser5 of J-2 and Ser10 of J-3 (corresponding to Ser46 and Ser247 of cdk5; J. Ma, personal communication).

5.3 Changes in O-GlcNAc, OGT and OGA in MCI and AD

As described in 1.3, different lines of evidence indicate that O-GlcNAc may play a role in the pathogenesis of AD. However, reports on O-GlcNAcylation in AD are contradicting and the underlying factors and causalities of O-GlcNAc changes are unknown. In this work, global O-GlcNAcylation as well as the involved enzymes OGT and OGA were analyzed in two distinct brain regions, the IPL and cerebellum, at different stages during AD progression.

5.3.1 Increased protein O-GlcNAcylation in IPL samples from AD subjects

The IPL, a subregion of the cerebral cortex, is strongly affected in AD, as demonstrated by findings of neurofibrillary tangles, amyloid plaques, grey matter atrophy, and glucose hypometabolism (Braak and Braak, 1991; Jacobs *et al.*, 2011; Ossenkoppele *et al.*, 2012).

Analysis of IPL samples revealed that cytosolic O-GlcNAcylation was significantly elevated in AD when compared to age-matched controls. Upregulation of O-GlcNAc in AD has been described previously; however, O-GlcNAcylation was elevated only in the detergent insoluble cytoskeletal fraction but not in the detergent soluble fraction (Griffith and Schmitz, 1995). These results stand in contrast to findings of other groups demonstrating a decrease in protein O-GlcNAcylation in AD brain (Robertson *et al.*, 2004; Liu *et al.*, 2004, 2008, 2009a,b). Furthermore, Yao and Coleman reported no difference in global O-GlcNAcylation in AD brain, with the exception of a reduced signal at 160 kDa corresponding to clathrin assembly protein-3 (Yao and Coleman, 1998). An overview of studies investigating O-GlcNAcylation in AD brains including applied methods and findings is provided in Table 19. Noteworthy, most studies analyzing frontal cortex samples demonstrated reduced O-GlcNAcylation in AD. Only the study by Griffith and Schmitz showed elevated O-GlcNAcylation in the frontal cortex; however, the observed increase in O-GlcNAcylation was markedly more pronounced in the parietal cortex (Griffith and Schmitz, 1995). In agreement, another study investigating IPL samples also demonstrated increased O-GlcNAcylation in AD albeit only on specific proteins (Di Domenico *et al.*, 2010).

To date, the most widely used anti-O-GlcNAc antibodies are CTD110.6 and RL2 (Comer *et al.*, 2001; Holt *et al.*, 1987; Snow *et al.*, 1987). However, these antibodies were raised against different O-GlcNAc epitopes and O-GlcNAc signal detection is noticeably different with both antibodies (Ahrend *et al.*, 2008; Borghgraef *et al.*, 2013; Tashima and Stanley, 2014). In general, the use of different antibodies and different detection methods as well as variances in analyzed brain regions and sample preparation may explain the observed discrepancies in O-GlcNAcylation in AD, clearly demonstrating the need for standardized analysis methods for O-GlcNAc detection in human brain samples.

Table 19: Overview of studies examining O-GlcNAcylation in AD brain

Brain region	O-GlcNAc changes in AD	Sample specification	Detection method	Additional information	Reference
Temporal, parietal, and frontal cortex and basal forebrain cerebellum	↑ ~	Detergent-insoluble cytoskeletal fraction	ELISA with anti-O-GlcNAc antibodies (HGAC 39 and HGAC 85) and [^{3}H]galactose labeling**	No change in detergent-soluble fraction	Griffith and Schmitz, 1995
Frontal cortex and middle frontal gyrus cerebellum	~ ↓ of band at 160 kDa ~	Cytosolic fraction*	[^{3}H]galactose labeling**	160 kDa protein was identified as clathrin assembly protein-3	Yao and Coleman, 1998
Frontal cortex	↓	Cytosolic fraction*	Radioimmuno dot blot with RL2 antibody		Liu *et al.*, 2004
not specified	↓	Heat-stable cytoskeletal preparations	[^{3}H]galactose labeling**	Tau protein is enriched in the analyzed fraction	Robertson *et al.*, 2004
Frontal cortex	↓	Cytosolic fraction*	Dot blot with RL2 antibody	O-GlcNAcylation correlated positively with the levels of GLUT1 and GLUT3	Liu *et al.*, 2008
Frontal cortex Cerebellar cortex	↓ ~	Cytosolic fraction*	Dot blot with RL2 antibody	Signals were normalized to actin expression; results were confirmed by immuno-fluorescence in the superior frontal gyrus	Liu *et al.*, 2009a
Frontal cortex	↓	Cytosolic fraction*	Dot blot and Western blot with RL2 antibody	Results from dot blot and Western blot analyses were combined	Liu *et al.*, 2009b
Hippocampus IPL	↑ / ↓ ↑	Homogenates	2D SDS-PAGE of wheat germ agglutinin-binding proteins	O-GlcNAcylation of protein 14-3-3γ was confirmed with CTD110.6 antibody	Di Domenico *et al.*; 2010

↑ = increased; ~ = unchanged; ↓ = decreased; * brain homogenates were centrifuged (> 1000 x g) and only supernatant was analyzed; ** [^{3}H]galactose labeling of terminal GlcNAc residues with galactosyltransferase; GLUT: glucose transporter.

Noteworthy in this work, O-GlcNAc signals demonstrated great inter- and intragroup pattern variations which have not been described previously. In many of the above listed studies O-GlcNAc was detected using dot blot or ELISA assays thereby precluding the possibility of investigating individual protein signals. In retrospect, it would have been interesting to compare O-GlcNAc bands to the Direct Blue staining of proteins, as strong O-GlcNAc signals may not correlate with high expression of a protein and vice versa.

Proteomics studies have demonstrated differential expression and glycosylation of various proteins in AD brain (Sultana *et al.*, 2006a; Owen *et al.*, 2009; Di Domenico *et al.*, 2010). However, only few 'O-GlcNAcomics' studies have been performed on human AD samples (e.g. Skorobatko *et al.*, 2011) and quantification of O-GlcNAc changes by MS is still quite complicated although great progress has been made in the recent years (Wang *et al.*, 2007; Khidekel *et al.*, 2007; Maury *et al.*, 2014). O-GlcNAcomics studies are currently underway (in cooperation with J.C. Triplett, Department of Chemistry, University of Kentucky) and may reveal the identity of proteins with altered O-GlcNAcylation in AD, i.e. the proteins with the apparent molecular weight of 27, 50, and 75 kDa (see Figure 13).

O-GlcNAc expression did not correlate with age or gender but O-GlcNAc seemed to correlate positively with disease severity, indexed by decreasing MMSE scores and increasing Braak stages. Reasons for the great variability in O-GlcNAc expression within the analyzed groups are unknown but it may be partially explained by natural heterogeneity between individuals. When comparing individuals of the same age, differences of similar magnitude have been demonstrated for cerebral glucose utilization (Kuhl *et al.*, 1982). The observed variations may also be explained by other patient-specific parameters (e.g. nutrition and life style). Furthermore, population based studies have repeatedly identified diabetes as a risk factor for AD and AD has been proposed to represent a brain-specific "type 3 diabetes" (Kuustisto *et al.*, 1997; Peila *et al.*, 2002; de la Monte and Wands, 2008). It would be highly interesting to investigate potential correlations of cerebral O-GlcNAc expression with diabetic status or cerebral glucose utilization.

5.3.2 Unaffected OGT expression in IPL samples from AD subjects

In an attempt to explain augmented O-GlcNAcylation in AD brain, O-GlcNAc cycling enzymes were investigated and the analysis of OGT yielded unexpected results. In general, OGT signal intensities were very weak and the most prominent signal corresponded to a band at approximately 105 kDa; this result could be validated with a second antibody against OGT. The molecular weight of this signal corresponds to mOGT (103 kDa) rather than to ncOGT (116 kDa) and as sample homogenates were used, mOGT is likely to be present in the samples (Hanover *et al.*, 2003). Conversely, in developing and aging rat brain marked

and stable expression of ncOGT but no significant expression of mOGT is observed (Liu *et al.*, 2012). At present, reasons for the detection of OGT with a molecular weight of 105 kDa are unknown.

Densitometric analysis of this signal revealed that despite increased O-GlcNAcylation, OGT expression in IPL samples from AD subjects was unaltered when compared to age-matched controls. This lack of a correlation between O-GlcNAc and OGT has previously been shown in aging rat brain where increased O-GlcNAcylation was in fact accompanied by decreased OGT expression (Fülöp *et al.*, 2008). Furthermore, OGT protein levels do not necessarily mirror OGT activity (Kreppel et al., 1997).

OGT activity in AD has not been analyzed previously and unfortunately it was also not investigated in this work as common OGT assays rely on [^{3}H]GlcNAc incorporation into peptides/proteins and the aforementioned ELISA-based OGT assay has not yet been tested for quantification purposes. Consequently, the relevance of unaltered OGT expression for augmented O-GlcNAcylation in AD brain cannot be discussed conclusively.

5.3.3 Reduced OGA expression in IPL samples from AD subjects

In contrast to OGT, OGA expression was significantly downregulated in IPL samples from subjects with AD and, most importantly, the observed decrease significantly correlated with augmented cytosolic O-GlcNAcylation. As for OGT, multiple OGA isoforms have been described with FL-OGA residing predominantly in the cytoplasm while NV-OGA is located to nuclei and lipid droplets (Comtesse *et al.*, 2001; Keembiyehetty *et al.*, 2011). As OGA was analyzed in sample homogenates, theoretically both isoforms could have been detected. Indeed, in addition to the prominent signal corresponding to FL-OGA, a second albeit weaker signal was detected at the apparent molecular weight of NV-OGA (data not shown). This finding was unexpected as the shorter isoform has been shown to be quickly downregulated in rat brain during embryonic development and was undetectable after birth let alone in adult animals (Liu *et al.*, 2012). Whether the detected band represents NV-OGA or whether NV-OGA expression is also downregulated in human brain remains to be determined.

A common protocol using pNP-GlcNAc as a substrate was applied to analyze OGA activity (Zachara *et al.*, 2011) and revealed significantly reduced OGA activity in AD brain. After normalization of OGA activity assay results to the corresponding OGA signal, no difference in OGA activity between AD cases and age-matched controls was observed. This suggests that reduced OGA expression is not compensated by increased OGA activity and this may therefore be responsible for the disruption of the O-GlcNAc cycling equilibrium in AD.

Reason(s) for decreased OGA expression in AD remain to be elucidated. In general, cellular protein levels are dependent on their synthesis and degradation rates. A recent whole transcriptome sequencing analysis discovered that while the OGA-encoding *MGEA5* gene was not differentially expressed, it showed alternative promoter usage and alternative splicing in AD (Twine *et al.*, 2011). Whether mRNA stability and/or translation of OGA may be altered in AD is currently unknown. Increased degradation of OGA by the ubiquitin-proteasome and/or autophagic-lysosomal system is unlikely as both pathways are perturbed in AD (reviewed in Ihara *et al.*, 2012). Furthermore, OGA represents a substrate for caspase-3 although cleavage of OGA does not affect the enzyme´s catalytic activity *in vitro* (Wells *et al.*, 2002a; Butkinaree *et al.*, 2008). Elevated levels of activated caspase-3 are found in AD brain (Su *et al.*, 2001) but it remains to be investigated whether OGA represents a substrate for caspase-3 *in vivo* and if this could affect OGA activity in AD.

5.3.4 No changes in O-GlcNAcylation in MCI and in the cerebellum

In addition to AD, brain samples from subjects with amnestic MCI were also analyzed. Amnestic MCI often represents an early stage of AD in which cognitive impairment is present but criteria for dementia are not yet met (Albert and Blacker, 2006). No significant changes were observed when comparing O-GlcNAcylation in IPL samples from MCI subjects with non-demented controls. Also OGT and OGA expression were unaffected. These data indicate that changes in O-GlcNAcylation are not an early event in the progression of AD.

In contrast to the IPL, the cerebellum seems to be less affected in AD (Braak *et al.*, 1989) and is often used as a control when analyzing pathological changes in AD. Accordingly, previous studies have found no significant changes in O-GlcNAcylation in cerebellar samples from AD patients (Griffith and Schmitz, 1995). In this work, cerebellar O-GlcNAc levels were unaltered in MCI but seemed slightly albeit not significantly decreased in AD. This is in agreement with a previous report analyzing a similarly small sample number (n = 6); in this study, mean O-GlcNAcylation was decreased by almost 40 % in AD cerebellum although due to great individual signal variation, this reduction was not statistically significant (Liu *et al.*, 2009a). Analysis of OGT and OGA expression in the cerebellum also revealed no significant changes in AD and MCI. Interestingly, O-GlcNAc signal pattern in cerebellum differed greatly from that in IPL, namely the highly varying signal bands at 27, 50 and 75 kDa were markedly weaker or even undetectable in cerebellar samples. Whether this is due to brain area-specific disparities in protein expression and/or O-GlcNAcylation or may be explained by the fact that the cerebellum is less affected by AD pathology is not known.

5.4 Potential causes and consequences of altered O-GlcNAcylation in AD

It is commonly accepted that impaired protein O-GlcNAcylation may contribute to AD pathogenesis although the underlying molecular mechanisms and causalities have yet to be elucidated (recently reviewed in Yuzwa and Vocadlo, 2014). Significant downregulation of OGA expression may solely be responsible for the herein observed increase in protein O-GlcNAcylation but it is more likely that the combination of various factors results in altered O-GlcNAcylation in AD. Some of these potential factors are discussed below and are summarized in Figure 25.

The role of glucose availability and metabolism

Impaired glucose transport and metabolism in AD brain has been reported by various groups (Kalaria and Harik, 1989; Simpson *et al.*, 1994; Fukuyama *et al.*, 1994). Furthermore, Liu *et al.* demonstrated a positive correlation between reduced expression of glucose transporters GLUT1 and GLUT3 and reduced O-GlcNAcylation in AD brain and suggested that lower flux of glucose through the HBP was responsible for the observed decrease in protein O-GlcNAcylation (Liu *et al.*, 2008). In accordance, starvation of mice has been demonstrated to reduce cerebral O-GlcNAcylation (Liu *et al.*, 2004). Lowering the glucose concentration in cell culture medium also decreased O-GlcNAc expression in cell culture studies. Interestingly, simultaneous OGA inhibition by PUGNAc not only precluded this decline but markedly increased O-GlcNAcylation (Liu *et al.*, 2004) strongly indicating that glucose availability is not a limiting factor for O-GlcNAcylation.

In agreement, O-GlcNAc´s role as a nutrient sensor was challenged by *in vitro* studies demonstrating increased O-GlcNAcylation despite glucose deprivation (Cheung and Hart, 2008; Taylor *et al.*, 2008; 2009; Zou *et al.*, 2012). While this finding was reproduced in different cell lines, the molecular mechanisms responsible remain obscure and may be cell type-specific. In N2a and in HepG2 (human hepatocellular carcinoma) cells, augmented O-GlcNAcylation despite reduced UDP-GlcNAc level was accompanied by decreased OGA and/or increased OGT expression (Cheung and Hart, 2008; Taylor *et al.*, 2008; 2009). In isolated cardiomyocytes, even a small reduction of the glucose concentration in cell culture medium resulted in upregulation of O-GlcNAc and concurrent downregulation of OGA expression (Zou *et al.*, 2012). Based on these studies, it may be speculated that the reduction of OGA expression could represent a regulatory mechanism by which cells may increase protein O-GlcNAcylation in response to acute nutrient deprivation. Importantly, complete glucose deprivation poses a non-physiological situation and even acute hypoglycemia may not model chronically impaired glucose availability in AD brain.

Nonetheless, these studies indicate that despite reduced glucose concentration protein O-GlcNAcylation can be significantly upregulated.

The role of oxidative stress

Augmented O-GlcNAcylation despite reduced glucose availability may also be explained based on O-GlcNAc´s role as a stress sensor. Various kinds of stress, including oxidative stress, have been shown to increase protein O-GlcNAcylation *in vitro* (Zachara *et al.*, 2004). Moreover, UDP-GlcNAc pools are susceptible to cellular stress, potentially via superoxide-induced inhibition of GAPDH and subsequent rerouting of glucose from glycolysis towards the HBP (Du *et al.*, 2000; see Figure 25). In the context of AD this is highly relevant, as a growing body of evidence indicates oxidative stress as an important player in AD (reviewed in Sultana *et al.*, 2006b). In agreement, GAPDH, amongst other proteins, is oxidized in AD and reduced activity of multiple glycolytic enzymes has been reported in AD brain (Meier-Ruge *et al.*, 1984; Sultana *et al.*, 2006a). In accordance with the mechanism proposed by Du *et al.*, malfunction of glycolytic enzymes in AD may divert glucose and its downstream metabolite fructose-6-phosphate to favor UDP-GlcNAc synthesis via the HBP thereby precluding a decline in UDP-GlcNAc concentration despite reduced intracellular glucose level. UDP-GlcNAc has not been investigated in the context of AD and to date, it is not known whether UDP-GlcNAc levels are altered in AD brain.

The role of O-GlcNAc cycling enzymes

OGT and OGA gene and protein expression as well as activity have been investigated in rodent aging and animal models of AD (Fülöp *et al.*, 2008; Chen *et al.*, 2012; Liu *et al.*, 2012; Yang *et al.*, 2012) but until this work, expression and activity of O-GlcNAc cycling enzymes had not been investigated in human AD samples. In general, OGT activity is regulated across a wide range of UDP-GlcNAc concentrations with the affinity of OGT towards different substrates being dependent on the level of UDP-GlcNAc (Kreppel and Hart, 1999). In contrast to other UDP-GlcNAc-utilizing enzymes, OGT has a very high affinity towards its donor substrate (Hirschberg and Snider, 1987; Haltiwanger *et al.*, 1992; Marshall *et al.*, 2003). Therefore, in conditions of insufficient HBP flux (maybe due to impaired transport of glucose into the cell), generated UDP-GlcNAc may preferentially be utilized for O-GlcNAcylation instead of being used in other metabolic pathways e.g. protein glycosylation in ER and Golgi (Figure 25).

Furthermore, both OGT and OGA are posttranslationally modified with O-GlcNAc and OGT is also tyrosine phosphorylated (Kreppel *et al.*, 1997; Lazarus *et al.*, 2006). Intriguingly, phosphorylation of OGT has been demonstrated to elevate OGT´s autoglycosylation and

activity *in vitro* (Whelan *et al.*, 2008) and hyperphosphorylation of different proteins has been described in AD (e.g. tau; Grundke-Iqbal *et al.*, 1986b). Whether OGT activity is altered in AD, remains to be investigated. Based on the intricate interplay of phosphorylation and O-GlcNAcylation it is conceivable that differential OGT posttranslational modifications, activity and/or substrate specificity, together with the herein reported decline in OGA expression/activity, may exacerbate the dysregulation of O-GlcNAc cycling in AD.

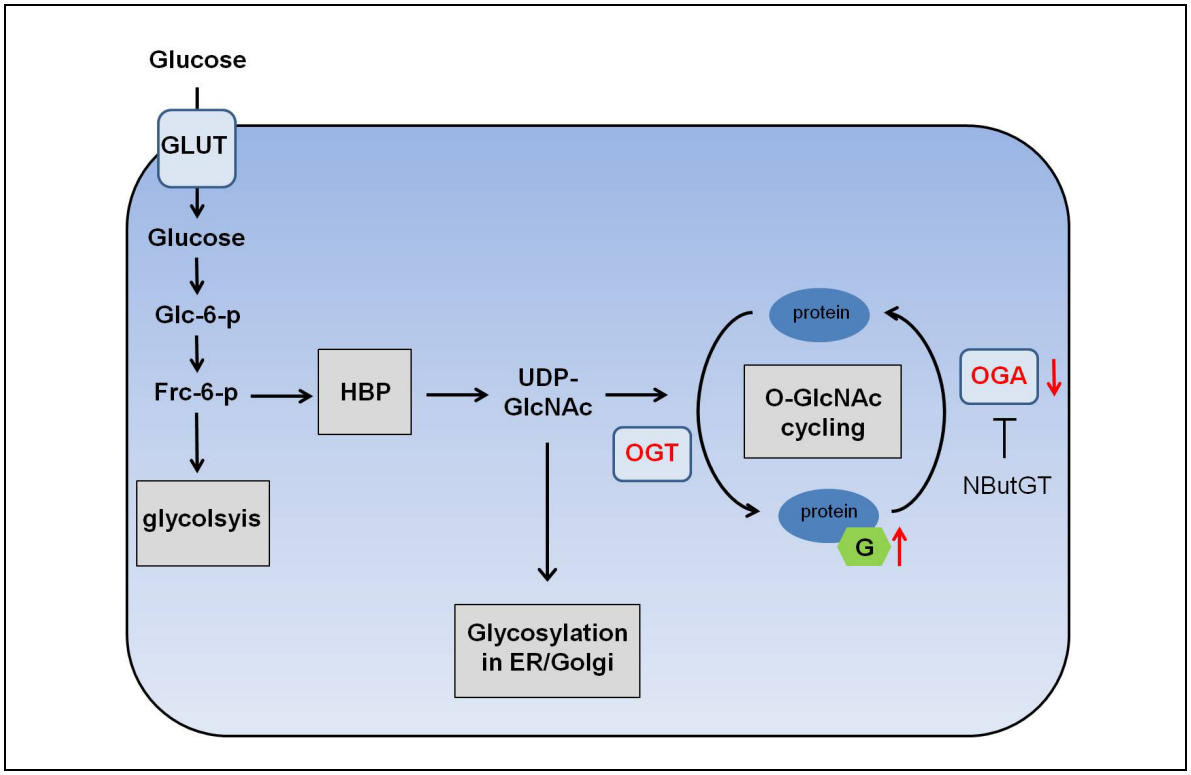

Figure 25: Dysregulation of O-GlcNAc cycling in AD

Glucose is transported across the blood brain barrier and into neurons by GLUT1 and GLUT3. After phosphorylation and isomerization, fructose-6-phosphate can be further metabolized through the glycolytic pathway or it can enter the HBP to generate UDP-GlcNAc. Using UDP-GlcNAc as substrate, OGT catalyzes the addition of O-GlcNAc to proteins while OGA removes this posttranslational modification. In AD brain, reduced expression of GLUTs, impaired glucose utilization and decreased activity of glycolytic enzymes has been demonstrated but potential effects on UDP-GlcNAc concentrations have not yet been analyzed (Meier-Ruge *et al.*, 1984; Kalaria and Harik, 1989; Simpson *et al.*, 1994; Fukuyama *et al.*, 1994; Liu *et al.*, 2008). In this work, significantly upregulated protein O-GlcNAcylation was demonstrated in IPL samples from subjects with AD. This increase was not accompanied by changes in OGT expression but correlated with significantly reduced OGA expression and activity. Results of the herein performed experiments are depicted in red. GLUT: glucose transporter; Glc-6-p: glucose-6-phosphate; Frc-6-p: fructose-6-phosphate; HBP: hexosamine biosynthetic pathway; OGT: O-GlcNAc transferase; G: O-GlcNAc; OGA: O-GlcNAc hydrolase; ↑: increase; ↓: decrease.

Possible implication(s) of altered O-GlcNAcylation for APP/Aβ metabolism in AD

In SY5Y-APP cells, increased O-GlcNAcylation of APP (after treatment with NButGT) did not affect sAPPα or sAPPβ levels indicating that APP-specific O-GlcNAcylation may not have a direct influence on APP processing. Similarly, it has been suggested that not the glycosylation status of APP itself but rather perturbed N-glycosylation of other cellular proteins may contribute to altered metabolism of APP (Pahlsson and Spitalnik, 1996). In accordance, modulation of global O-GlcNAc levels may affect function and/or activity of many different proteins including secretases, phosphatases and/or kinases (e.g. cdk5) and may thereby indirectly affect APP processing. Supporting this hypothesis, nicastrin, a member of the γ-secretase complex, has recently been shown to be O-GlcNAcylated and its modification significantly decreased γ-secretase activity *in vitro* (Kim *et al.*, 2013). In AD, altered O-GlcNAcylation due to reduced OGA expression could have far-reaching consequences as a myriad of proteins and molecular pathways may be implicated.

Understanding the role of O-GlcNAcylation in the pathogenesis of AD is highly significant, especially in light of a growing number of groups investigating the therapeutic potential of OGA inhibition in different AD mouse models (Yuzwa *et al.*, 2012; Kim *et al.*, 2013; Graham *et al.*, 2014). For example, Kim *et al.* demonstrated that NButGT treatment of transgenic mice decreased Aβ plaque load and levels of (insoluble) Aβ and had positive effects on memory (Kim *et al.*, 2013). Noteworthy, in this study, long-term OGA inhibition was initiated before the onset of AD symptoms. As results of this work indicate that altered O-GlcNAcylation is a late event in AD progression, it would be highly interesting to analyze potential effects of OGA inhibition initiated at a later time-point. Also, it remains to be investigated whether OGA inhibition still exerts positive effects when OGA expression is downregulated as shown in this work.

6 Summary

O-linked N-acetylglucosamine (O-GlcNAc) has been extensively studied in the context of Alzheimer disease (AD) but the potential role(s) of this posttranslational modification in the pathogenesis of AD as well as the underlying causes and consequences of altered O-GlcNAcylation in AD are unknown.

In this work, the role of O-GlcNAc in different aspects of AD pathology was investigated. In addition, a recently developed *in vitro* O-GlcNAc transferase (OGT) assay was refined and implemented.

The role of O-GlcNAc in the processing of the amyloid precursor protein (APP) was investigated in cell culture using human neuroblastoma cells overexpressing wild-type APP_{695}. Treatment of cells with Alloxan, a fairly unspecific inhibitor of OGT, was expected to reduce global O-GlcNAc expression. Also, based on the “yin-yang” hypothesis, treatment with PMA, an activator of protein kinase C, was expected to reduce O-GlcNAcylation. In this work however, only inconsistent effects of Alloxan and PMA treatments on O-GlcNAc expression were observed. In contrast, treatment of the cells with a highly specific inhibitor of O-GlcNAc hydrolase (OGA) resulted in significantly increased global and APP-specific O-GlcNAcylation but had no effect on the levels of secreted APP fragmented sAPPα and sAPPβ in conditioned medium.

Further studies aimed to identify (potential) changes in composition and quantity of endogenous Aβ peptides as well as to identify the site(s) of O-GlcNAcylation on different APP peptides. In this work however, only synthetic Aβ species and unmodified APP peptides could be detected by MALDI-TOF mass spectrometry.

In addition, based on previous preliminary studies, O-GlcNAcylation of cyclin-dependent kinase 5 (cdk5) was analyzed as cdk5, amongst other kinases, phosphorylates APP and may be implicated in AD pathogenesis. *In vitro* OGT assay was performed with cdk5 and synthetic peptides thereof. While no O-GlcNAc was detected on cdk5 peptides, O-GlcNAcylation of recombinant cdk5 could be demonstrated. Whether cdk5 is O-GlcNAcylated *in vivo* as well as the potential functional role of O-GlcNAcylation of cdk5 remain to be elucidated.

Furthermore, a recently established OGT assay on nitrocellulose membrane was successfully altered into an ELISA-based OGT assay using the nuclear pore protein Nup62 as a substrate. A great advantage of this assay is that it can be used for the rapid screening

of different proteins for possible O-GlcNAcylation or for the testing of potential OGT inhibitors without the need for radioactive compounds.

Finally, the expression of O-GlcNAc and O-GlcNAc cycling enzymes OGT and OGA was investigated in post-mortem brain samples of subjects with AD and age-matched controls. To analyze the time course of potential changes in the progression of the disease the same parameters were also investigated in the brains of subjects with amnestic mild cognitive impairment (MCI), an early stage of AD. Analyses were performed in samples from two distinct brain areas, the inferior parietal lobule (IPL) which is strongly affected in AD and the cerebellum which is largely spared by AD pathology. In IPL samples from subjects with AD, significantly increased O-GlcNAcylation was observed when compared to age-matched controls. While no difference in OGT expression was detected, augmented O-GlcNAc levels correlated with decreased OGA expression and activity. No such changes were observed in IPL samples from subjects with amnestic MCI or in cerebellar samples from subjects with AD or MCI, implying that O-GlcNAc is enhanced only in brain regions affected by AD pathology and that increased O-GlcNAcylation only occurs in late stages of AD.

Taken together, results of this work indicate that O-GlcNAc may not be directly involved in the processing of APP and that changes in O-GlcNAcylation may be a consequence rather than a cause of AD pathology. In conclusion, together with previous studies, this work demonstrates that the role of O-GlcNAc in the pathogenesis of AD remains elusive and that further studies are needed before O-GlcNAcylation may be regarded as a novel target for AD therapy.

References

Ahrend M, Käberich A, Fergen M, Schmitz B (2008). Immunochemical methods for the rapid screening of the O-glycosidically linked N-acetylglucosamine modification of proteins. *Methods Mol Biol* **446**: 267–280.

Albert MS, Blacker D (2006). Mild cognitive impairment and dementia. *Annu Rev Clin Psychol* **2**: 379–388.

Alzheimer A (1907). Über eine eigenartige Erkrankung der Hirnrinde. *Allg Z Psychiat Psych-Gerichtl Med* 64:146–148.

Ando K, Iijima KI, Elliott JI, Kirino Y, Suzuki T (2001). Phosphorylation-dependent regulation of the interaction of amyloid precursor protein with Fe65 affects the production of β-amyloid. *J Biol Chem* **276**(43): 40353–40361.

Arnold CS, Johnson GV, Cole RN, Dong DL, Lee M, Hart GW (1996). The microtubule-associated protein tau is extensively modified with O-linked N-acetylglucosamine. *J Biol Chem* **271**(46): 28741–28744.

Artimo P, Jonnalagedda M, Arnold K, Baratin D, Csardi G, Castro E de, Duvaud S, Flegel V, Fortier A, Gasteiger E, Grosdidier A, Hernandez C, Ioannidis V, Kuznetsov D, Liechti R, Moretti S, Mostaguir K, Redaschi N, Rossier G, Xenarios I, Stockinger H (2012). ExPASy: SIB bioinformatics resource portal. *Nucleic Acids Res* **40**: W597-603.

Balzen S (2010). Untersuchungen zur O-GlcNAc-Glykosylierung von Proteinen aus Endothel- und Skelettmuskelzellen. (Dissertation)

Beausoleil SA, Jedrychowski M, Schwartz D, Elias JE, Villen J, Li J, Cohn MA, Cantley LC, Gygi SP (2004). Large-scale characterization of HeLa cell nuclear phosphoproteins. *Proc Natl Acad Sci U S A* **101**(33): 12130–12135.

Belyaev ND, Kellett, Katherine A B, Beckett C, Makova NZ, Revett TJ, Nalivaeva NN, Hooper NM, Turner AJ (2010). The transcriptionally active amyloid precursor protein (APP) intracellular domain is preferentially produced from the 695 isoform of APP in a β-secretase-dependent pathway. *J Biol Chem* **285**(53): 41443–41454.

Bennett BD, Babu-Khan S, Loeloff R, Louis JC, Curran E, Citron M, Vassar R (2000). Expression analysis of BACE2 in brain and peripheral tissues. *J Biol Chem* **275**(27): 20647–20651.

Bertram L, Blacker D, Mullin K, Keeney D, Jones J, Basu S, Yhu S, McInnis MG, Go RC, Vekrellis K, Selkoe DJ, Saunders AJ, Tanzi RE (2000). Evidence for genetic linkage of Alzheimer's disease to chromosome 10q. *Science* **290**(5500): 2302–2303.

Bertram L, Tanzi RE (2005). The genetic epidemiology of neurodegenerative disease. *J Clin Invest* **115**(6): 1449–1457.

Bond MR, Hanover JA (2013). O-GlcNAc cycling: a link between metabolism and chronic disease. *Annu Rev Nutr* **33**:205-229.

Borghgraef P, Menuet C, Theunis C, Louis JV, Devijver H, Maurin H, Smet-Nocca C, Lippens G, Hilaire G, Gijsen H, Moechars D, van Leuven F (2013). Increasing brain protein O-GlcNAc-ylation mitigates breathing defects and mortality of Tau.P301L mice. *PLoS ONE* **8**(12): e84442.

Braak H, Braak E, Bohl J, Lang W (1989). Alzheimer´s disease: amyloid plaques in the cerebellum. *J Neurol Sci* **93**(2-3): 277–287.

Braak H, Braak E (1991). Neuropathological stageing of Alzheimer-related changes. *Acta Neuropathol* **82**(4): 239–259.

Braak H, Braak E (1997). Frequency of stages of Alzheimer-related lesions in different age categories. *Neurobiol Aging* **18**(4): 351-357.

Bredesen DE, John V, Galvan V (2010). Importance of the caspase cleavage site in amyloid-β protein precursor. *J Alzheimers Dis* **22**(1): 57–63.

Brunholz S, Sisodia S, Lorenzo A, Deyts C, Kins S, Morfini G (2012). Axonal transport of APP and the spatial regulation of APP cleavage and function in neuronal cells. *Exp Brain Res* **217**(3-4): 353–364.

Bullock WO, Fernandez JM, Short JM (1987). XL1-Blue: a high efficiency plasmid transforming recA Escherichia coli strain with β-galactosidase selection. *Bio Technisques* **5**(4): 376–379.

Burdick D, Soreghan B, Kwon M, Kosmoski J, Knauer M, Henschen A, Yates J, Cotman C, Glabe C (1992). Assembly and aggregation properties of synthetic Alzheimer's A4/β amyloid peptide analogs. *J Biol Chem* **267**(1): 546–554.

Buse MG (2006). Hexosamines, insulin resistance, and the complications of diabetes: current status. *Am J Physiol Endocrinol Metab* **290**(1): E1-E8.

Butkinaree C, Cheung WD, Park S, Park K, Barber M, Hart GW (2008). Characterization of β-N-acetylglucosaminidase cleavage by caspase-3 during apoptosis. *J Biol Chem* **283**(35): 23557–23566.

Butkinaree C, Park K, Hart GW (2010). O-linked β-N-acetylglucosamine (O-GlcNAc): Extensive crosstalk with phosphorylation to regulate signaling and transcription in response to nutrients and stress. *Biochim Biophys Acta* **1800**(2): 96–106.

Buxbaum JD, Liu KN, Luo Y, Slack JL, Stocking KL, Peschon JJ, Johnson RS, Castner BJ, Cerretti DP, Black RA (1998). Evidence that tumor necrosis factor α converting enzyme is involved in regulated α-secretase cleavage of the Alzheimer amyloid protein precursor. *J Biol Chem* **273**(43): 27765–27767.

Cao X, Südhof TC (2001). A transcriptionally correction of transcriptively active complex of APP with Fe65 and histone acetyltransferase Tip60. *Science* **293**(5527): 115–120.

Cappai R, White AR (1999). Amyloid β. *Int J Biochem Cell Biol* **31**(9): 885–889.

Castellani RJ, Rolston RK, Smith MA (2010). Alzheimer disease. *Dis Mon* **56**(9): 484–546.

Chalkley RJ, Burlingame AL (2001). Identification of GlcNAcylation sites of peptides and α-crystallin using Q-TOF mass spectrometry. *J Am Soc Mass Spectrom* **12**(10): 1106–1113.

Chang K, Kim H, Ha T, Ha J, Shin KY, Jeong YH, Lee J, Park C, Kim S, Baik T, Suh Y (2006). Phosphorylation of amyloid precursor protein (APP) at Thr668 regulates the nuclear translocation of the APP intracellular domain and induces neurodegeneration. *Mol Cell Biol* **26**(11): 4327–4338.

Chatham JC, Marchase RB (2010). Protein O-GlcNAcylation: A critical regulator of the cellular response to stress. *Curr Signal Transduct Ther* **5**(1): 49–59.

Chen Y, Tian Z, Liang Z, Sun S, Dai C, Lee MH, LaFerla FM, Grundke-Iqbal I, Iqbal K, Liu F, Gong C (2012). Brain gene expression of a sporadic (icv-STZ Mouse) and a familial mouse model (3xTg-AD mouse) of Alzheimer's disease. *PLoS ONE* **7**(12): e51432.

Cheng X, Hart GW (2001). Alternative O-glycosylation/O-phosphorylation of serine-16 in murine estrogen receptor β: post-translational regulation of turnover and transactivation activity. *J Biol Chem* **276**(13): 10570–10575.

Cheung WD, Hart GW (2008). AMP-activated protein kinase and p38 MAPK activate O-GlcNAcylation of neuronal proteins during glucose deprivation. *J Biol Chem* **283**(19): 13009–13020.

Chow VW, Mattson MP, Wong PC, Gleichmann M (2010). An overview of APP processing enzymes and products. *Neuromolecular Med* **12**(1): 1–12.

Clarke AJ, Hurtado-Guerrero R, Pathak S, Schüttelkopf AW, Borodkin V, Shepherd SM, Ibrahim, Adel FM, van Aalten, DMF (2008). Structural insights into mechanism and specificity of O-GlcNAc transferase. *EMBO J* **27**(20): 2780–2788.

Cole RN, Hart GW (2001). Cytosolic O-glycosylation is abundant in nerve terminals. *J Neurochem* **79**(5): 1080-1089.

Comer FI, Hart GW (2000). O-Glycosylation of nuclear and cytosolic proteins. Dynamic interplay between O-GlcNAc and O-phosphate. *J Biol Chem* **275**(38): 29179–29182.

Comer FI, Hart GW (2001). Reciprocity between O-GlcNAc and O-phosphate on the carboxyl terminal domain of RNA polymerase II. *Biochemistry* **40**(26): 7845–7852.

Comer FI, Vosseller K, Wells L, Accavitti MA, Hart GW (2001). Characterization of a mouse monoclonal antibody specific for O-linked N-acetylglucosamine. *Anal Biochem* **293**(2): 169–177.

Comtesse N, Maldener E, Meese E (2001). Identification of a nuclear variant of MGEA5, a cytoplasmic hyaluronidase and a β-N-acetylglucosaminidase. *Biochem Biophys Res Commun* **283**(3): 634–640.

Crawford GL, Hart GW, Whiteheart SW (2008). Murine platelets are not regulated by O-linked β-N-acetylglucosamine. *Arch Biochem Biophys* **474**(1): 220–224.

Cruz JC, Tsai L (2004). Cdk5 deregulation in the pathogenesis of Alzheimer's disease. *Trends Mol Med* **10**(9): 452–458.

Daigle I, Li C (1993). apl-1, a Caenorhabditis elegans gene encoding a protein related to the human β-amyloid protein precursor. *Proc Natl Acad Sci U S A* **90**(24): 12045–12049.

Davis DG, Schmitt FA, Wekstein DR, Markesbery WR (1999). Alzheimer neuropathologic alterations in aged cognitively normal subjects. *J Neuropathol Exp Neurol* **58**(4): 376–388.

de la Monte SM, Wands JR (2008). Alzheimer's disease is type 3 diabetes-evidence reviewed. *J Diabetes Sci Technol* **2**(6): 1101–1113.

Dehennaut V, Lefebvre T, Sellier C, Leroy Y, Gross B, Walker S, Cacan R, Michalski J, Vilain J, Bodart J (2007). O-linked N-acetylglucosaminyltransferase inhibition prevents G2/M transition in Xenopus laevis oocytes. *J Biol Chem* **282**(17): 12527–12536.

Di Domenico F, Owen JB, Sultana R, Sowell RA, Perluigi M, Cini C, Cai J, Pierce WM, Butterfield DA (2010). The wheat germ agglutinin-fractionated proteome of subjects with Alzheimer's disease and mild cognitive impairment hippocampus and inferior parietal lobule: Implications for disease pathogenesis and progression. *J Neurosci Res* **88**(16): 3566–3577.

Dias WB, Cheung WD, Hart GW (2012). O-GlcNAcylation of kinases. *Biochem Biophys Res Commun* **422**(2): 224–228.

Dong DL, Hart GW (1994). Purification and characterization of an O-GlcNAc selective N-acetyl-β-D-glucosaminidase from rat spleen cytosol. *J Biol Chem* **269**(30): 19321–19330.

Du XL, Edelstein D, Rossetti L, Fantus IG, Goldberg H, Ziyadeh F, Wu J, Brownlee M (2000). Hyperglycemia-induced mitochondrial superoxide overproduction activates the hexosamine pathway and induces plasminogen activator inhibitor-1 expression by increasing Sp1 glycosylation. *Proc Natl Acad Sci U S A* **97**(22): 12222–12226.

Duggirala R, Blangero J, Almasy L, Dyer TD, Williams KL, Leach RJ, O'Connell P, Stern MP (1999). Linkage of type 2 diabetes mellitus and of age at onset to a genetic location on chromosome 10q in Mexican Americans. *Am J Hum Genet* **64**(4): 1127–1140.

Dyrks T, Monning U, Beyreuther K, Turner J (1994). Amyloid precursor protein secretion and β A4 amyloid generation are not mutually exclusive. *FEBS Lett* **349**(2): 210–214.

Dyrks T, Weidemann A, Multhaup G, Salbaum JM, Lemaire HG, Kang J, Muller-Hill B, Masters CL, Beyreuther K (1988). Identification, transmembrane orientation and biogenesis of the amyloid A4 precursor of Alzheimer's disease. *EMBO J* **7**(4): 949–957.

Edbauer D, Willem M, Lammich S, Steiner H, Haass C (2002). Insulin-degrading enzyme rapidly removes the β-amyloid precursor protein intracellular domain (AICD). *J Biol Chem* **277**(16): 13389–13393.

Ehehalt R, Keller P, Haass C, Thiele C, Simons K (2003). Amyloidogenic processing of the Alzheimer β-amyloid precursor protein depends on lipid rafts. *J Cell Biol* **160**(1): 113–123.

Eisenstein M (2011). Genetics: finding risk factors. *Nature* **475**(7355): S20-2.

Esch FS, Keim PS, Beattie EC, Blacher RW, Culwell AR, Oltersdorf T, McClure D, Ward PJ (1990). Cleavage of amyloid β peptide during constitutive processing of its precursor. *Science* **248**(4959): 1122–1124.

Folstein MF, Folstein SE, McHugh PR (1975). "Mini-mental state". A practical method for grading the cognitive state of patients for the clinician. *J Psychiatr Res* **12**(3): 189-198.

Förster S, Gehrig B, Balzen S, Diestel S, Schmitz B (2012). Analytical tools for the identification of O-GlcNAc modified protein: from Western blots to mass spectrometric sequencing. (Poster)

Forsythe ME, Love DC, Lazarus BD, Kim EJ, Prinz WA, Ashwell G, Krause MW, Hanover JA (2006). Caenorhabditis elegans ortholog of a diabetes susceptibility locus: oga-1 (O-GlcNAcase) knockout impacts O-GlcNAc cycling, metabolism, and dauer. *Proc Natl Acad Sci U S A* **103**(32): 11952–11957.

Francis R, McGrath G, Zhang J, Ruddy DA, Sym M, Apfeld J, Nicoll M, Maxwell M, Hai B, Ellis MC, Parks AL, Xu W, Li J, Gurney M, Myers RL, Himes CS, Hiebsch R, Ruble C, Nye JS, Curtis D (2002). aph-1 and pen-2 are required for Notch pathway signaling, γ-secretase cleavage of βAPP, and presenilin protein accumulation. *Dev Cell* **3**(1): 85–97.

Fukuyama H, Ogawa M, Yamauchi H, Yamaguchi S, Kimura J, Yonekura Y, Konishi J (1994). Altered cerebral energy metabolism in Alzheimer's disease: a PET study. *J Nucl Med* **35**(1): 1–6.

Fülöp N, Feng W, Xing D, He K, Not LG, Brocks CA, Marchase RB, Miller AP, Chatham JC (2008). Aging leads to increased levels of protein O-linked N-acetylglucosamine in heart, aorta, brain and skeletal muscle in Brown-Norway rats. *Biogerontology* **9**(3): 139–151.

Gandy S, Czernik AJ, Greengard P (1988). Phosphorylation of Alzheimer disease amyloid precursor peptide by protein kinase C and Ca2+/calmodulin-dependent protein kinase II. *Proc Natl Acad Sci U S A* **85**(16): 6218–6221.

Gao Y, Wells L, Comer FI, Parker GJ, Hart GW (2001). Dynamic O-glycosylation of nuclear and cytosolic proteins: cloning and characterization of a neutral, cytosolic β-N-acetylglucosaminidase from human brain. *J Biol Chem* **276**(13): 9838–9845.

Gloster TM, Zandberg WF, Heinonen JE, Shen DL, Deng L, Vocadlo DJ (2011). Hijacking a biosynthetic pathway yields a glycosyltransferase inhibitor within cells. *Nat Chem Biol* **7**(3): 174–181.

Godenschweger I (2007). Untersuchungen der O-GlcNAc Modifikation der rekombinant hergestellten Kinase CdK5. (Diploma thesis)

Goebel-Stengel M, Stengel A, Tache Y, Reeve, Joseph R Jr (2011). The importance of using the optimal plasticware and glassware in studies involving peptides. *Anal Biochem* **414**(1): 38–46.

Gollner UF (2002). Untersuchungen zur Bedeutung der N-Acetylglucosaminylierung für die proteolytische Spaltung der schwedischen Mutante des β-Amyloid Precursor Proteins. (Dissertation)

Gonzales RA, Greger, P H Jr, Baker SP, Ganz NI, Bolden C, Raizada MK, Crews FT (1987). Phorbol esters inhibit agonist-stimulated phosphoinositide hydrolysis in neuronal primary cultures. *Brain Res* **465**(1-2): 59–66.

Gouras GK, Tsai J, Näslund J, Vincent B, Edgar M, Checler F, Greenfield JP, Haroutunian V, Buxbaum JD, Xu H, Greengard P, Relkin NR (2000). Intraneuronal Aβ42 accumulation in human brain. *Am J Pathol* **156**(1): 15–20.

Graham DL, Gray AJ, Joyce JA, Yu D, O'Moore J, Carlson GA, Shearman MS, Dellovade TL, Hering H (2014). Increased O-GlcNAcylation reduces pathological tau without affecting its normal phosphorylation in a mouse model of tauopathy. *Neuropharmacology* **79**: 307–313.

Graham ME, Thaysen-Andersen M, Bache N, Craft GE, Larsen MR, Packer NH, Robinson PJ (2011). A novel post-translational modification in nerve terminals: O-linked N-acetylglucosamine phosphorylation. *J Proteome Res* **10**(6): 2725–2733.

Greene SJ, Killiany RJ (2010). Subregions of the inferior parietal lobule are affected in the progression to Alzheimer's disease. *Neurobiol Aging* **31**(8): 1304–1311.

Griffith LS, Mathes M, Schmitz B (1995). β-amyloid precursor protein is modified with O-linked N-acetylglucosamine. *J Neurosci Res* **41**(2): 270–278.

Griffith LS, Schmitz B (1995). O-linked N-acetylglucosamine is upregulated in Alzheimer brains. *Biochem Biophys Res Commun* **213**(2): 424–431.

Griffith LS, Schmitz B (1999). O-linked N-acetylglucosamine levels in cerebellar neurons respond reciprocally to pertubations of phosphorylation. *Eur J Biochem* **262**(3): 824–831.

Gross BJ, Kraybill BC, Walker S (2005). Discovery of O-GlcNAc transferase inhibitors. *J Am Chem Soc* **127**(42): 14588–14589.

Grundke-Iqbal I, Iqbal K, Quinlan M, Tung YC, Zaidi MS, Wisniewski HM (1986a). Microtubule-associated protein tau. A component of Alzheimer paired helical filaments. *J Biol Chem* **261**(13): 6084–6089.

Grundke-Iqbal I, Iqbal K, Tung YC, Quinlan M, Wisniewski HM, Binder LI (1986b). Abnormal phosphorylation of the microtubule-associated protein tau (tau) in Alzheimer cytoskeletal pathology. *Proc Natl Acad Sci U S A* **83**(13): 4913–4917.

Guinez C, Mir A, Dehennaut V, Cacan R, Harduin-Lepers A, Michalski J, Lefebvre T (2008). Protein ubiquitination is modulated by O-GlcNAc glycosylation. *FASEB J* **22**(8): 2901–2911.

Gupta R, Brunak S (2002). Prediction of glycosylation across the human proteome and the correlation to protein function. *Pac Symp Biocomput*: 310–322.

Gurel Z, Zaro BW, Pratt MR, Sheibani N (2014). Identification of O-GlcNAc modification targets in mouse retinal pericytes: implication of p53 in pathogenesis of diabetic retinopathy. *PLoS ONE* **9**(5): e95561.

Haass C, Koo EH, Mellon A, Hung AY, Selkoe DJ (1992a). Targeting of cell-surface β-amyloid precursor protein to lysosomes: alternative processing into amyloid-bearing fragments. *Nature* **357**(6378): 500–503.

Haass C, Schlossmacher MG, Hung AY, Vigo-Pelfrey C, Mellon A, Ostaszewski BL, Lieberburg I, Koo EH, Schenk D, Teplow DB (1992b). Amyloid β-peptide is produced by cultured cells during normal metabolism. *Nature* **359**(6393): 322–325.

Haass C, Kaether C, Thinakaran G, Sisodia S (2012). Trafficking and proteolytic processing of APP. *Cold Spring Harb Perspect Med* **2**(5): a006270.

Haltiwanger RS, Blomberg MA, Hart GW (1992). Glycosylation of nuclear and cytoplasmic proteins. Purification and characterization of a uridine diphospho-N-acetylglucosamine:polypeptide β-N-acetylglucosaminyl-transferase. *J Biol Chem* **267**(13): 9005–9013.

Haltiwanger RS, Holt GD, Hart GW (1990). Enzymatic addition of O-GlcNAc to nuclear and cytoplasmic proteins. Identification of a uridine diphospho-N-acetylglucosamine:peptide β-N-acetylglucosaminyl-transferase. *J Biol Chem* **265**(5): 2563–2568.

Hanover JA, Forsythe ME, Hennessey PT, Brodigan TM, Love DC, Ashwell G, Krause M (2005). A Caenorhabditis elegans model of insulin resistance: altered macronutrient storage and dauer formation in an OGT-1 knockout. *Proc Natl Acad Sci U S A* **102**(32): 11266–11271.

Hanover JA, Yu S, Lubas WB, Shin SH, Ragano-Caracciola M, Kochran J, Love DC (2003). Mitochondrial and nucleocytoplasmic isoforms of O-linked GlcNAc transferase encoded by a single mammalian gene. *Arch Biochem Biophys* **409**(2): 287–297.

Hardy JA, Higgins GA (1992). Alzheimer's disease: the amyloid cascade hypothesis. *Science* **256**(5054): 184–185.

Harris B, Pereira I, Parkin E (2009). Targeting ADAM10 to lipid rafts in neuroblastoma SH-SY5Y cells impairs amyloidogenic processing of the amyloid precursor protein. *Brain Res* **1296**: 203–215.

Hart GW, Greis KD, Dong LY, Blomberg MA, Chou TY, Jiang MS, Roquemore EP, Snow DM, Kreppel LK, Cole RN (1995). O-linked N-acetylglucosamine: the "yin-yang" of Ser/Thr phosphorylation? Nuclear and cytoplasmic glycosylation. *Adv Exp Med Biol* **376**: 115–123.

Hart GW, Housley MP, Slawson C (2007). Cycling of O-linked β-N-acetylglucosamine on nucleocytoplasmic proteins. *Nature* **446**(7139): 1017–1022.

Heber S, Herms J, Gajic V, Hainfellner J, Aguzzi A, Rülicke T, von Kretzschmar H, von Koch C, Sisodia S, Tremml P, Lipp HP, Wolfer DP, Müller U (2000). Mice with combined gene knock-outs reveal essential and partially redundant functions of amyloid precursor protein family members. *J Neurosci* **20**(21): 7951–7963.

Hébert SS, Serneels L, Tolia A, Craessaerts K, Derks C, Filippov MA, Müller U, de Strooper B (2006). Regulated intramembrane proteolysis of amyloid precursor protein and regulation of expression of putative target genes. *EMBO Rep* **7**(7): 739–745.

Heckel D, Comtesse N, Brass N, Blin N, Zang KD, Meese E (1998). Novel immunogenic antigen homologous to hyaluronidase in meningioma. *Hum Mol Genet* **7**(12): 1859–1872.

Herms J, Anliker B, Heber S, Ring S, Fuhrmann M, Kretzschmar H, Sisodia S, Müller U (2004). Cortical dysplasia resembling human type 2 lissencephaly in mice lacking all three APP family members. *EMBO J* **23**(20): 4106–4115.

Hirschberg CB, Snider MD (1987). Topography of glycosylation in the rough endoplasmic reticulum and Golgi apparatus. *Annu Rev Biochem* **56**: 63–87.

Ho S, Wang K, Whisenhunt TR, Huang P, Zhu X, Kudlow JE, Paterson AJ (2010). O-GlcNAcylation enhances FOXO4 transcriptional regulation in response to stress. *FEBS Lett* **584**(1): 49–54.

Hoffmann BR, Liu Y, Mosher DF (2012). Modification of EGF-like module 1 of thrombospondin-1, an animal extracellular protein, by O-linked N-acetylglucosamine. *PLoS ONE* **7**(3): e32762.

Holt GD, Hart GW (1986). The subcellular distribution of terminal N-acetylglucosamine moieties. Localization of a novel protein-saccharide linkage, O-linked GlcNAc. *J Biol Chem* **261**(17): 8049–8057.

Holt GD, Snow CM, Senior A, Haltiwanger RS, Gerace L, Hart GW (1987). Nuclear pore complex glycoproteins contain cytoplasmically disposed O-linked N-acetylglucosamine. *J Cell Biol* **104**(5): 1157–1164.

Horsch M, Hoesch L, Vasella A, Rast DM (1991). N-acetylglucosaminono-1,5-lactone oxime and the corresponding (phenylcarbamoyl)oxime. Novel and potent inhibitors of β-N-acetylglucosaminidase. *Eur J Biochem* **197**(3): 815–818.

Hu P, Shimoji S, Hart GW (2010). Site-specific interplay between O-GlcNAcylation and phosphorylation in cellular regulation. *FEBS Lett* **584**(12): 2526–2538.

Hu Y, Belke D, Suarez J, Swanson E, Clark R, Hoshijima M, Dillmann WH (2005). Adenovirus-mediated overexpression of O-GlcNAcase improves contractile function in the diabetic heart. *Circ Res* **96**(9): 1006–1013.

Hu Y, Suarez J, Fricovsky E, Wang H, Scott BT, Trauger SA, Han W, Hu Y, Oyeleye MO, Dillmann WH (2009). Increased enzymatic O-GlcNAcylation of mitochondrial proteins impairs mitochondrial function in cardiac myocytes exposed to high glucose. *J Biol Chem* **284**(1): 547–555.

Hung AY, Haass C, Nitsch RM, Qiu WQ, Citron M, Wurtman RJ, Growdon JH, Selkoe DJ (1993). Activation of protein kinase C inhibits cellular production of the amyloid β-protein. *J Biol Chem* **268**(31): 22959–22962.

Huse JT, Pijak DS, Leslie GJ, Lee VM, Doms RW (2000). Maturation and endosomal targeting of β-site amyloid precursor protein-cleaving enzyme. The Alzheimer's disease β-secretase. *J Biol Chem* **275**(43): 33729–33737.

Ida N, Hartmann T, Pantel J, Schröder J, Zerfass R, Förstl H, Sandbrink R, Masters CL, Beyreuther K (1996). Analysis of heterogeneous A4 peptides in human cerebrospinal fluid and blood by a newly developed sensitive Western blot assay. *J Biol Chem* **271**(37): 22908–22914.

Ihara Y, Morishima-Kawashima M, Nixon R (2012). The ubiquitin-proteasome system and the autophagic-lysosomal system in Alzheimer disease. *Cold Spring Harb Perspect Med* **2**(8).

Iijima K, Ando K, Takeda S, Satoh Y, Seki T, Itohara S, Greengard P, Kirino Y, Nairn AC, Suzuki T (2000). Neuron-specific phosphorylation of Alzheimer's β-amyloid precursor protein by cyclin-dependent kinase 5. *J Neurochem* **75**(3): 1085–1091.

Invitrogen (2007a). Click-iT™ O-GlcNAc Enzymatic Labeling System. www.lifetechnologies.com/content/sfs/manuals/mpC33368.pdf (14.10.2014).

Invitrogen (2007b). Click-iT™ Protein Analysis Detection Kits. www.lifetechnologies.com/content/sfs/manuals/mpC33370.pdf (14.10.2014).

Iqbal K, Alonso, Alejandra del C, Chen S, Chohan MO, El-Akkad E, Gong C, Khatoon S, Li B, Liu F, Rahman A, Tanimukai H, Grundke-Iqbal I (2005). Tau pathology in Alzheimer disease and other tauopathies. *Biochim Biophys Acta* **1739**(2-3): 198–210.

Issad T, Kuo M (2008). O-GlcNAc modification of transcription factors, glucose sensing and glucotoxicity. *Trends Endocrinol Metab* **19**(10): 380–389.

Iwatsubo T, Odaka A, Suzuki N, Mizusawa H, Nukina N, Ihara Y (1994). Visualization of Aβ 42(43) and Aβ 40 in senile plaques with end-specific Aβ monoclonals: evidence that an initially deposited species is Aβ 42(43). *Neuron* **13**(1): 45–53.

Iyer SPN, Akimoto Y, Hart GW (2003). Identification and cloning of a novel family of coiled-coil domain proteins that interact with O-GlcNAc transferase. *J Biol Chem* **278**(7): 5399–5409.

Jacobs HIL, Van Boxtel MPJ, Uylings HBM, Gronenschild EHBM, Verhey FR, Jolles J (2011). Atrophy of the parietal lobe in preclinical dementia. *Brain Cogn* **75**(2): 154–163.

Jacobsen KT, Iverfeldt K (2009). Amyloid precursor protein and its homologues: a family of proteolysis-dependent receptors. *Cell Mol Life Sci* **66**(14): 2299–2318.

Jacobsen KT, Iverfeldt K (2011). O-GlcNAcylation increases non-amyloidogenic processing of the amyloid-β precursor protein (APP). *Biochem Biophys Res Commun* **404**(3): 882–886.

Jarrett JT, Berger EP, Lansbury, PT Jr (1993). The C-terminus of the β protein is critical in amyloidogenesis. *Ann N Y Acad Sci* **695**: 144–148.

Jarvik L, Greenson H (1987). About a peculiar disease of the cerebral cortex. By Alois Alzheimer, 1907 (Translated by L. Jarvik and H. Greenson). *Alzheimer Dis Assoc Disord* **1**(1): 3–8.

Jínek M, Rehwinkel J, Lazarus BD, Izaurralde E, Hanover JA, Conti E (2004). The superhelical TPR-repeat domain of O-linked GlcNAc transferase exhibits structural similarities to importin α. *Nat Struct Mol Biol* **11**(10): 1001–1007.

Kaether C, Lammich S, Edbauer D, Ertl M, Rietdorf J, Capell A, Steiner H, Haass C (2002). Presenilin-1 affects trafficking and processing of βAPP and is targeted in a complex with nicastrin to the plasma membrane. *J Cell Biol* **158**(3): 551–561.

Kalaria RN, Harik SI (1989). Reduced glucose transporter at the blood-brain barrier and in cerebral cortex in Alzheimer disease. *J Neurochem* **53**(4): 1083–1088.

Kang J, Lemaire HG, Unterbeck A, Salbaum JM, Masters CL, Grzeschik KH, Multhaup G, Beyreuther K, Müller-Hill B (1987). The precursor of Alzheimer's disease amyloid A4 protein resembles a cell-surface receptor. *Nature* **325**(6106): 733–736.

Kang J, Müller-Hill B (1990). Differential splicing of Alzheimer's disease amyloid A4 precursor RNA in rat tissues: PreA4(695) mRNA is predominantly produced in rat and human brain. *Biochem Biophys Res Commun* **166**(3): 1192–1200.

Kearse KP, Hart GW (1991). Lymphocyte activation induces rapid changes in nuclear and cytoplasmic glycoproteins. *Proc Natl Acad Sci U S A* **88**(5): 1701–1705.

Keembiyehetty CN, Krzeslak A, Love DC, Hanover JA (2011). A lipid-droplet-targeted O-GlcNAcase isoform is a key regulator of the proteasome. *J Cell Sci* **124**(Pt 16): 2851–2860.

Keller BO, Sui J, Young AB, Whittal RM (2008). Interferences and contaminants encountered in modern mass spectrometry. *Anal Chim Acta* **627**(1): 71-81.

Kellersmann J (2003). Der Einfluss der O-GlcNAc-Modifikation auf das Prozessieren des Amyloid Precursor Proteins (APP) sowie auf die Regulation der Cdk5. (Dissertation)

Kelly WG, Dahmus ME, Hart GW (1993). RNA polymerase II is a glycoprotein. Modification of the COOH-terminal domain by O-GlcNAc. *J Biol Chem* **268**(14): 10416–10424.

Khidekel N, Arndt S, Lamarre-Vincent N, Lippert A, Poulin-Kerstien KG, Ramakrishnan B, Qasba PK, Hsieh-Wilson LC (2003). A chemoenzymatic approach toward the rapid and sensitive detection of O-GlcNAc posttranslational modifications. *J Am Chem Soc* **125**(52): 16162–16163.

Khidekel N, Ficarro SB, Clark PM, Bryan MC, Swaney DL, Rexach JE, Sun YE, Coon JJ, Peters EC, Hsieh-Wilson LC (2007). Probing the dynamics of O-GlcNAc glycosylation in the brain using quantitative proteomics. *Nat Chem Biol* **3**(6): 339–348.

Kim C, Nam DW, Park SY, Song H, Hong HS, Boo JH, Jung ES, Kim Y, Baek JY, Kim KS, Cho JW, Mook-Jung I (2013). O-linked β-N-acetylglucosaminidase inhibitor attenuates β-amyloid plaque and rescues memory impairment. *Neurobiol Aging* **34**(1): 275–285.

Kim EJ, Abramowitz LK, Bond MR, Love DC, Kang DW, Leucke HF, Kang DW, Ahn J, Hanover JA (2014). Versatile O-GlcNAc transferase assay for high-throughput identification of enzyme variants, substrates, and inhibitors. *Bioconjug Chem* **25**(6): 1025–1030.

Kim Y, Lee KJ, Jeon H, Yu YG (2006). Protein kinase CK2 is inhibited by human nucleolar phosphoprotein p140 in an inositol hexakisphosphate-dependent manner. *J Biol Chem* **281**(48): 36752–36757.

Klafki HW, Wiltfang J, Staufenbiel M (1996). Electrophoretic separation of βA4 peptides (1-40) and (1-42). *Anal Biochem* **237**(1): 24–29.

Koike H, Tomioka S, Sorimachi H, Saido TC, Maruyama K, Okuyama A, Fujisawa-Sehara A, Ohno S, Suzuki K, Ishiura S (1999). Membrane-anchored metalloprotease MDC9 has an α-secretase activity responsible for processing the amyloid precursor protein. *Biochem J* **343**(Pt 2): 371–375.

Konrad RJ, Zhang F, Hale JE, Knierman MD, Becker GW, Kudlow JE (2002). Alloxan is an inhibitor of the enzyme O-linked N-acetylglucosamine transferase. *Biochem Biophys Res Commun* **293**(1): 207–212.

Koo EH, Squazzo SL (1994). Evidence that production and release of amyloid β-protein involves the endocytic pathway. *J Biol Chem* **269**(26): 17386–17389.

Koo EH, Squazzo SL, Selkoe DJ, Koo CH (1996). Trafficking of cell-surface amyloid β-protein precursor. I. Secretion, endocytosis and recycling as detected by labeled monoclonal antibody. *J Cell Sci* **109**(Pt 5): 991–998.

Köpke E, Tung YC, Shaikh S, Alonso AC, Iqbal K, Grundke-Iqbal I (1993). Microtubule-associated protein tau. Abnormal phosphorylation of a non-paired helical filament pool in Alzheimer disease. *J Biol Chem* **268**(32): 24374–24384.

Kreppel LK, Blomberg MA, Hart GW (1997). Dynamic glycosylation of nuclear and cytosolic proteins. Cloning and characterization of a unique O-GlcNAc transferase with multiple tetratricopeptide repeats. *J Biol Chem* **272**(14): 9308–9315.

Kreppel LK, Hart GW (1999). Regulation of a cytosolic and nuclear O-GlcNAc transferase. Role of the tetratricopeptide repeats. *J Biol Chem* **274**(45): 32015–32022.

Kuhl DE, Metter EJ, Riege WH, Phelps ME (1982). Effects of human aging on patterns of local cerebral glucose utilization determined by the 18Ffluorodeoxyglucose method. *J Cereb Blood Flow Metab* **2**(2): 163–171.

Kuhn P, Wang H, Dislich B, Colombo A, Zeitschel U, Ellwart JW, Kremmer E, Rossner S, Lichtenthaler SF (2010). ADAM10 is the physiologically relevant, constitutive α-secretase of the amyloid precursor protein in primary neurons. *EMBO J* **29**(17): 3020–3032.

Kurogochi M, Matsushita T, Nishimura S (2004). Post-translational modifications on proteins: facile and efficient procedure for the identification of O-glycosylation sites by MALDI-LIFT-TOF/TOF mass spectrometry. *Angew Chem Int Ed Engl* **43**(31): 4071–4075.

Kuusisto J, Koivisto K, Mykkanen L, Helkala EL, Vanhanen M, Hanninen T, Kervinen K, Kesaniemi YA, Riekkinen PJ, Laakso M (1997). Association between features of the insulin resistance syndrome and Alzheimer's disease independently of apolipoprotein E4 phenotype: cross sectional population based study. *BMJ* **315**(7115): 1045–1049.

LaFerla FM, Green KN, Oddo S (2007). Intracellular amyloid-β in Alzheimer's disease. *Nat Rev Neurosci* **8**(7): 499–509.

Lamb JR, Tugendreich S, Hieter P (1995). Tetratrico peptide repeat interactions: to TPR or not to TPR? *Trends Biochem Sci* **20**(7): 257–259.

Lammich S, Kojro E, Postina R, Gilbert S, Pfeiffer R, Jasionowski M, Haass C, Fahrenholz F (1999). Constitutive and regulated α-secretase cleavage of Alzheimer's amyloid precursor protein by a disintegrin metalloprotease. *Proc Natl Acad Sci U S A* **96**(7): 3922–3927.

Lazarus BD, Love DC, Hanover JA (2006). Recombinant O-GlcNAc transferase isoforms: identification of O-GlcNAcase, yes tyrosine kinase, and tau as isoform-specific substrates. *Glycobiology* **16**(5): 415–421.

Lee M, Kao S, Lemere CA, Xia W, Tseng H, Zhou Y, Neve R, Ahlijanian MK, Tsai L (2003). APP processing is regulated by cytoplasmic phosphorylation. *J Cell Biol* **163**(1): 83–95.

Lee TN, Alborn WE, Knierman MD, Konrad RJ (2006). Alloxan is an inhibitor of O-GlcNAc-selective N-acetyl-β-D-glucosaminidase. *Biochem Biophys Res Commun* **350**(4): 1038–1043.

Lehman DM, Fu D, Freeman AB, Hunt KJ, Leach RJ, Johnson-Pais T, Hamlington J, Dyer TD, Arya R, Abboud H, Göring HHH, Duggirala R, Blangero J, Konrad RJ, Stern MP (2005). A single nucleotide polymorphism in MGEA5 encoding O-GlcNAc-selective N-acetyl-β-D glucosaminidase is associated with type 2 diabetes in Mexican Americans. *Diabetes* **54**(4): 1214–1221.

Lenzen S (2008). The mechanisms of alloxan- and streptozotocin-induced diabetes. *Diabetologia* **51**(2): 216–226.

Lew J, Huang QQ, Qi Z, Winkfein RJ, Aebersold R, Hunt T, Wang JH (1994). A brain-specific activator of cyclin-dependent kinase 5. *Nature* **371**(6496): 423–426.

Liu F, Iqbal K, Grundke-Iqbal I, Hart GW, Gong C (2004). O-GlcNAcylation regulates phosphorylation of tau: a mechanism involved in Alzheimer's disease. *Proc Natl Acad Sci U S A* **101**(29): 10804–10809.

Liu F, Shi J, Tanimukai H, Gu J, Gu J, Grundke-Iqbal I, Iqbal K, Gong C (2009a). Reduced O-GlcNAcylation links lower brain glucose metabolism and tau pathology in Alzheimer's disease. *Brain* **132**(Pt 7): 1820–1832.

Liu Y, Li X, Yu Y, Shi J, Liang Z, Run X, Li Y, Dai C, Grundke-Iqbal I, Iqbal K, Liu F, Gong C (2012). Developmental regulation of protein O-GlcNAcylation, O-GlcNAc transferase, and O-GlcNAcase in mammalian brain. *PLoS ONE* **7**(8): e43724.

Liu Y, Liu F, Grundke-Iqbal I, Iqbal K, Gong C (2009b). Brain glucose transporters, O-GlcNAcylation and phosphorylation of tau in diabetes and Alzheimer's disease. *J Neurochem* **111**(1): 242–249.

Liu Y, Liu F, Iqbal K, Grundke-Iqbal I, Gong C (2008). Decreased glucose transporters correlate to abnormal hyperphosphorylation of tau in Alzheimer disease. *FEBS Lett* **582**(2): 359–364.

Love DC, Kochan J, Cathey RL, Shin S, Hanover JA (2003). Mitochondrial and nucleocytoplasmic targeting of O-linked GlcNAc transferase. *J Cell Sci* **116**(Pt 4): 647–654.

Lubas WA, Frank DW, Krause M, Hanover JA (1997). O-Linked GlcNAc transferase is a conserved nucleocytoplasmic protein containing tetratricopeptide repeats. *J Biol Chem* **272**(14): 9316–9324.

Lubas WA, Hanover JA (2000). Functional expression of O-linked GlcNAc transferase. Domain structure and substrate specificity. *J Biol Chem* **275**(15): 10983–10988.

Lubas WA, Smith M, Starr CM, Hanover JA (1995). Analysis of nuclear pore protein p62 glycosylation. *Biochemistry* **34**(5): 1686–1694.

Lue LF, Kuo YM, Roher AE, Brachova L, Shen Y, Sue L, Beach T, Kurth JH, Rydel RE, Rogers J (1999). Soluble amyloid β peptide concentration as a predictor of synaptic change in Alzheimer's disease. *Am J Pathol* **155**(3): 853–862.

Luo Y, Bolon B, Kahn S, Bennett BD, Babu-Khan S, Denis P, Fan W, Kha H, Zhang J, Gong Y, Martin L, Louis JC, Yan Q, Richards WG, Citron M, Vassar R (2001). Mice deficient in BACE1, the Alzheimer's β-secretase, have normal phenotype and abolished β-amyloid generation. *Nat Neurosci* **4**(3): 231–232.

Ma J, Hart GW (2014). O-GlcNAc profiling: from proteins to proteomes. *Clin Proteomics* **11**(1): 8.

Macauley MS, Bubb AK, Martinez-Fleites C, Davies GJ, Vocadlo DJ (2008). Elevation of global O-GlcNAc levels in 3T3-L1 adipocytes by selective inhibition of O-GlcNAcase does not induce insulin resistance. *J Biol Chem* **283**(50): 34687–34695.

Macauley MS, Shan X, Yuzwa SA, Gloster TM, Vocadlo DJ (2010). Elevation of Global O-GlcNAc in rodents using a selective O-GlcNAcase inhibitor does not cause insulin resistance or perturb glucohomeostasis. *Chem Biol* **17**(9): 949–958.

Macauley MS, Vocadlo DJ (2009). Enzymatic characterization and inhibition of the nuclear variant of human O-GlcNAcase. *Carbohydr Res* **344**(9): 1079–1084.

Macauley MS, Whitworth GE, Debowski AW, Chin D, Vocadlo DJ (2005). O-GlcNAcase uses substrate-assisted catalysis: kinetic analysis and development of highly selective mechanism-inspired inhibitors. *J Biol Chem* **280**(27): 25313–25322.

Marshall S, Bacote V, Traxinger RR (1991). Discovery of a metabolic pathway mediating glucose-induced desensitization of the glucose transport system. Role of hexosamine biosynthesis in the induction of insulin resistance. *J Biol Chem* **266**(8): 4706–4712.

Marshall S, Duong T, Orbus RJ, Rumberger JM, Okuyama R (2003). Measurement of UDP-N-acetylglucosaminyl transferase (OGT) in brain cytosol and characterization of anti-OGT antibodies. *Anal Biochem* **314**(2): 169–179.

Martin JC, Fadda E, Ito K, Woods RJ (2014). Defining the structural origin of the substrate sequence independence of O-GlcNAcase using a combination of molecular docking and dynamics simulation. *Glycobiology* **24**(1): 85–96.

Masters CL, Simms G, Weinman NA, Multhaup G, McDonald BL, Beyreuther K (1985). Amyloid plaque core protein in Alzheimer disease and Down syndrome. *Proc Natl Acad Sci U S A* **82**(12): 4245–4249.

Matsuura A, Ito M, Sakaidani Y, Kondo T, Murakami K, Furukawa K, Nadano D, Matsuda T, Okajima T (2008). O-linked N-acetylglucosamine is present on the extracellular domain of notch receptors. *J Biol Chem* **283**(51): 35486–35495.

Maury JJP, Ng D, Bi X, Bardor M, Choo AB (2014). Multiple reaction monitoring mass spectrometry for the discovery and quantification of O-GlcNAc-modified proteins. *Anal Chem* **86**(1): 395–402.

McClain DA, Lubas WA, Cooksey RC, Hazel M, Parker GJ, Love DC, Hanover JA (2002). Altered glycan-dependent signaling induces insulin resistance and hyperleptinemia. *Proc Natl Acad Sci U S A* **99**(16): 10695–10699.

Meier-Ruge W, Iwangoff P, Reichlmeier K (1984). Neurochemical enzyme changes in Alzheimer's and Pick's disease. *Arch Gerontol Geriatr* **3**(2): 161–165.

Mikesh LM, Ueberheide B, Chi A, Coon JJ, Syka JEP, Shabanowitz J, Hunt DF (2006). The utility of ETD mass spectrometry in proteomic analysis. *Biochim Biophys Acta* **1764**(12): 1811–1822.

Mori C, Spooner ET, Wisniewsk KE, Wisniewski TM, Yamaguch H, Saido TC, Tolan DR, Selkoe DJ, Lemere CA (2002). Intraneuronal Aβ42 accumulation in Down syndrome brain. *Amyloid* **9**(2): 88–102.

Myers SA, Daou S, Affar EB, Burlingame A (2013). Electron transfer dissociation (ETD): the mass spectrometric breakthrough essential for O-GlcNAc protein site assignments-a study of the O-GlcNAcylated protein host cell factor C1. *Proteomics* **13**(6): 982–991.

Naslund J, Haroutunian V, Mohs R, Davis KL, Davies P, Greengard P, Buxbaum JD (2000). Correlation between elevated levels of amyloid β-peptide in the brain and cognitive decline. *JAMA* **283**(12): 1571–1577.

Näslund J, Schierhorn A, Hellman U, Lannfelt L, Roses AD, Tjernberg LO, Silberring J, Gandy SE, Winblad B, Greengard P (1994). Relative abundance of Alzheimer Aβ amyloid peptide variants in Alzheimer disease and normal aging. *Proc Natl Acad Sci U S A* **91**(18): 8378–8382.

Nordstedt C, Caporaso GL, Thyberg J, Gandy SE, Greengard P (1993). Identification of the Alzheimer β/A4 amyloid precursor protein in clathrin-coated vesicles purified from PC12 cells. *J Biol Chem* **268**(1): 608–612.

Nowak J (2011). Changes in the O-GlcNAcylation of cdk5 in SH-SY5Y APP cells after different sphingolipid treatments - Influences on the Alzheimer´s Disease Pathology? (Master thesis)

Öckl P (2007). Etablierung von Immunpräzipitation/MALDI-ToF MS zur Untersuchung des Einflusses der O-GlcNAc-Modifikation auf die Bildung der Alzheimer Aβ-Peptid-Spezies. (Diploma thesis)

O'Donnell N, Zachara NE, Hart GW, Marth JD (2004). Ogt-dependent X-chromosome-linked protein glycosylation is a requisite modification in somatic cell function and embryo viability. *Mol Cell Biol* **24**(4): 1680–1690.

Ohyagi Y, Takahashi K, Kamegai M, Tabira T (1990). Developmental and differential expression of β amyloid protein precursor mRNAs in mouse brain. *Biochem Biophys Res Commun* **167**(1): 54–60.

Oishi M, Nairn AC, Czernik AJ, Lim GS, Isohara T, Gandy SE, Greengard P, Suzuki T (1997). The cytoplasmic domain of Alzheimer's amyloid precursor protein is phosphorylated at Thr654, Ser655, and Thr668 in adult rat brain and cultured cells. *Mol Med* **3**(2): 111–123.

Okuyama R, Marshall S (2003). UDP-N-acetylglucosaminyl transferase (OGT) in brain tissue: temperature sensitivity and subcellular distribution of cytosolic and nuclear enzyme. *J Neurochem* **86**(5): 1271–1280.

Ossenkoppele R, Zwan MD, Tolboom N, van Assema DME, Adriaanse SF, Kloet RW, Boellaard R, Windhorst AD, Barkhof F, Lammertsma AA, Scheltens P, van der Flier WM, van Berckel BNM (2012). Amyloid burden and metabolic function in early-onset Alzheimer's disease: parietal lobe involvement. *Brain* **135**(Pt 7): 2115–2125.

Owen JB, Di Domenico F, Sultana R, Perluigi M, Cini C, Pierce WM, Butterfield DA (2009). Proteomics-determined differences in the concanavalin-A-fractionated proteome of hippocampus and inferior parietal lobule in subjects with Alzheimer's disease and mild cognitive impairment: implications for progression of AD. *J Proteome Res* **8**(2): 471–482.

Parkin ET, Watt NT, Hussain I, Eckman EA, Eckman CB, Manson JC, Baybutt HN, Turner AJ, Hooper NM (2007). Cellular prion protein regulates β-secretase cleavage of the Alzheimer's amyloid precursor protein. *Proc Natl Acad Sci U S A* **104**(26): 11062–11067.

Pahlsson P, Spitalnik SL (1996). The role of glycosylation in synthesis and secretion of β-amyloid precursor protein by Chinese hamster ovary cells. *Arch Biochem Biophys* **331**(2): 177-186.

Peila R, Rodriguez BL, Launer LJ (2002). Type 2 diabetes, APOE gene, and the risk for dementia and related pathologies: The Honolulu-Asia Aging Study. *Diabetes* **51**(4): 1256–1262.

Petersen RC (2004). Mild cognitive impairment as a diagnostic entity. *J Intern Med* **256**(3): 183–194.

Poenaru L, Dreyfus JC (1973). Electrophoretic study of hexosaminidases. Hexosaminidase C. *Clin Chim Acta* **43**(3): 439–442.

Portelius E, Westman-Brinkmalm A, Zetterberg H, Blennow K (2006). Determination of β-amyloid peptide signatures in cerebrospinal fluid using immunoprecipitation-mass spectrometry. *J Proteome Res* **5**(4): 1010–1016.

Postina R, Schroeder A, Dewachter I, Bohl J, Schmitt U, Kojro E, Prinzen C, Endres K, Hiemke C, Blessing M, Flamez P, Dequenne A, Godaux E, van Leuven F, Fahrenholz F (2004). A disintegrin-metalloproteinase prevents amyloid plaque formation and hippocampal defects in an Alzheimer disease mouse model. *J Clin Invest* **113**(10): 1456–1464.

Prince M, Bryce R, Albanese E, Wimo A, Ribeiro W, Ferri CP (2013). The global prevalence of dementia: a systematic review and metaanalysis. *Alzheimers Dement* **9**(1): 63-75.e2.

Qi-Takahara Y, Morishima-Kawashima M, Tanimura Y, Dolios G, Hirotani N, Horikoshi Y, Kametani F, Maeda M, Saido TC, Wang R, Ihara Y (2005). Longer forms of amyloid β protein: implications for the mechanism of intramembrane cleavage by γ-secretase. *J Neurosci* **25**(2): 436–445.

Qiu Z, Naten DL, Liston JC, Yess J, Rebeck GW (2001). A novel approach for studying endogenous Aβ processing using cultured primary neurons isolated from APP transgenic mice. *Exp Neurol* **170**(1): 186–194.

Ramakrishnan B, Qasba PK (2002). Structure-based design of β 1,4-galactosyltransferase I (β 4Gal-T1) with equally efficient N-acetylgalactosaminyltransferase activity: point mutation broadens β 4Gal-T1 donor specificity. *J Biol Chem* **277**(23): 20833–20839.

Ranuncolo SM, Ghosh S, Hanover JA, Hart GW, Lewis BA (2012). Evidence of the involvement of O-GlcNAc-modified human RNA polymerase II CTD in transcription in vitro and in vivo. *J Biol Chem* **287**(28): 23549–23561.

Rao FV, Dorfmueller HC, Villa F, Allwood M, Eggleston IM, van Aalten DMF (2006). Structural insights into the mechanism and inhibition of eukaryotic O-GlcNAc hydrolysis. *EMBO J* **25**(7): 1569–1578.

Rechsteiner M, Rogers SW (1996). PEST sequences and regulation by proteolysis. *Trends Biochem Sci* **21**(7): 267–271.

Rexach JE, Rogers CJ, Yu S, Tao J, Sun YE, Hsieh-Wilson LC (2010). Quantification of O-glycosylation stoichiometry and dynamics using resolvable mass tags. *Nat Chem Biol* **6**(9): 645–651.

Riddell DR, Christie G, Hussain I, Dingwall C (2001). Compartmentalization of β-secretase (Asp2) into low-buoyant density, noncaveolar lipid rafts. *Curr Biol* **11**(16): 1288–1293.

Robertson LA, Moya KL, Breen KC (2004). The potential role of tau protein O-glycosylation in Alzheimer's disease. *J Alzheimers Dis* **6**(5): 489–495.

Robinson KA, Ball LE, Buse MG (2007). Reduction of O-GlcNAc protein modification does not prevent insulin resistance in 3T3-L1 adipocytes. *Am J Physiol Endocrinol Metab* **292**(3): E884-90.

Rosen DR, Martin-Morris L, Luo LQ, White K (1989). A Drosophila gene encoding a protein resembling the human β-amyloid protein precursor. *Proc Natl Acad Sci U S A* **86**(7): 2478–2482.

Rostovtsev VV, Green LG, Fokin VV, Sharpless KB (2002). A stepwise huisgen cycloaddition process: copper(I)-catalyzed regioselective "ligation" of azides and terminal alkynes. *Angew Chem Int Ed Engl* **41**(14): 2596–2599.

Rumble B, Retallack R, Hilbich C, Simms G, Multhaup G, Martins R, Hockey A, Montgomery P, Beyreuther K, Masters CL (1989). Amyloid A4 protein and its precursor in Down's syndrome and Alzheimer's disease. *N Engl J Med* **320**(22): 1446–1452.

Sabrowski J (2012). Implementierung einer ELISA-basierten Methode zur Verifizierung potentieller intrazellulärer Interaktionspartner von humanem NCAM. (Diploma thesis)

Sano Y, Nakaya T, Pedrini S, Takeda S, Iijima-Ando K, Iijima K, Mathews PM, Itohara S, Gandy S, Suzuki T (2006). Physiological mouse brain Aβ levels are not related to the phosphorylation state of threonine-668 of Alzheimer's APP. *PLoS ONE* **1**: e51.

Sastre M (2010). Troubleshooting methods for APP processing in vitro. *J Pharmacol Toxicol Methods* **61**(2): 86–91.

Schimpl M, Borodkin VS, Gray LJ, van Aalten DMF (2012). Synergy of peptide and sugar in O-GlcNAcase substrate recognition. *Chem Biol* **19**(2): 173–178.

Schmechel DE, Saunders AM, Strittmatter WJ, Crain BJ, Hulette CM, Joo SH, Pericak-Vance MA, Goldgaber D, Roses AD (1993). Increased amyloid β-peptide deposition in cerebral cortex as a consequence of apolipoprotein E genotype in late-onset Alzheimer disease. *Proc Natl Acad Sci U S A* **90**(20): 9649–9653.

Schmitt K (2009). Nachweis der Aktivität der O-GlcNAc Transferase und Glykosylierung der CdK5. (Diploma thesis)

Seeger M, Nordstedt C, Petanceska S, Kovacs DM, Gouras GK, Hahne S, Fraser P, Levesque L, Czernik AJ, George-Hyslop PS, Sisodia SS, Thinakaran G, Tanzi RE, Greengard P, Gandy S (1997). Evidence for phosphorylation and oligomeric assembly of presenilin 1. *Proc Natl Acad Sci U S A* **94**(10): 5090–5094.

Sehlin D, Englund H, Simu B, Karlsson M, Ingelsson M, Nikolajeff F, Lannfelt L, Pettersson FE (2012). Large aggregates are the major soluble Aβ species in AD brain fractionated with density gradient ultracentrifugation. *PLoS ONE* **7**(2): e32014.

Selkoe DJ (2001). Alzheimer's disease: genes, proteins, and therapy. *Physiol Rev* **81**(2): 741–766.

Selkoe DJ (2011). Alzheimer's disease. *Cold Spring Harb Perspect Biol* **3**(7).

Shafi R, Iyer SP, Ellies LG, O'Donnell N, Marek KW, Chui D, Hart GW, Marth JD (2000). The O-GlcNAc transferase gene resides on the X chromosome and is essential for embryonic stem cell viability and mouse ontogeny. *Proc Natl Acad Sci U S A* **97**(11): 5735–5739.

Sharma P, Sharma M, Amin ND, Albers RW, Pant HC (1999b). Regulation of cyclin-dependent kinase 5 catalytic activity by phosphorylation. *Proc Natl Acad Sci U S A* **96**(20): 11156–11160.

Sharma P, Steinbach PJ, Sharma M, Amin ND, Barchi JJ Jr, Pant HC (1999a). Identification of substrate binding site of cyclin-dependent kinase 5. *J Biol Chem* **274**(14): 9600–9606.

Shen DL, Gloster TM, Yuzwa SA, Vocadlo DJ (2012). Insights into O-linked N-acetylglucosamine (O-GlcNAc) processing and dynamics through kinetic analysis of O-GlcNAc transferase and O-GlcNAcase activity on protein substrates. *J Biol Chem* **287**(19): 15395–15408.

Simpson IA, Chundu KR, Davies-Hill T, Honer WG, Davies P (1994). Decreased concentrations of GLUT1 and GLUT3 glucose transporters in the brains of patients with Alzheimer's disease. *Ann Neurol* **35**(5): 546–551.

Sisodia SS (1992). β-amyloid precursor protein cleavage by a membrane-bound protease. *Proc Natl Acad Sci U S A* **89**(13): 6075–6079.

Skorobogatko YV, Deuso J, Adolf-Bryfogle J, Nowak MG, Gong Y, Lippa CF, Vosseller K (2011). Human Alzheimer's disease synaptic O-GlcNAc site mapping and iTRAQ expression proteomics with ion trap mass spectrometry. *Amino Acids* **40**(3): 765–779.

Skovronsky DM, Doms RW, Lee VM (1998). Detection of a novel intraneuronal pool of insoluble amyloid β protein that accumulates with time in culture. *J Cell Biol* **141**(4): 1031–1039.

Slawson C, Lakshmanan T, Knapp S, Hart GW (2008). A mitotic GlcNAcylation/phosphorylation signaling complex alters the posttranslational state of the cytoskeletal protein vimentin. *Mol Biol Cell* **19**(10): 4130–4140.

Slawson C, Zachara NE, Vosseller K, Cheung WD, Lane MD, Hart GW (2005). Perturbations in O-linked β-N-acetylglucosamine protein modification cause severe defects in mitotic progression and cytokinesis. *J Biol Chem* **280**(38): 32944–32956.

Smet-Nocca C, Broncel M, Wieruszeski J, Tokarski C, Hanoulle X, Leroy A, Landrieu I, Rolando C, Lippens G, Hackenberger CPR (2011). Identification of O-GlcNAc sites within peptides of the Tau protein and their impact on phosphorylation. *Mol Biosyst* **7**(5): 1420–1429.

Snow CM, Senior A, Gerace L (1987). Monoclonal antibodies identify a group of nuclear pore complex glycoproteins. *J Cell Biol* **104**(5): 1143–1156.

Strempel N (2010). Untersuchungen zur O-GlcNAc-Modifikation eines GST-Nup62-Fusionsproteins, der rekombinanten CdK5 und des C-Terminus des Amyloid Precursor Proteins. (Diploma thesis)

Strittmatter WJ, Saunders AM, Schmechel D, Pericak-Vance M, Enghild J, Salvesen GS, Roses AD (1993). Apolipoprotein E: high-avidity binding to β-amyloid and increased frequency of type 4 allele in late-onset familial Alzheimer disease. *Proc Natl Acad Sci U S A* **90**(5): 1977–1981.

Studier FW, Moffatt BA (1986). Use of bacteriophage T7 RNA polymerase to direct selective high-level expression of cloned genes. *J Mol Biol* **189**(1): 113–130.

Su JH, Zhao M, Anderson AJ, Srinivasan A, Cotman CW (2001). Activated caspase-3 expression in Alzheimer's and aged control brain: correlation with Alzheimer pathology. *Brain Res* **898**(2): 350–357.

Suckau D, Resemann A, Schuerenberg M, Hufnagel P, Franzen J, Holle A (2003). A novel MALDI LIFT-TOF/TOF mass spectrometer for proteomics. *Anal Bioanal Chem* **376**(7): 952–965.

Sultana R, Boyd-Kimball D, Poon HF, Cai J, Pierce WM, Klein JB, Merchant M, Markesbery WR, Butterfield DA (2006a). Redox proteomics identification of oxidized proteins in Alzheimer's disease hippocampus and cerebellum: an approach to understand pathological and biochemical alterations in AD. *Neurobiol Aging* **27**(11): 1564–1576.

Sultana R, Perluigi M, Butterfield DA (2006b). Protein oxidation and lipid peroxidation in brain of subjects with Alzheimer's disease: insights into mechanism of neurodegeneration from redox proteomics. *Antioxid Redox Signal* **8**(11-12): 2021–2037.

Suzuki T, Nairn AC, Gandy SE, Greengard P (1992). Phosphorylation of Alzheimer amyloid precursor protein by protein kinase C. *Neuroscience* **48**(4): 755–761.

Swerdlow PS, Finley D, Varshavsky A (1986). Enhancement of immunoblot sensitivity by heating of hydrated filters. *Anal Biochem* **156**(1): 147–153.

Tallent MK, Varghis N, Skorobogatko Y, Hernandez-Cuebas L, Whelan K, Vocadlo DJ, Vosseller K (2009). In vivo modulation of O-GlcNAc levels regulates hippocampal synaptic plasticity through interplay with phosphorylation. *J Biol Chem* **284**(1): 174–181.

Tang BL (2009). Neuronal protein trafficking associated with Alzheimer disease: from APP and BACE1 to glutamate receptors. *Cell Adh Migr* **3**(1): 118–128.

Tashima Y, Stanley P (2014). Antibodies that detect O-linked β-D-N-acetylglucosamine on the extracellular domain of cell surface glycoproteins. *J Biol Chem* **289**(16): 11132–11142.

Taylor RP, Geisler TS, Chambers JH, McClain DA (2009). Up-regulation of O-GlcNAc transferase with glucose deprivation in HepG2 cells is mediated by decreased hexosamine pathway flux. *J Biol Chem* **284**(6): 3425–3432.

Taylor RP, Parker GJ, Hazel MW, Soesanto Y, Fuller W, Yazzie MJ, McClain DA (2008). Glucose deprivation stimulates O-GlcNAc modification of proteins through up-regulation of O-linked N-acetylglucosaminyl-transferase. *J Biol Chem* **283**(10): 6050–6057.

The UniProt Consortium (2014). Activities at the Universal Protein Resource (UniProt). *Nucleic Acids Res* **42**: D191-8.

Thinakaran G, Koo EH (2008). Amyloid precursor protein trafficking, processing, and function. *J Biol Chem* **283**(44): 29615–29619.

Thornton E, Vink R, Blumbergs PC, Van Den Heuvel C (2006). Soluble amyloid precursor protein α reduces neuronal injury and improves functional outcome following diffuse traumatic brain injury in rats. *Brain Res* **1094**(1): 38–46.

Toleman C, Paterson AJ, Whisenhunt TR, Kudlow JE (2004). Characterization of the histone acetyltransferase (HAT) domain of a bifunctional protein with activable O-GlcNAcase and HAT activities. *J Biol Chem* **279**(51): 53665–53673.

Torres CR, Hart GW (1984). Topography and polypeptide distribution of terminal N-acetylglucosamine residues on the surfaces of intact lymphocytes. Evidence for O-linked GlcNAc. *J Biol Chem* **259**(5): 3308–3317.

Tritz J (2010). Untersuchungen zur Aktivität der rekombinanten O-GlcNAc-Transferase sowie zum Einfluss von Glucosamin und NButGT auf die O-GlcNAc-Modifikation in SY5Y-Zellen. (Diploma thesis)

Tsai LH, Delalle I, Caviness VS Jr, Chae T, Harlow E (1994). p35 is a neural-specific regulatory subunit of cyclin-dependent kinase 5. *Nature* **371**(6496): 419–423.

Twine NA, Janitz K, Wilkins MR, Janitz M (2011). Whole transcriptome sequencing reveals gene expression and splicing differences in brain regions affected by Alzheimer's disease. *PLoS ONE* **6**(1): e16266.

Uljon SN, Mazzarelli L, Chait BT, Wang R (2000). Analysis of proteins and peptides directly from biological fluids by immunoprecipitation/mass spectrometry. *Methods Mol Biol* **146**: 439–452.

Vassar R, Bennett BD, Babu-Khan S, Kahn S, Mendiaz EA, Denis P, Teplow DB, Ross S, Amarante P, Loeloff R, Luo Y, Fisher S, Fuller J, Edenson S, Lile J, Jarosinski MA, Biere AL, Curran E, Burgess T, Louis JC, Collins F, Treanor J, Rogers G, Citron M (1999). β-secretase cleavage of Alzheimer's amyloid precursor protein by the transmembrane aspartic protease BACE. *Science* **286**(5440): 735–741.

Vetrivel KS, Thinakaran G (2010). Membrane rafts in Alzheimer's disease β-amyloid production. *Biochim Biophys Acta* **1801**(8): 860–867.

von Rotz RC, Kohli BM, Bosset J, Meier M, Suzuki T, Nitsch RM, Konietzko U (2004). The APP intracellular domain forms nuclear multiprotein complexes and regulates the transcription of its own precursor. *J Cell Sci* **117**(Pt 19): 4435–4448.

Vosseller K, Trinidad JC, Chalkley RJ, Specht CG, Thalhammer A, Lynn AJ, Snedecor JO, Guan S, Medzihradszky KF, Maltby DA, Schoepfer R, Burlingame AL (2006). O-linked N-acetylglucosamine proteomics of postsynaptic density preparations using lectin weak affinity chromatography and mass spectrometry. *Mol Cell Proteomics* **5**(5): 923–934.

Walsh DM, Tseng BP, Rydel RE, Podlisny MB, Selkoe DJ (2000). The oligomerization of amyloid β-protein begins intracellularly in cells derived from human brain. *Biochemistry* **39**(35): 10831–10839.

Wang P, Lazarus BD, Forsythe ME, Love DC, Krause MW, Hanover JA (2012). O-GlcNAc cycling mutants modulate proteotoxicity in Caenorhabditis elegans models of human neurodegenerative diseases. *Proc Natl Acad Sci U S A* **109**(43): 17669–17674.

Wang R, Sweeney D, Gandy SE, Sisodia SS (1996). The profile of soluble amyloid β protein in cultured cell media. Detection and quantification of amyloid β protein and variants by immunoprecipitation-mass spectrometry. *J Biol Chem* **271**(50): 31894–31902.

Wang Z, Gucek M, Hart GW (2008). Cross-talk between GlcNAcylation and phosphorylation: site-specific phosphorylation dynamics in response to globally elevated O-GlcNAc. *Proc Natl Acad Sci U S A* **105**(37): 13793–13798.

Wang Z, Hart GW (2008). Glycomic Approaches to Study GlcNAcylation: Protein Identification, Site-mapping, and Site-specific O-GlcNAc Quantitation. *Clin Proteom* **4**(1-2): 5–13.

Wang Z, Pandey A, Hart GW (2007). Dynamic interplay between O-linked N-acetylglucosaminylation and glycogen synthase kinase-3-dependent phosphorylation. *Mol Cell Proteomics* **6**(8): 1365–1379.

Wasco W, Bupp K, Magendantz M, Gusella JF, Tanzi RE, Solomon F (1992). Identification of a mouse brain cDNA that encodes a protein related to the Alzheimer disease-associated amyloid β protein precursor. *Proc Natl Acad Sci U S A* **89**(22): 10758–10762.

Wasco W, Gurubhagavatula S, Paradis MD, Romano DM, Sisodia SS, Hyman BT, Neve RL, Tanzi RE (1993). Isolation and characterization of APLP2 encoding a homologue of the Alzheimer's associated amyloid β protein precursor. *Nat Genet* **5**(1): 95–100.

Weidemann A, König G, Bunke D, Fischer P, Salbaum JM, Masters CL, Beyreuther K (1989). Identification, biogenesis, and localization of precursors of Alzheimer's disease A4 amyloid protein. *Cell* **57**(1): 115–126.

Weingarten MD, Lockwood AH, Hwo SY, Kirschner MW (1975). A protein factor essential for microtubule assembly. *Proc Natl Acad Sci U S A* **72**(5): 1858–1862.

Wells L, Vosseller K, Hart GW (2003). A role for N-acetylglucosamine as a nutrient sensor and mediator of insulin resistance. *Cell Mol Life Sci* **60**(2): 222–228.

Wells L, Gao Y, Mahoney JA, Vosseller K, Chen C, Rosen A, Hart GW (2002a). Dynamic O-glycosylation of nuclear and cytosolic proteins: further characterization of the nucleocytoplasmic β-N-acetylglucosaminidase, O-GlcNAcase. *J Biol Chem* **277**(3): 1755–1761.

Wells L, Kreppel LK, Comer FI, Wadzinski BE, Hart GW (2004). O-GlcNAc transferase is in a functional complex with protein phosphatase 1 catalytic subunits. *J Biol Chem* **279**(37): 38466–38470.

Wells L, Vosseller K, Cole RN, Cronshaw JM, Matunis MJ, Hart GW (2002b). Mapping sites of O-GlcNAc modification using affinity tags for serine and threonine post-translational modifications. *Mol Cell Proteomics* **1**(10): 791–804.

Werner S (2004). Untersuchungen zur O-GlcNAc Modifikation neuraler Proteine. (Dissertation)

Westermeier R (2005). *Electrophoresis in Practice*. 4th ed.: Wiley-VCH.

Whelan SA, Dias WB, Thiruneelakantapillai L, Lane MD, Hart GW (2010). Regulation of insulin receptor substrate 1 (IRS-1)/AKT kinase-mediated insulin signaling by O-Linked β-N-acetylglucosamine in 3T3-L1 adipocytes. *J Biol Chem* **285**(8): 5204–5211.

Whelan SA, Lane MD, Hart GW (2008). Regulation of the O-linked β-N-acetylglucosamine transferase by insulin signaling. *J Biol Chem* **283**(31): 21411–21417.

Whisenhunt TR, Yang X, Bowe DB, Paterson AJ, Van Tine BA, Kudlow JE (2006). Disrupting the enzyme complex regulating O-GlcNAcylation blocks signaling and development. *Glycobiology* **16**(6): 551–563.

Wiltfang J, Arold N, Neuhoff V (1991). A new multiphasic buffer system for sodium dodecyl sulfate-polyacrylamide gel electrophoresis of proteins and peptides with molecular masses 100,000-1000, and their detection with picomolar sensitivity. *Electrophoresis* **12**(5): 352–366.

Wirths O, Multhaup G, Bayer TA (2004). A modified β-amyloid hypothesis: intraneuronal accumulation of the β-amyloid peptide--the first step of a fatal cascade. *J Neurochem* **91**(3): 513–520.

Wobst H, Förster S, Laurini C, Sekulla A, Dreiseidler M, Höhfeld J, Schmitz B, Diestel S (2012). UCHL1 regulates ubiquitination and recycling of the neural cell adhesion molecule NCAM. *FEBS J* **279**(23): 4398–4409.

Wolfe MS, Xia W, Ostaszewski BL, Diehl TS, Kimberly WT, Selkoe DJ (1999). Two transmembrane aspartates in presenilin-1 required for presenilin endoproteolysis and γ-secretase activity. *Nature* **398**(6727): 513–517.

Wu Z, Kinslow C, Pettigrew KD, Rapoport SI, Schapiro MB (1998). Role of familial factors in late-onset Alzheimer disease as a function of age. *Alzheimer Dis Assoc Disord* **12**(3): 190–197.

Yang WH, Kim JE, Nam HW, Ju JW, Kim HS, Kim YS, Cho JW (2006). Modification of p53 with O-linked N-acetylglucosamine regulates p53 activity and stability. *Nat Cell Biol* **8**(10): 1074–1083.

Yang X, Ongusaha PP, Miles PD, Havstad JC, Zhang F, So WV, Kudlow JE, Michell RH, Olefsky JM, Field SJ, Evans RM (2008). Phosphoinositide signalling links O-GlcNAc transferase to insulin resistance. *Nature* **451**(7181): 964–969.

Yang YR, Song M, Lee H, Jeon Y, Choi E, Jang H, Moon HY, Byun H, Kim E, Kim DH, Lee MN, Koh A, Ghim J, Choi JH, Lee-Kwon W, Kim KT, Ryu SH, Suh P (2012). O-GlcNAcase is essential for embryonic development and maintenance of genomic stability. *Aging Cell* **11**(3): 439–448.

Yao PJ, Coleman PD (1998). Reduction of O-linked N-acetylglucosamine-modified assembly protein-3 in Alzheimer's disease. *J Neurosci* **18**(7): 2399–2411.

Yu G, Nishimura M, Arawaka S, Levitan D, Zhang L, Tandon A, Song YQ, Rogaeva E, Chen F, Kawarai T, Supala A, Levesque L, Yu H, Yang DS, Holmes E, Milman P, Liang Y, Zhang DM, Xu DH, Sato C,

Rogaev E, Smith M, Janus C, Zhang Y, Aebersold R, Farrer LS, Sorbi S, Bruni A, Fraser P, St George-Hyslop P (2000). Nicastrin modulates presenilin-mediated notch/glp-1 signal transduction and βAPP processing. *Nature* **407**(6800): 48–54.

Yuzwa SA, Cheung AH, Okon M, McIntosh LP, Vocadlo DJ (2014). O-GlcNAc modification of tau directly inhibits its aggregation without perturbing the conformational properties of tau monomers. *J Mol Biol* **426**(8): 1736–1752.

Yuzwa SA, Macauley MS, Heinonen JE, Shan X, Dennis RJ, He Y, Whitworth GE, Stubbs KA, McEachern EJ, Davies GJ, Vocadlo DJ (2008). A potent mechanism-inspired O-GlcNAcase inhibitor that blocks phosphorylation of tau in vivo. *Nat Chem Biol* **4**(8): 483–490.

Yuzwa SA, Shan X, Macauley MS, Clark T, Skorobogatko Y, Vosseller K, Vocadlo DJ (2012). Increasing O-GlcNAc slows neurodegeneration and stabilizes tau against aggregation. *Nat Chem Biol* **8**(4): 393–399.

Yuzwa SA, Vocadlo DJ (2014). O-GlcNAc and neurodegeneration: biochemical mechanisms and potential roles in Alzheimer's disease and beyond. *Chem Soc Rev* **43**(19): 6839–6858.

Zachara NE, O'Donnell N, Cheung WD, Mercer JJ, Marth JD, Hart GW (2004). Dynamic O-GlcNAc modification of nucleocytoplasmic proteins in response to stress. A survival response of mammalian cells. *J Biol Chem* **279**(29): 30133–30142.

Zachara NE, Vosseller K, Hart GW (2011). Detection and analysis of proteins modified by O-linked N-acetylglucosamine. *Curr Protoc Protein Sci* **Chapter 12**: Unit12.8.

Zhang F, Su K, Yang X, Bowe DB, Paterson AJ, Kudlow JE (2003). O-GlcNAc modification is an endogenous inhibitor of the proteasome. *Cell* **115**(6): 715–725.

Zhang Y, McLaughlin R, Goodyer C, LeBlanc A (2002). Selective cytotoxicity of intracellular amyloid β peptide1-42 through p53 and Bax in cultured primary human neurons. *J Cell Biol* **156**(3): 519–529.

Zheng H, Jiang M, Trumbauer ME, Sirinathsinghji DJ, Hopkins R, Smith DW, Heavens RP, Dawson GR, Boyce S, Conner MW, Stevens KA, Slunt HH, Sisoda SS, Chen HY, Van der Ploeg LH (1995). β-Amyloid precursor protein-deficient mice show reactive gliosis and decreased locomotor activity. *Cell* **81**(4): 525–531.

Zou K, Kim D, Kakio A, Byun K, Gong J, Kim J, Kim M, Sawamura N, Nishimoto S, Matsuzaki K, Lee B, Yanagisawa K, Michikawa M (2003). Amyloid β-protein (Aβ)1-40 protects neurons from damage induced by Aβ1-42 in culture and in rat brain. *J Neurochem* **87**(3): 609–619.

Zou L, Zhu-Mauldin X, Marchase RB, Paterson AJ, Liu J, Yang Q, Chatham JC (2012). Glucose deprivation-induced increase in protein O-GlcNAcylation in cardiomyocytes is calcium-dependent. *J Biol Chem* **287**(41): 34419–34431.

Appendix

A. Plasmid pBJG1-Nup62

Plasmid was generated from pBJG1-hNCAM180cyt by excision of hNCAM180cyt and insertion of the Nup62 coding sequence with deleted stop codon using *Bam*HI and *Xho*I restriction enzymes.

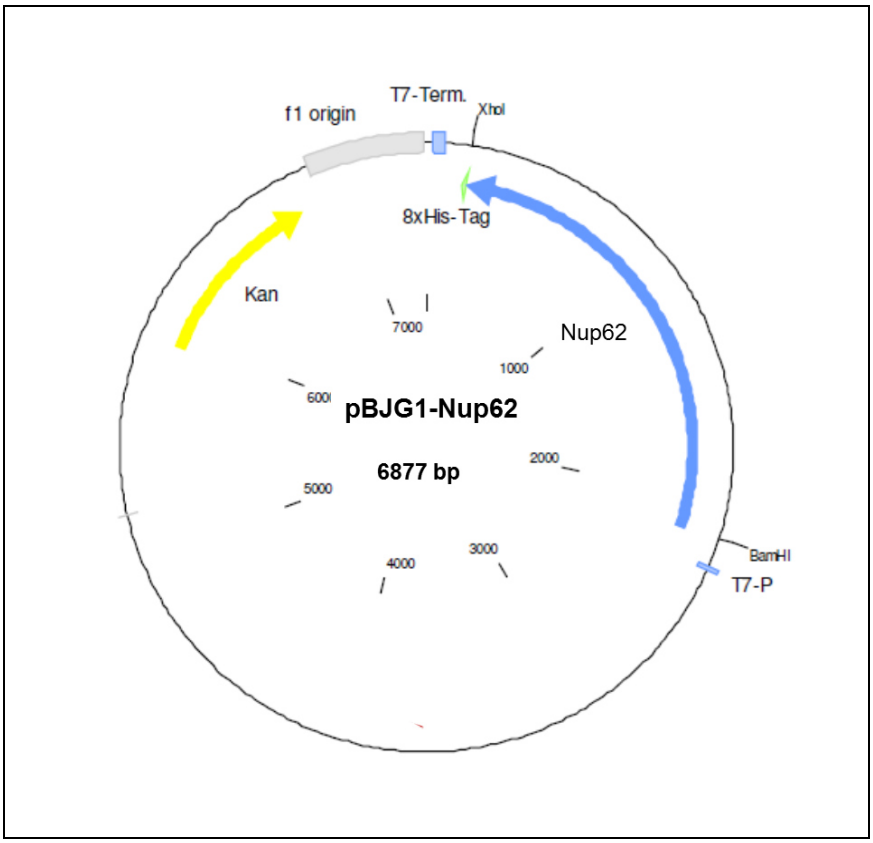

Figure 26: Plasmid map pBJG1-Nup62
T7-Term: T7 Terminator; T7-P: T7 Promotor; Kan: Kanamycin; bp: base pairs

B. Human Brain samples

Clinical and pathological information on human brain tissue samples used in this work.

Table 20: Clinical and pathological information of IPL samples

Case #	Sample ID	Gender	Age at death	PMI (h)	Braak stage	MMSE score
C1	1065	M	87	3.5	IV	24
C2	1070	M	82	2.25	I	29
C3	1063	F	86	3.75	I	29
C4	1131	F	80	2.25	I	28
C5	1161	F	84	2.42	0	30
C6	1103	F	76	10	I	29
C7	1146	F	93	2.75	II	29
C8	1106	M	79	1.75	II	29
C9	1142	M	92	3.25	0	30
C10	1127	F	91	1.25	II	29
C11	1092	F	86	1.75	I	29
C12	1159	F	86	3.25	0	28
C13	1163	F	84	2.93	I	26
MCI1	1164	F	88	3	III	28
MCI2	1130	F	99	2	V	22
MCI3	1178	F	96	2.42	IV	27
MCI4	1083	F	88	9.83	V	17
MCI5	1122	M	87	2.75	IV	27
MCI6	1152	M	84	3.5	IV	24
MCI7	1087	F	82	2.9	III	29
MCI8	1065	M	87	3.5	IV	24
MCI9	1077	M	87	2.25	III	21
MCI10	1059	M	93	4.25	IV	21
AD1	1199	M	88	2.67	VI	11
AD2	1128	F	86	2.67	VI	0
AD3	1085	F	84	5	VI	18
AD4	1215	F	91	3	V	13
AD5	1192	F	93	2.75	V	0
AD6	1073	F	83	4	V	4
AD7	1072	F	75	2.33	VI	22
AD8	1058	M	78	3.67	VI	19
AD9	1028	M	82	4	VI	
AD10	807	M	93	3.08	VI	14
AD11	960	F	81	2.25	V	13

Case #	Sample ID	Gender	Age at death	PMI (h)	Braak stage	MMSE score
AD12	854	F	79	3.45	VI	16
AD13	1061	F	80	2.75	VI	22

C: control; MCI: mild cognitive impairment; AD: Alzheimer disease; F: female; M: male; Age of death (in years); PMI: post-mortem interval (in hours); MMSE: Mini-Mental State Examination.

Table 21: Clinical and pathological information of cerebellum samples

Case #	Sample ID	Gender	Age at Death	PMI (h)	Braak stage	MMSE Score
C1	1063	F	86	3.75	I	29
C2	1092	F	86	1.75	I	29
C3	1095	F	90	4.08	I	29
C4	1103	F	76	10	I	29
C5	1106	M	79	1.75	II	29
C6	1089	M	74	4	I	26
C7	1070	M	82	2.25	I	29
C8	1066	M	81	2	II	30
MCI 1	1130	F	99	2	V	22
MCI 2	1164	F	88	3	III	28
MCI 3	1083	F	88	9.38	V	17
MCI 4	1178	F	96	2.42	IV	27
MCI 5	1122	M	87	2.75	IV	27
MCI 6	1065	M	87	3.5	IV	24
MCI 7	1087	F	82	2.9	III	29
MCI 8	1059	M	93	4.25	IV	21
AD1	1058	M	78	3.67	VI	19
AD2	1074	M	81	2.92	VI	21
AD3	1060	M	77	3	VI	
AD4	1192	F	93	2.75	V	0
AD5	1215	F	91	3	V	13
AD6	1199	M	88	2.67	VI	11
AD7	1128	F	86	2.67	VI	0
AD8	1085	F	84	5	VI	18

C: control; MCI: mild cognitive impairment; AD: Alzheimer disease; F: female; M: male; Age of death (in years); PMI: post-mortem interval (in hours); MMSE: Mini-Mental State Examination.

C. Exemplary MS results of Aβ-IP

SY5Y-APP cells were subjected to various treatments; conditioned media was harvested and stored at -80°C until further analysis. Aβ-IP was performed as described in 3.4.7. Briefly, 0.1 % Triton X-100 was added to 1 ml conditioned medium and Aβ was immunoprecipitated with 4G8 antibody and Protein G-sepharose. As a positive control, 1 µl 1 µM $Aβ_{12-28}$ solution was added to the sample. Beads were washed with IP wash buffer, 25 mM $NaHCO_3$ and finally with DI water. Bound peptides were eluted from beads with 0.1 % TFA. 1 µl sample was applied to the target spot, immediately mixed with 1 µl matrix (α-CHCA in 30 % ACN / 0.1 % TFA, saturated solution) and air-dried. Samples were analyzed by MALDI-TOF MS.

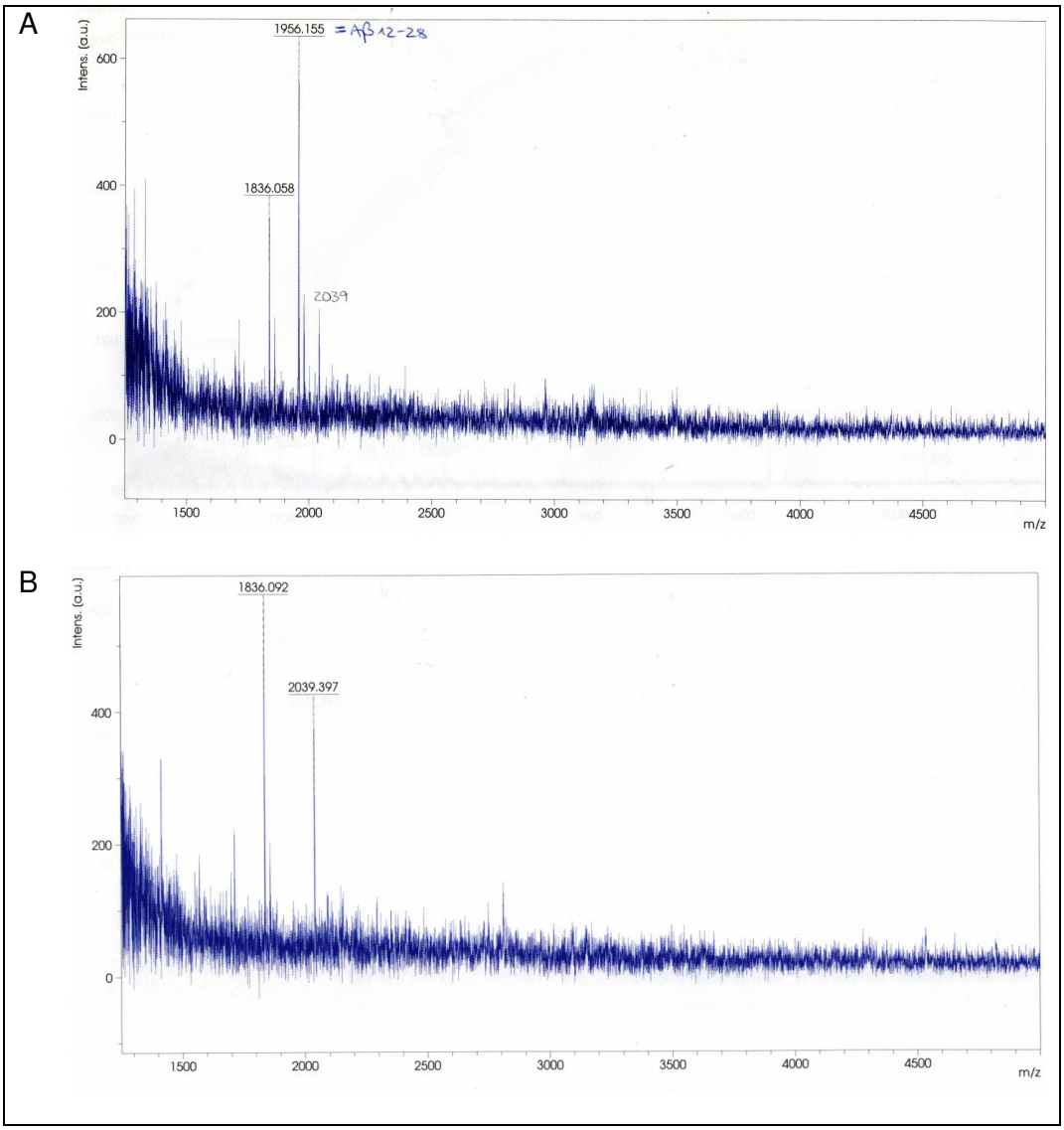

Figure 27: Exemplary mass spectra after Aβ-IP from conditioned media of SY5Y-APP cells

SY5Y-APP cells were treated for 24 hours with 30 µM NButGT **(A)** or DMSO **(B)**. Aβ was immunoprecipitated from conditioned medium and analyzed by MALDI-TOF MS. **(A)** Mass spectrum after Aβ-IP from conditioned medium supplemented with $Aβ_{12-28}$. **(B)** Mass spectrum after Aβ-IP from conditioned medium (DMSO). To exclude low mass chemical noise, MS data were acquired across the 1300-5000 m/z range Molecular mass of $Aβ_{12-28}$: 1956 Da; m/z: mass-to-charge ratio; Intens. [a.u]: Intensitiy, measured in arbitrary units.

D. Individual results of two OGA activity assays

OGA activity assay was performed twice with n = 3 each. Both times, protein estimation after sample preparation revealed that one of the samples was too dilute to continue with. OGA activity assay was performed as described in 3.6. Reactions were stopped after 120 or 150 minutes, respectively. Absorption at 405 nm was measured and released GlcNAc was calculated as described in 3.6. Enzyme activity units were calculated by dividing the µM GlcNAc released by the incubation time (in minutes).

Table 22: Results of OGA activity assay 1

Sample ID	OD_{405}	Mean OD_{405}	sample - blank	µM GlcNAc released	Enzyme activity units *
Blank	0.058 0.055	0.057			
C13	0.442 0.438	0.440	0.384	3.104	0.026
C3	0.545 0.582	0.564	0.508	4.108	0.034
AD1	0.171 0.195	0.183	0.127	1.024	0.009
AD3	0.247 0.243	0.245	0.189	1.526	0.013
AD5	0.355 0.359	0.357	0.300	2.432	0.020

*Enzyme activity units are measured in µM GlcNAc released / 120 minutes

Table 23: Results of OGA activity assay 2

Sample ID	OD_{405}	Mean OD_{405}	sample - blank	µM GlcNAc released	Enzyme activity units *
Blank	0.059 0.077	0.068			
C2	0.474 0.464	0.469	0.401	3.246	0.022
C7	0.485 0.499	0.492	0.424	3.432	0.023
C11	0.439 0.452	0.446	0.378	3.060	0.020
AD8	0.344 0.357	0.351	0.283	2.291	0.015
AD9	0.381 0.384	0.383	0.315	2.550	0.017

*Enzyme activity units are measured in µM GlcNAc released / 150 minutes

E. *In silico* O-GlcNAcylation of cdk5

Amino acid sequence of cdk5 was obtained from UniProt (UniProt accession number Q00535) and FASTA sequence was analyzed for potential O-GlcNAcylation with YinOYang 1.2 Prediction Server.

```
Name:  Sequence          Length:  292
MQKYEKLEKIGEGTYGTVFKAKNRETHEIVALKRVRLDDDDEGVPSSALREICLLKELKHKNIVRLHDVLHSDKKLTLVF      80
EFCDQDLKKYFDSCNGDLDPEIVKSFLFQLLKGLGFCHSRNVLHRDLKPQNLLINRNGELKLADFGLARAFGIPVRCYSA     160
EVVTLWYRPPDVLFGAKLYSTSIDMWSAGCIFAELANAGRPLFPGNDVDDQLKRIFRLLGTPTEEQWPSMTKLPDYKPYP     240
MYPATTSLVNVVPKLNATGRDLLQNLLKCNPVQRISAEEALQHPYFSDFCPP
.............................................G.................................      80
.....................................................................................     160
.....................................................................................     240
....GYG.....................................................


-------------------------------------------------------------------------------
SeqName     Residue  O-GlcNAc  Potential  Thresh.  Thresh.   NetPhos  YinOYang?
                      result   (o-glcnac)   (1)      (2)    potential
                                                          (Thresh=0.5)
-------------------------------------------------------------------------------
Sequence       46  S    +        0.4191    0.4115   0.5051
Sequence      245  T    +        0.4917    0.4426   0.5470
Sequence      246  T*   +        0.5219    0.4438   0.5486     0.759       *
Sequence      247  S    +        0.5097    0.4427   0.5472
-------------------------------------------------------------------------------
```

Figure 28: Sites of potential O-GlcNAcylation of cdk5

Amino acid sequence of human cdk5 was imported into YinOYang 1.2 Prediction Server. Analysis settings were as follows: check yin-yang site prediction, Output: show only positive sites, NetPhos threshold: 0.5. +: O-GlcNAc predicted; *: yin-yang site

Danksagung

Ich danke Frau Prof. Brigitte Schmitz (em.) für die Vergabe des Themas sowie die gute Betreuung während der letzten Jahre. Des Weiteren möchte ich Herrn Prof. Norbert Koch, Herrn Prof. Jörg Höhfeld und Frau PD Simone Diestel für die Übernahme der Ämter der weiteren Gutachter danken.

Mein herzlicher Dank gilt allen jetzigen und ehemaligen MitarbeiterInnen der Abteilung Biochemie bzw. Human Metabolomics für das angenehme Arbeitsklima und Ihre stete Unterstützung im Labor - und außerhalb. Ganz besonders möchte ich Bernd Gehrig für die massenspektrometrischen Analysen danken sowie für die ausführlichen Erklärungen und die Geduld, mit der er versucht hat mir die Massenspektrometrie näherzubringen. Bei Hilke Wobst, Simone Diestel und Anni Dahmen möchte ich mich noch einmal besonders für Ihre Unterstützung, die konstruktive Kritik und die vielen - nicht nur fachspezifischen - Diskussionen in der letzten Phase der Promotion bedanken.

Außerdem danke ich Herrn Prof. D. Allan Butterfield dafür, dass er mir die Möglichkeit gegeben hat einen wichtigen Teil meiner Arbeit in seinem Labor an der University of Kentucky durchzuführen. Auch seinen MitarbeiterInnen, allen voran Dr. Rukhsana Sultana, Judy Triplett und Mollie Fraim, möchte ich danken, dass sie mich so herzlich in ihr Labor aufgenommen und unterstützt haben. Außerdem danke ich dem Gleichstellungsbüro der Uni Bonn für die kleine finanzielle Unterstützung in Kentucky.

Als letztes möchte ich mich an dieser Stelle ganz herzlich bei meiner Familie und Freunden bedanken, die mich während meiner gesamten Promotion unterstützt haben und sich geduldig immer wieder seltsame O-GlcNAc-Probleme angehört haben!

Abschlusserklärung

Hiermit erkläre ich, die vorgelegte Arbeit selbstständig verfasst und keine anderen als die angegebenen Hilfsmittel benutzt, sowie alle Stellen der Arbeit, die anderen Werken im Wortlaut oder Sinn nach entnommen sind, kenntlich gemacht zu haben

Köln, 21.10.2014

Sarah Förster